L-MT-16-016

ENCLOSURE 2

AREVA, INC.

CALCULATION 11042-0205, Revision 3

TITLE:

61BTH ITCP and OTCP Closure Weld Flaw Evaluation

90 pages follow

<table>
<tr><td rowspan="3">AREVA</td><td rowspan="3">Form 3.2-1
Calculation Cover Sheet
TIP 3.2 (Revision 10)</td><td>Calculation No.</td><td>11042-0205</td></tr>
<tr><td>Revision No.</td><td>3</td></tr>
<tr><td colspan="2">Page 1 of 90</td></tr>
<tr><td>DCR NO (if applicable):
11042-025 Revision 0</td><td>PROJECT NAME:</td><td colspan="2">NUHOMS® 61BTH Type 1 DSCs for Monticello Nuclear Generating Plant</td></tr>
<tr><td>PROJECT NO: 11042</td><td>CLIENT:</td><td colspan="2">Xcel Energy</td></tr>
<tr><td colspan="4">CALCULATION TITLE:
61BTH ITCP and OTCP Closure Weld Flaw Evaluation</td></tr>
<tr><td colspan="4">SUMMARY DESCRIPTION:
1) Calculation Summary
This calculation qualifies Monticello DSC-16, a 61BTH Type 1 DSC, for all design basis loads in consideration of observed flaws in the Inner Top Cover Plate (ITCP) and Outer Top Cover Plate (OTCP) closure welds..

2) Storage Media Location
- Coldstor - /areva_tn/11042/11042-0205-000
- Coldstor - /areva_tn/11042/11042-0205-002</td></tr>
<tr><td colspan="4">If original issue, is licensing review per TIP 3.5 required? N/A
Yes ☐ No ☐ (explain below) Licensing Review No.:</td></tr>
<tr><td colspan="2">Software utilized (subject to test requirements of TIP 3.3):
ANSYS</td><td>Software Version:
14.0</td><td>Software Log Revision
R-31</td></tr>
<tr><td colspan="3">Calculation is complete

Originator Name and Signature: Jeff Pieper [signature]</td><td>Date: 3/10/16</td></tr>
<tr><td colspan="3">Calculation has been checked for consistency, completeness, and correctness

Checker Name and Signature: Gabriel Lomas [signature: Gabriel J. Lomas]</td><td>Date:
3/10/16</td></tr>
<tr><td colspan="3">Calculation is approved for use

Project Engineer Name and Signature: [signature] HAROON Raheel 2016.03.21 17:41:22 -04'00'</td><td>Date:
3/21/16</td></tr>
</table>

REVISION SUMMARY

Rev.	Description	Affected Pages	Affected Data
0	Initial Issue	All	All
1	Revised per DCR 11042-022 Revision 0. Made editorial clarifications, updated information from revised Reference calculations, removed extraneous sensitivity analyses.	1-10, 13, 14, 17, 18, 21, 22, 24-34, 36, 45, 46, 48-50, 59-77	Removed extraneous data.
2	Revised per DCR 11042-023 Revision 0. Added elastic-plastic analyses in Appendix A. Additional discussion and clarifications added throughout.	1-4, 6-10, 13-17, 19-22, 24, 27-29, 31, 33-35, 44, 60, 62-63, 68-78, Appendix A (79-87)	Added files in Appendix A
3	Revised per DCR 11042-025 Revision 0 to address RAI-2-1. Clarified limit load vs elastic plastic results. Added Table 7. Added additional results plots in Appendix A.	1-7, 13, 15, 21, 22, 29, 35, 36, 45, 46, 81, 82, 90	None

TABLE OF CONTENTS

Page

LIST OF TABLES

LIST OF FIGURES

Page

1.0 PURPOSE

The purpose of this calculation is to evaluate DSC-16 at the Monticello Nuclear Generating Plant (MNGP) per ASME Section III criteria in consideration of flaws observed in the Inner and Outer Top Cover Plate (ITCP and OTCP) closure welds. The flaws are documented in the Reference 5.1 Phased Array Ultrasonic Testing (PAUT) inspection report. The canister is a 61BTH Type 1 design. The ASME Section III Subsection NB Code limits on primary stress are evaluated using the limit load analysis criteria prescribed in the Code [Ref. 5.7]. Additional elastic-plastic analyses are performed to document the actual predicted strains in the welds and to demonstrate adequate margin against plastic collapse.

The body of this calculation is predominately concerned with the limit load analyses, including several finite element model mesh sensitivity analyses. The limit load analyses demonstrate satisfaction of the ASME NB limits on primary stress.

The elastic-plastic analyses are performed in Appendix A and the results are summarized in Section 7.0 and Table 7. The elastic plastic analyses demonstrate adequate margin against the material ductility limits and against plastic collapse.

2.0 ASSUMPTIONS

1. The ITCP weld to the siphon and vent block and the welds of the siphon and vent port cover plates are inaccessible for PAUT inspection. Approximately 11" are obscured due to the location of the siphon and vent block. Whereas the main circumferential lid-to-shell welds are made with an automated welding machine, some manual welding was performed around the siphon/vent block and ports. As discussed in Section 3.4, a strength reduction factor of 0.8 is considered for both the ITCP and OTCP welds. This factor accounts for the siphon and vent block welds and uncertainties in the UT technique.

   Note that the bounding flaws evaluated in this analysis are treated as full circumferential flaws. In other words, it is not assumed that the siphon and vent block is free of flaws, but rather contains the same bounding flaws as the examined welds. The geometry of the siphon and vent block is not assumed in this analysis. It is assumed that the stresses in the circular configuration bound the stresses that would be computed for a configuration that explicitly includes the siphon and vent block.

2. The longitudinal seams in the canister shell caused attenuation in the PAUT energy beam at locations 24.3" to 24.8" and 129.5" to 130" [Ref. 5.1] that can potentially diminish the effectiveness of the examination in these half inch areas. These regions are considered limited examination zones. It is assumed that the flaws observed outside of these regions are representative, and that no larger or more bounding flaws exist in the regions behind the canister seam welds. The use of the 0.8 weld strength reduction factor discussed above in Assumption 1 accounts for any uncertainty in this region.

3. [Not used]

4. The flaws are considered to be planar cracks lying on circumferential planes, parallel with the longitudinal axis of the cask. (I.e. the crack tips are pointed in the axial directions of the cask). This is a conservative flaw orientation since the welds primarily resist normal stresses in the plane of the lids due to plate bending caused by DSC internal pressure. Also, during the side drop loading, normal stresses in the plane of the lids resist the ovalizing mode of shell deformation.

   This flaw orientation is also conservative for through-thickness shear stresses in the lid welds since it maximizes the reduction in available shear area. (A flaw of equal length, but placed at an angle, would result in less reduction of the weld throat thickness).

5. Many of the flaws identified in the Reference 5.1 PAUT examination report lie in very similar locations within the weld cross section. As discussed in detail in Section 3.2, flaws that lie in similar radial and axial positions within the weld are considered bounded by a representative "group flaw." The locations and sizes of the "group flaws" are chosen conservatively to ensure they are bounding of the individual flaws.

6. The analysis is based on the nominal dimensions of the components as shown in the design drawings [References 5.3 and 5.4] including the as-fabricated radial gap between the outer diameter of the lids and the inner diameter of the DSC shell. Although weld shrinkage will close this gap during closure operations, the resulting compressive load path between the lids and shell is conservatively ignored. Further discussion is provided in Section 4.3.

3.0 DESIGN INPUT/DATA

3.1 DSC Geometry

The 61BTH Type 1 DSC geometry is detailed in the Reference 5.3 and 5.4 drawings. The Reference 5.5 drawing shows the details for the final ITCP and OTCP closure field welds. Sketches from Reference 5.1 and details from References 5.3 and 5.4 are shown in Figure 1 through Figure 4.

The material for all structural components (DSC Shell, OTCP, and ITCP) is SA-240 Type 304 stainless steel.

The shield plug material is SA-36 carbon steel.

The DSC shell is 0.5" nominal thickness.

The ITCP is 0.75" nominal thickness. Per the Reference 5.5 drawing, it is welded to the DSC shell and vent/siphon block with a 3/16" groove weld. However, the ITCP lid groove (weld prep) is 0.25" minimum, and it was confirmed that the weld is also 0.25" [Ref. 5.1].

The OTCP is 1.25" nominal thickness. It is welded to the DSC shell with a 1/2" groove weld.

The ITCP and OTCP closure welds (with the exception of the ITCP welds around the vent/siphon block and the welds of the vent and siphon port cover plates) are made using the GTAW process with an automated welder. This is a non-flux type of weld. The vent/siphon block and the vent and siphon port cover plate welds are performed manually, also using a non-flux process.

3.2 Flaw Details and Geometry

Various sets of bounding flaws are chosen for the detailed analyses based on the flaw dimensions in Reference 5.1 and the discussion below. Note that flaws are identified in this calculation using the numerical flaw listings in the Reference 5.1 inspection report.

3.2.1 Outer Top Cover Plate

3.2.1.1 Case 1

Figure 5 shows all of the OTCP weld flaws from Reference 5.1 plotted on an outline of the DSC geometry. Figure 6 shows a similar plot but with the main cluster of flaws bounded by a box, and showing a representative "group flaw" for this region. The longest flaw within the group region is 31.7" long and the tallest flaw is 0.14" high. Therefore, the bounding flaw for this region is taken as a full circumferential flaw, 0.14" in height.

Note that all flaws in the group region were reviewed to ensure that no two flaws in close circumferential proximity, considered as being joined, would produce a taller flaw. For example, OTCP Flaw #9 and OTCP Flaw #10 are within 0.17" of each other in the circumferential direction, but their combined height is only 0.47-0.38=0.09". Therefore these flaws, considered combined, are bounded by the 0.14" high group flaw.

The radial and axial positions of the bounding flaw were chosen to be at the center of the group region. This radial position is within the critical failure plane of the weld (i.e. a plane containing the minimum weld throat thickness of 0.5").

Figure 6 also shows additional information about the flaws outside of the group region. OTCP Flaw #2 is intermittent around the entire circumference of the DSC. Therefore this flaw, at 0.12" in height, is considered a full circumferential flaw. Since OTCP Flaw #14 is in close proximity to Flaw #2, it is conservatively considered joined to OTCP Flaw #2, and the combined flaw height is considered to be present around the entire circumference. The combined flaw height is determined based on the geometry to be 0.195".

As seen in Figure 6, OTCP Flaw #20 is remote from the group region and from OTCP Flaw #s 2 and 14. OTCP Flaw #20 is only 0.32" in length, and only 0.07" in height. This flaw is separated from OTCP Flaw #19 by 0.36" in the circumferential direction and by 0.19" in the axial direction. It is separated from OTCP Flaw #21 by 1.66" in the circumferential direction and by 0.23" in the axial direction. Since extension of the flaws under the postulated loading is negligible (since only one cycle of the critical loads is applied) this flaw will not join with the adjacent flaws. Additionally, since OTCP Flaw #20 is much smaller than the critical surface flaw size of 0.29" from Reference 5.17, it is not considered explicitly in the FEA analyses and is considered bounded by the other modeled flaws which are very conservative.

Similarly, OTCP Flaw #3 is remote from all flaws with the exception of OTCP Flaw #2. However, OTCP Flaw #3 is very small, only 0.18" long and 0.09" tall. Inspection of the PAUT plots (see Page 22 of Reference 5.1) also shows that OTCP Flaw #2, which is considered as fully continuous in this analysis, is actually very intermittent at the circumferential position of OTCP Flaw #3. Furthermore, OTCP Flaw #3 is much smaller than the critical subsurface flaw size of 0.29" from Reference 5.17. Therefore, it is not considered explicitly in the FEA analyses and is considered bounded by the other modeled flaws which are very conservative.

Figure 7 shows the first bounding flaw set considered for the OTCP in the ANSYS collapse analyses.

3.2.1.2 Case 2

The discussion above and the flaw locations shown in Figure 5 through Figure 7 are based primarily on the tabulated flaw data from Reference 5.1. Since OTCP Flaw #2 is intermittent around the circumference of the weld, a closer inspection of the PAUT scan images is performed, and an additional flaw set for the OTCP is created. In this additional case, the location of OTCP Flaw #2 is based on the PAUT scan image of the flaw at the circumferential position of OTCP Flaw #14, which is the only additional flaw that could be considered to interact with OTCP Flaw #2. Based on the PAUT scan images, the flaws are located as seen in Figure 8. In this case the height of both Flaw #2 and Flaw #7 are estimated based on the PAUT scan images and are conservatively larger than the flaw heights tabulated in Reference 5.1.

3.2.2 Inner Top Cover Plate

Figure 9 shows all of the ITCP weld flaws from Reference 5.1 plotted on an outline of the DSC geometry. All but two of the flaws are clustered in the region of the weld root at the inner surface of the DSC shell. Figure 10 shows the bounding flaw set considered for the ITCP in the ANSYS collapse analyses. Both the representative group flaw and ITCP Flaw #7 are considered to be full circumferential flaws. ITCP Flaw #11 is remote from all other flaws (in the circumferential direction) and is therefore considered bounded by the representative group flaw. The representative group flaw for the ITCP is conservatively placed at the tension side of the weld when resisting internal pressure.

All of the ITCP flaws documented in Reference 5.1 were reviewed to ensure that no two (or more) flaws, which are in close proximity to each other, could be considered as combined and therefore creating a more critical flaw. The following cases are considered in particular:

- ITCP Flaw #2 and Flaw #3 are within 0.12" from each other in the circumferential position, but their maximum combined height (1.58-1.49 = 0.09") is bounded by the group flaw height of 0.09".

- ITCP Flaw #5 and Flaw #8 partially overlaps with Flaw #6 in the circumferential direction and would have a combined height of 0.15". However, Flaw #5 (0.15" in length) and Flaw #8 (0.14" in length) are extremely small. Due to their overlap in the circumferential direction, their combined length would be only 0.16", and therefore would not affect the global or local stability of the weld. This very short region with a potential 0.15" high flaw is bounded by the full-circumferential representation of the modeled flaws.

- ITCP Flaw #10 is within 0.04" of Flaw #12 in the circumferential direction. The individual flaws are 0.05" tall and 0.04" tall, respectively, and 0.49" long and 0.18" long, respectively. They are also separated in the axial direction by 0.09". Postulating a flaw from the bottom of Flaw #12 to the top of Flaw #10 would imply a height of 0.18". However, the combined-height region would be over a very short length and would not affect the global or local stability of the weld. Therefore this postulated combined flaw is considered bounded by the full-circumferential representation of the modeled flaws.

It is noted that based on Figure 9 and Figure 10, ITCP Flaw #7 appears to be in the base metal of the inner top cover plate. It is likely that the flaw is actually at the fusion / heat affected region between the weld metal

and the base metal. The ANSYS models used in this calculation place the flaw at 0.81" inward from the outer surface of the DSC shell whereas the tabulated data in Reference 5.1 places the flaw at 0.80" from the outer surface. The 0.01" discrepancy is considered negligible. The exact location of the flaw is not considered critical in light of the significant margin that is available (See Section 7.0) and the generally very conservative idealization of the flaws (i.e. full circumferential).

3.3 Material Properties

The material properties for the DSC structure are taken from Reference 5.11. The properties of the two materials of construction, SA-240 Type 304 stainless steel and SA-36 carbon steel, are provided in Table 4 and Table 5, respectively. The weld metal is considered to be composed of the same properties as the base metal, as the welds are made with the non-flux GTAW method [Reference 5.14] using bare metal ER308 (stainless) filler material. The tensile strength of the ER308 electrode (80 ksi at room temperature [Ref. 5.15]) is slightly greater than the type 304 base metal (75 ksi at room temperature [Ref. 5.16]). The yield stress value of the weld metal is assumed to be equal to or greater than the base metal. Therefore, the treatment of the weld metal as being identical to the base metal is appropriate for the Section III limit load analyses and the elastic-plastic analyses performed in this calculation.

Temperatures used for material properties are discussed in Section 4.2 and are shown in Table 3.

Poisson's ratio for all modeled parts is taken as 0.29.

Weight density for SA-240 Type 304 is taken as 0.285 lb/in^3.

Weight density for SA-36 is taken as 0.284 lb/in^3.

3.4 Design Criteria

All of the applicable design basis loading conditions are considered in accordance with the requirements of ASME Section III Subsection NB [Ref. 5.7]. Section 4.1 details the methods used to perform the code [Ref. 5.7] qualifications. Section 4.2 details the selection of the bounding load cases.

The mockup used in the PAUT process development contained weld manufacturing flaws intentionally distributed in locations that would be expected with the weld process used for the DSC lid closure welds. Approximately 30% of those flaws were placed at the weld root and 27% were placed near the weld toe to demonstrate that they could be reliably detected in the presence of typical geometric responses from those regions. The flaws include incomplete root penetration, lack of fusion, and tungsten inclusions. AREVA document 54-PQ-114-001 [Ref. 5.19], Section 8.0, provides images of the UT responses for these flaws and demonstrates that the PAUT process can effectively detect these flaws. Furthermore, the qualification performed on the blind mockup provides objective evidence that detection of flaws in these regions of the weld is not a problem. The blind mockup used for qualification contained a similar percentage/number and distribution of flaws as the development mockup. Although the flaw information for the blind mockup cannot be disclosed in order to preserve the security of the mockup for future qualifications, EPRI and NRC personnel present at the demonstration have reviewed that information. In addition, uncertainties in the PAUT examination are accounted for by using a 0.8 reduction factor on the limit load and a 0.8 reduction factor on the material ductility for the elastic-plastic analyses. This factor, which is in agreement with ISG-15 [Ref. 5.20], conservatively accounts for any additional limitations in the efficacy of the PAUT examinations and also accounts for the inaccessible area around the vent and siphon block as well as the geometric reflectors at the root and near the toe of the weld.

4.0 METHODOLOGY

4.1 Analysis Method and Acceptance Criteria

The 61BTH DSC including the ITCP and OTCP welds are designed and analyzed per ASME Section III Subsection NB (the Code) [Ref. 5.7] in the Reference 5.2 calculation. The presence of the ITCP and OTCP weld flaws will cause high local stresses and complex stress fields that will render an elastic analysis (such as those performed in Reference 5.2) very difficult. Therefore, the flaws are explicitly included in the finite element models as "design features", and the applicable ASME code [Ref. 5.7] stress limits are evaluated as described below.

Primary Stress Limits

In order to satisfy the primary stress limits of Reference 5.7 paragraphs NB-3221.1, NB-3221.2, and NB-3221.3, a Limit Analysis will be performed per Paragraph NB-3228.1. The acceptance criterion is that the specified loadings not exceed two-thirds of the lower bound collapse load, as determined using an ideally plastic (non-strain hardening) material model, with the yield stress set at a value of 1.5*S_m. This criterion is used for evaluation of the Service Level A and B load cases discussed in Section 4.2.

Note that Service Level C acceptance criteria are generally 20% greater than Service Level A criteria, per Paragraph NB-3224 of Reference 5.7. This information is used in the discussion in Section 4.2 to eliminate some non-critical load cases.

For the Service Level D loadings (accident level internal pressure and side drop), the rules of ASME Section III Appendix F Paragraph F-1341.3 [Ref. 5.9] are used, which indicate that the loads "shall not exceed 90% of the limit analysis collapse load using a yield stress which is the lesser of 2.3S_m and 0.7S_u." This criterion is used for evaluation of the Service Level D load cases discussed in Section 4.2.

An additional increase factor of 1/0.8=1.25 is applied to the required limit load collapse pressure in order to account for the weld strength reduction factor of 0.8 to account for UT sensitivity and inaccessible weld regions discussed in Section 3.4. Typically, the weld strength reduction factor is applied to the weld allowable stress during qualification. In the case of limit-load analysis, reduction of the material yield stress is applicable. The reduction in yield stress would have a direct, 1:1 correlation to the calculated lower bound collapse pressure due to the perfectly-plastic (i.e. non-strain hardening) material model. In this analysis, rather than decrease the material yield stress the required calculated collapse pressure is increased by the factor of 1.25.

Note that the Service Level D criterion is essentially 2.1 times greater than the Service Level A/B criterion, as calculated below. This information is used in the discussion in Section 4.2 to eliminate some non-critical load cases.

At a temperature of 500 °F, the limit load yield stress for SA-240 Type 304 for Service Levels A/B and D are 26.3 ksi and 40.3 ksi, respectively.

The code [Ref. 5.7] required factors against the lower bound collapse load as determined by the limit load analyses for Service Levels A/B and D are 1.5 and 1.11, respectively.

The ratio of the acceptance criteria is therefore: $\frac{(40.3\times 1.5)}{(26.3 * 1.1)} = 2.1$.
(i.e. the Service level A/B criteria are 2.1 times as severe)

Limit Load Analysis Background

ASME Section III Subsection NB provides only a basic description of the Limit Load analysis technique. A more thorough description is provided in ASME Section VIII Division 2 Paragraph 5.2.3 [Ref. 5.18]:

> *Limit-load analysis addresses the failure modes of ductile rupture and the onset of gross plastic deformation (plastic collapse)...*
>
> *Limit-Load analysis provides an alternative to elastic analysis and stress linearization and the satisfaction of primary stress limits...*
>
> *Displacements and strains indicated by a limit analysis have no physical meaning.*
>
> *Limit load analysis is based on the theory of limit analysis that defines a lower bound to the limit load of a structure as the solution of a numerical model with the following properties:*
>
> 1. *The material model is elastic-perfectly plastic with a specified yield strength.*
>
> 2. *The strain-displacement relations are those of small displacement theory.*
>
> *The limit load is the load that causes overall structural instability. This point is indicated by the inability to achieve an equilibrium solution for a small increase in load (i.e. the solution will not converge).*

Separately, in order to address questions on the potential for material rupture due to potentially high plastic strains, supplemental elastic-plastic analyses are performed in Section 10.0 (Appendix A).

Material Ductility Limits

In order to show adequate margin against material failure at regions of high localized plastic strain, elastic-plastic analyses are performed in Appendix A. The peak strain values are compared against the material minimum specified elongation limit reduced by the weld uncertainty factor of 0.8 discussed in Section 3.4.

Primary Plus Secondary Stress Limits

The Code [Ref. 5.7] also prescribes limits on primary plus secondary stresses for Service Levels A and B [Ref. 5.7 Paragraph NB-3222.2]. Secondary stresses may be developed in the DSC due to differential thermal expansion of the interconnected parts and thermal gradients within the structure. The code stress limit for primary plus secondary stress (calculated on an elastic basis) is $3S_m$. However, as shown in Ref. 5.7 Figure NB-3222-1, rules for exceeding the $3S_m$ limit are provided in Paragraph NB-3228.5, which states that "the $3S_m$ limit ... may be exceeded provided that the requirements of (a) through (f) below are met."

Requirement (a) states that "the range of primary plus secondary membrane plus bending stress intensity, excluding thermal bending stresses, shall be $\leq 3S_m$." This provision is related to the potential for "plastic strain concentrations" occurring in "localized areas of the structure", and the potential for these concentrations to affect the "fatigue behavior, ratcheting behavior, or buckling behavior of the structure" [Ref. 5.7 Paragraph NB-3228.1]. Requirements (b) through (d) are also limitations related to fatigue and thermal stress ratchet. As detailed in Section 10.5 of Reference 5.2, the DSC is exempt from fatigue analysis requirements since all of the criteria in NB-3222.4 of Reference 5.7 are satisfied. Similarly, since the DSC

thermal loads are not cyclic in nature (other than small daily and seasonal fluctuations), thermal stress ratchet is not a concern. Therefore, the $3S_m$ limit as it relates to fatigue is not applicable.

Requirement (e) requires that the component temperature be less than 800 °F for austenitic stainless steel. The maximum DSC shell temperature (entire shell including the lid region) is 611 °F (See Table 3). Therefore this requirement is satisfied.

Requirement (f) states that the material must have a specified yield stress to ultimate stress ratio of less than 0.8. For the 61BTH DSC which used SA-240 Type 304 steel, the ratio is 30/75 = 0.4. Therefore this requirement is satisfied.

Based on the discussion above (primarily the fact that cyclic conditions are not a design factor for the DSC), there is no need to consider limits on primary plus secondary stresses. Therefore, thermal stresses are not included in this analysis.

<u>Special Stress Limits</u>

In addition to the primary and primary plus secondary stress limits the Code [Ref. 5.7] also imposes Special Stress Limits as detailed in paragraph NB-3227. The applicable special stress limits are discussed below in relation to the DSC top end cover plate welds.

Bearing Loads: There are no significant bearing loads affecting the ITCP and OTCP closure welds during Service Level A, B, or C loading. During the Service Level D side drop event, bearing stress exists at the contact surface between the DSC and Transfer Cask. However, as noted in ASME Section III Appendix F [Ref. 5.9] paragraph F-1331.3, bearing stress need only be evaluated for pinned and/or bolted joints. Therefore this special stress limit is not applicable to this evaluation.

Pure Shear: Although the ITCP and OTCP closure welds are loaded in shear by internal pressure loading, the stress state is not pure shear due to the additional bending stresses. Paragraph NB-3227.2 of Reference 5.7 clarifies that this stress limit is applicable to "for example, keys, shear rings, screw threads." Therefore this special stress limit is not applicable to this evaluation.

Progressive Distortion of Nonintegral Connections: The ITCP and OTCP closure welds are integral and therefore not nonintegral connections. Furthermore, there are no sources of significant cyclic loading that would cause progressive distortion of the DSC. Therefore this special stress limit is not applicable to this evaluation.

Triaxial Stress: The purpose of the code [Ref. 5.7] limit on triaxial stress is to provide protection against failure due to uniform triaxial tension [Ref. 5.13 Chapter 4.5]. Internal pressure in the DSC and bending of the cover plates may cause tension in the weld in the radial and circumferential directions, but there is no source for tension in the axial direction. Therefore failure due to hydrostatic tension in the weld metal is not credible. Therefore this special stress limit is not applicable to this evaluation.

<u>Fracture and Flaw Extension</u>

Although linear-type flaws have been identified in the structure, the critical failure mode of the welds is plastic collapse. Under one-time loading, elastic and plastic crack extension are not a concern for the very tough type 304 stainless steel materials of the DSC shell, OTCP, and ITCP. This conclusion is supported by ASME Section XI Article C-4000 "Determination of Failure Model" [Ref. 5.10] which states that for austenitic

wrought material and non-flux welds, "plastic collapse is the controlling failure mode." Note that the 61BTH Type 1 DSC OTCP and ITCP closure welds are made with the GTAW method [Reference 5.14] which is a non-flux type of weld.

Additionally, there is no source for fatigue flaw extension. The only cyclic loads on the DSC are minor daily and seasonal temperature fluctuations. Therefore, cyclic fatigue growth of the flaws in not a credible phenomenon.

Combined with the discussions above, the limit load analysis of the DSC top cover plates and closure welds is sufficient to satisfy all of the applicable stress criteria of the Code [Ref. 5.7].

Residual Stress

Residual stress due to welding is a secondary stress and therefore is not considered in the limit load analyses performed in this calculation, as the Section III Code [Ref. 5.7] does not require it in the limit load analysis.

4.2 Load Cases

Table 1 lists the design basis load combinations for the 61BTH DSC. This calculation is concerned with all load cases beginning with the inner top cover plate weld, identified as Load FL-6 in Table 1.

The loading conditions of interest in this evaluation are internal and external pressure and inertial loads due to handling, transfer, seismic, and accidental drop conditions.

As discussed in Section 4.1, secondary (thermal) loading is not considered.

Note that the discussions below, and the analyses performed in this calculation, are based on the conservative design values for internal pressure loading, rather than the actual calculated values of internal pressure. Table 2 summarizes the conservative design values as well as the actual calculated values.

Temperatures used for the material properties for each Service Level condition are listed in Table 3 and discussed further in the paragraphs below.

Service Level A

The bounding Service Level A load combination for the DSC top end cover plates and welds is load case TR-5 which combines the hot ambient condition with internal pressure and 1g axial inertial loading. The other directions of inertial loading are not considered critical since their effects are not directly additive to the internal pressure loading, and furthermore they are bounded by the 75g side drop load discussed further below.

The 1g axial load will cause the DSC payload weight (fuel, basket, holddown ring, shield plug) to bear against the ITCP. The total maximum payload weight is 75,811 lbs conservatively including the weights of the ITCP and OTCP [Ref. 5.2 Section 10.2]. The equivalent uniform pressure applied to the top-end components is therefore:

$$P_{fuel,1g} = \frac{75{,}811}{\frac{\pi}{4} \times (66.25in)^2} = 22.0\,psi$$

Where the inner diameter of the DSC shell is 66.25 inches.

Therefore, the bounding Service Level A case is a uniform 10 psi internal pressure (for a Type 1 DSC) plus an additional 22.0 psi acting on the shield plug in the outward axial direction of the DSC Shell. Conservatively, this analysis considers the combined 10+22=32 psi load as a uniform internal pressure in the DSC Shell. This is very conservative since the fuel pressure load which is applied to the inner surface of the shield plug would in reality be distributed to the perimeter of the ITCP as a line load by the significant stiffness of the 7-inch thick shield plug. In other words, the approach used in this calculation maximizes the bending loads on the cover plates and therefore maximizes the loading on the closure welds.

Note that the cases with external pressure loading are discussed below.

Service Level B

The bounding Service Level B load combination for the DSC top end cover plates and welds is the combination of the hot ambient condition with the off-normal internal pressure of 20 psi (LD-6). All of the other Service Level B conditions, such as ram push/pull loads, do not affect the top end components. Therefore, the bounding Service Level B case is a uniform 20 psi internal pressure. Since the pressure loading is smaller (20 psi for SL B versus 32 psi for SL A as described above), the temperature used for SL A (500 °F) bounds the maximum SL B temperatures (416 °F), and since the same limit load acceptance criterion is used for Service Levels A and B, this case is bounded by Service Level A.

Service Level C

The bounding Service Level C load combination for the DSC top end cover plates and welds is one that bounds HSM-4 and HSM-8 which combines the hot ambient condition, normal internal pressure (20 psi), and seismic loading. However, the seismic loads are bounded by the handling loads [Ref. 5.2 Section 7.8] discussed above for Service Level A. In addition, the acceptance criteria for Level C limit load analysis is greater than Service Levels A and B. Therefore, all Service Level C conditions are bounded by the Service Level A case described above.

Note that the other Service Level C cases (such as LD-7 and UL-7) are for accident condition DSC ram push/pull loads. These loads do not affect the DSC top end components. Therefore they are not applicable to this analysis.

Note that cases with external pressure loading are discussed below.

Service Level D

Three load combinations are found to be critical for Service Level D loading of the DSC top end components, namely:

- accident level internal pressure
- corner drop
- side drop

The first load combination is bounded by HSM-5 or HSM-6 which consist of 65 psi internal pressure due to HSM blocked vent thermal conditions. This load is not combined with any other load that affects the top-end components. Therefore, the first bounding Service Level D load case considered in this analysis is 65 psi internal pressure. Note that in this condition the maximum DSC shell temperature is 611 °F and 625 °F is conservatively used in this analysis (See Table 3).

The other Service Level D conditions consist of the drop events and accident-level seismic loading. The accident seismic loads are bounded by the handling loads [Ref. 5.2 Section 7.8] discussed above for Service Level A. The end-drop load is not a credible event [see footnote 12 to Table 1] but was used in the original calculation [Ref. 5.2] to bound the corner drop event. However, that analysis produced negligible load in the top cover plate welds due to the idealized boundary conditions. As a result of an RAI by the NRC, the corner drop is considered using an alternate idealization that maximizes the load in the top cover plate welds. In this case, the 25-g corner drop load has an axial component that may be considered to load the top end cover plates with the inertia of the fuel, shield plug, hold-down ring, ITCP and OTCP. This case is evaluated in Section 6.4.

The 75g side drop load TR-10 is considered a critical load case and is evaluated in detail. Note that this load case represents 75x more load than the Service Level A 1g inertial loads. As discussed in Section 4.1, the Service Level D acceptance criterion is only 2.1 times less stringent than the Service Level A/B criterion. Therefore, evaluation of the 75g side drop case using the Service Level D criterion is bounding of the Service Level A transverse inertial loading. (Also, as discussed in Section 4.3, the boundary conditions used for the 75g side drop analysis are conservative and representative of the boundary conditions encountered for the Service Level A inertial loads and seismic loading.) The 75g side drop case also includes the off-normal internal pressure of 20 psi, as shown in Table 1.

Note that the side drop event TR-10 occurs during transfer operations which result in a maximum DSC shell temperature of 500 °F as shown in Table 3. The higher Service Level D temperature of 625 °F discussed above occurs only during DSC storage in the HSM, and therefore is not combined with the side drop loading.

External Pressure Loading

External pressure is present on the DSC in load cases DD-2 (vacuum drying, Service Level A) and HSM-9/10 (flood load, Service Level C). (The load cases with hydrostatic external pressure are due to the cask annulus being filled with water while the cask and DSC are in the vertical position. In this case the pressure load varies from zero at the top of the DSC to a maximum value at the bottom of the cask. Since the external pressure near the cover plates is essentially zero, these cases are not critical and are not considered further in this calculation.)

In load case DD-2, the external pressure is 14.7 psi (full vacuum). This pressure is bounded by the Service Level B off-normal pressure (20 psi) and therefore primary stresses in the cover plates and welds are bounded by the internal pressure load cases. Stability concerns of the DSC shell are not affected by the presence of weld flaws since they are at the end of the cask, remote from the locations at which buckling would occur. Additionally, the external pressure is resisted directly by the shield plug and the shield plug support ring, rather than by the OTCP and ITCP welds. Therefore external pressure load case DD-2 is not critical and is not considered further in this analysis.

In load case HSM-9/10, the flood load is due to a 50-foot static head of water, which is equivalent to 22 psi external pressure [Ref. 5.2 Section 7.9]. This pressure is bounded by the 32 psi internal pressure considered for Service Level A discussed above. Therefore the flood load case HSM-9/10 is bounded by the other internal pressure load cases.

Summary

The bounding load cases considered for the limit load collapse analyses are therefore:

(See Table 3 for temperature references)

(See Section 4.1 for explanation of the 1.5 and 1.11 factors for Service levels A/B and D, respectively, and also for the 0.8 factor which accounts for limitations in the weld examination and inaccessible weld regions, as discussed in Section 2.0, Assumption No. 1.

Service Level A/B: 32 psi Uniform Internal Pressure, Properties at 500 °F
(Accounts for internal pressure + inertial load of DSC contents onto Lid)
Limit load collapse pressure required to satisfy criteria: 1.5*32/0.8 = 60 psi

Service Level D-1: 65 psi Uniform Internal Pressure, Properties at 625 °F
Limit load collapse pressure required to satisfy criteria: 1.11*65/0.8 = 90.2 psi

Service Level D-2: 75g Side Drop Acceleration plus 20 psi Uniform Internal Pressure, Properties at 500°F.
Limit load collapse acceleration required to satisfy criteria: 1.11*75/0.8 = 104 g

For the elastic-plastic analyses performed in Appendix A, the same bounding load cases described above are performed in order to predict plastic strains for comparison to the material strain limits and to demonstrate adequate margin against collapse.

4.3 FEA Model Details

Several finite element models of the top half of the 61BTH DSC are constructed in ANSYS based on the Reference 5.3, 5.4, 5.5 drawings. The models fall into two basic categories: axisymmetric (2D) and half-symmetric (3D).

The axisymmetric models use ANSYS plane element type PLANE182, a 4-node axisymmetric plane element with non-linear capabilities. Each node has 2 degrees of freedom (translation in the X (radial) and Y (axial) directions). The default element options are used in the analysis. Sensitivity studies were performed to ensure that there were no adverse effects on the results due to the potential shear locking of the elements. (Sensitivity runs used KEYOPTION 1=3 to invoke the simplified enhanced strain formulation to relieve shear locking.) Additional discussion of the sensitivity analyses is provided in Section 6.0.

Contact between the ITCP and OTCP is simulated using nodal coupling in the Y (axial) direction. (See Section 6.1.2 for a sensitivity study using contact elements at this interface.)

No contact is defined between the opposing faces of the weld flaws. In other words, whereas compressive loading normal to the plane of the flaw may in reality be transmitted via compression through the crack face surfaces, this load path is ignored. This is conservative, and considered necessary since it is difficult (or impossible) to deduce from the PAUT data what separation may exist between the two faces of the flaws.

Also, no contact is considered between the DSC shell inner diameter and the ITCP and OTCP outer diameters. As seen in Figure 4, the fabricated dimensions of the lids and shell result in small radial gaps between the outer diameter of the lids and the inner surface of the shell. During the welding process, these gaps close, but since a small remaining gap cannot be ruled out, this analysis conservatively assumes that the as-fabricated gap exists, as shown in Figure 4. Even if the lids deflect in the analysis such that the gaps would close, the resulting contact/compressive load path is conservatively neglected. This is conservative since it forces all loads in the lid to travel through the weld, rather than through compression between the lids and shell.

Figure 11 and Figure 12 show images of the axisymmetric model. Loading and boundary conditions are discussed in the following sections. These sections are focused on the limit load analyses. See Appendix A for discussion of the elastic-plastic analyses.

The 3D, half-symmetric model uses ANSYS solid element type SOLID185, an 8-node brick (or 6-node prism) element with non-linear capabilities. Each node has 3 degrees of freedom (translation in the X, Y, and Z directions). The default element options are used in the analysis. Sensitivity studies were performed to ensure that the mesh was adequate. Additional discussion of the sensitivity analyses is provided in Section 6.0.

Contact in the half-symmetry model is defined using ANSYS element types CONT173 and TARGE170. Contact is defined between the following interfaces:

- OTCP to ITCP
- ITCP to Shield Plug
- Shield Plug outer diameter to DSC Shell
- Shield Plug bottom surface to Support Ring
- Support Ring to DSC Shell

The default contact parameters are used, although the contact stiffness is reduced in some cases to aid in convergence. Due to the large contact areas and since the contact areas are generally remote from the critical stress regions, the contact stiffness is not considered a critical parameter. The default contact parameters include: [Reference 5.6]

- Penetration tolerance factor: Default value = 0.1. This parameter controls the acceptable level of penetration of the contact node into the target surface, based on the depth of the element underlying the target element.
- Pinball region scale factor: Default Value = 1.0. This parameter controls the extents of the region around each contact node that is checked for contact with target segments. The default volume is a sphere of radius 4*depth of the underlying element.
- KeyOption 2: Contact algorithm: Default = Augmented Lagrangian. The contact method is an iterative penalty method where the contact pressure is augmented during the equilibrium iterations so that the final penetration is within the acceptable tolerance.
- KeyOption 4: Location of contact detection point: Default = On Gauss Point. Other options include using the nodal points, normal to either the contact surface or the target surface. The default option is suggested for general cases.

Other features and controls of the CONTA173 elements are related to advanced features (bonded contact, cohesion, etc.) and initial penetration and gap controls which are not utilized in this analysis.

Figure 19 through Figure 21 show images of the half-symmetry model. Loading and boundary conditions are discussed in the following sections.

Table 6 shows a summary of the ANSYS models and analyses which are performed. Further details on the various ANSYS models are provided below.

4.3.1 Axisymmetric Case #1

The first case considered is a combination of OTCP Flaw Set #1 and the ITCP bounding flaw set discussed in Sections 3.2.1.1 and 3.2.2, respectively. The mesh and flaw details for this case, called Axisymmetric Case #1, are shown in Figure 13 and Figure 14.

The mesh shown in these figures was created based on a basic goal of having at least 4 elements across the thickness of the net sections of the weld, as reduced by the flaws. In order to investigate the effects of mesh density, a refined mesh was created for this case, as shown in Figure 15. Since the sensitivity model shown in Figure 15 only refined the weld region an additional model was created as shown in Figure 16 to ensure a sufficient mesh in the lid interior region.

This model, and all of the other axisymmetric models discussed below, are used for analysis of uniform internal pressure loading. The model is constrained in the radial direction at the axis of symmetry and in the axial direction at the bottom cut of the DSC shell near the mid-length of the cask (remote from the top end components of interest.) The pressure loading is applied to the internal pressure boundary (bottom surface of ITCP, surface of ITCP weld to Shell, and Shell inner surface). (See Section 6.1.2 for a sensitivity analysis where internal pressure is included on the ITCP weld root flaw internal surfaces.)

4.3.2 Axisymmetric Case #2

The second case considered is a combination of OTCP Flaw Set #2 and the ITCP bounding flaw set discussed in Sections 3.2.1.2 and 3.2.2, respectively. The mesh and flaw details for this case, called Axisymmetric Case #2, are shown in Figure 17 and Figure 18 for the refined mesh. Based on the results of the Axisymmetric Case #1 (See Section 6.1.2), the initial mesh level described above for Case #1 would be sufficient. However, since the run times remained reasonable, a refined mesh model (weld and lid interior regions) was generated and is used for Case #2.

4.3.3 Axisymmetric Case #0

In order to study the effect of the flaws, a 3rd case is considered in which the flaws are removed and the as-designed collapse load is determined. Only the refined mesh model (weld and lid interior regions) is considered. The mesh is identical to Figure 16 but the coincident nodes along the crack faces are merged.

4.3.4 Half-Symmetry (3D) Case #1

The 3D model is based on the Axisymmetric Case #1. (Analysis results showed that there was negligible difference in the results from Axisymmetric Case #1 and Case #2. The total projected cross-sectional area of the flaws in Case #1 is greater than Case #2. Therefore, Case #1 is considered critical for the side drop loading).

The same flaw pattern is modeled, but the initial mesh is slightly less refined in order to obtain reasonable run times. Mesh sensitivity studies are described below. The half-symmetry model is used for internal pressure loading (as a benchmark case to study the effects of mesh refinement) and also for side-drop loading.

The shield plug support ring is connected to the DSC shell at the two corners using nodal DOF couples to represent the fillet welds used to join the two parts.

In order to improve the numerical stability of the ANSYS model, soft springs (COMBIN14) elements are used to connect the shield plug to the support ring. The springs have a stiffness of 1 lb/in. The low stiffness combined with the very small relative deflections between these parts results in negligible internal force in the springs. The forces in the springs at the final converged solution are reviewed to confirm that the spring forces are small.

In all load cases, symmetry conditions are applied to the cut face of the model. Axial constraints are applied at the bottom cut of the DSC shell near the mid-length of the cask (remote from the top end components of interest.) For the internal pressure load case, the model was further reduced to a 90-degree model and symmetry constraints were placed on both cut faces of the model.

The purpose of this calculation is to evaluate the effects of the closure weld flaws and qualify the welds and any other components affected by the welds. All other aspects of the DSC (such as the shell remote from the welds) are not in the scope of this calculation. The modeling approach (loads and boundary conditions) for the side drop event are considered in light of this purpose and are described in the following paragraphs.

For the side drop cases, the OD of the canister shell is constrained in the vertical (drop) direction for a small sector (approximately 1.5" inches or 2.8 degrees) of assumed contact. In reality the DSC is supported inside the Transfer Cask (TC) during this event. Therefore the true boundary condition would either be a line of contact along a TC rail (which is 3" wide) or a line of contact at areas remote from the rails. As deformations increase, the area of contact would also increase. As discussed below in Section 4.4, deflections are over-estimated in a limit load analysis. Therefore, the area of contact with the TC rail or inner surface is assumed to be constant. This conservatively neglects the increase in contact area that would occur during the drop deformations. Additionally, this boundary condition is representative of the DSC storage condition inside the HSM, where the DSC rests on the 3-inch wide steel rails.

As discussed in the Reference 5.2 calculation, the DSC payload (basket and fuel) are located approximately 21.5 inches away from the ITCP and are therefore considered to have no effect on the DSC lid components. The effect of the basket and fuel loading on the DSC shell is considered in the basket design-basis calculation for side-drop loading. The basket hold-down ring is a grid-type structure that does not represent significant weight and is of sufficient strength and stiffness to be self-supporting during the side drop and not significantly affect the DSC shell and adjacent regions. Therefore, as in the Reference 5.2 calculation, the DSC payload is not considered as affecting the top-end components and the weight is applied as a pressure along a strip of elements at the impact region, beginning approximately 23" below the ITCP. Since the loads

are essentially applied directly over the supported (impact) region of the DSC shell, they have no appreciable effect on the shell deformations.

Images of the Half-Symmetry model are shown in Figure 19 to Figure 21.

In order to study the adequacy of the mesh for the half-symmetry model, an internal pressure load case was performed and compared to the results of the axisymmetric case refined mesh. This study confirms the adequacy of the mesh in the cross-section of the 3D model. In order to evaluate the mesh in the circumferential direction, a model was created with a refined mesh in the regions of the model showing large plastic strains (the impact region) and locations where tensile stress is expected in the weld (at the 90-degree location where the lid resists ovalization of the DSC shell). This model is shown Figure 22.

4.3.5 Half-Symmetry (3D) Case #0

In order to study the effect of the flaws, an additional case is considered in which the flaws are removed from the model and the as-designed side drop limit load capacity is determined.

4.4 Limit Load Solution Details

As discussed in Section 4.1, this calculation is based on predicting the lower-bound collapse loads of the DSC based on limit load analysis. All materials are modeled as elastic-perfectly plastic[1], with yield stress values based on the limit load analysis requirements of the ASME code [Ref. 5.7]. Table 3 lists the temperatures used for each load case, and the values of the material properties are shown in Table 4 and Table 5.

The prescribed loads are applied to the model, and then are increased linearly until the solution fails to converge.

The analyses use small deflection theory (NLGEOM,OFF). This is conservative since deflections are unrealistically high in a limit load analysis due to the lower-bound non-strain-hardening material properties that are used. If large deflections were to be considered, the beneficial effects of OTCP and ITCP membrane action and of increased contact areas would be over-estimated, resulting in non-conservative effects. This was verified with a sensitivity study using NLGEOM,ON, which resulted in much higher collapse pressures. This confirmed that using NLGEOM,OFF is appropriate, and conservative.

In addition, Paragraph 5.2.3.1 of Reference 5.18 states that small displacement theory is to be used in a limit load analysis.

[1] "Elastic-perfectly plastic is standard mechanics of materials term that describes an idealized material that behaves in a linear-elastic manner up to the yield point, and thereafter is perfectly-plastic, i.e. non-strain hardening.

5.0 REFERENCES

5.1. AREVA Document No. 180-9236022-000. NDE Services Final Report. "Monticello, DSC-16, Phased Array UT Examination Results of the Inner and Outer Top Cover Lid Welds." Revision 0.

5.2. AREVA (Transnuclear) Calculation No. NUH61BTH-0200 Revision 0. "NUHOMS-61BTH Type 1 Dry Shielded Canister Shell Assembly Structural Analysis."

5.3. AREVA (Transnuclear) Drawing No. NUH61BTH-3000 Revision 8. "NUHOMS 61BTH Type 1 DSC Main Assembly."

5.4. AREVA (Transnuclear) Drawing No. NUH61BTH-3001 Revision 4. "NUHOMS 61BTH Type 1 DSC Shell Assembly."

5.5. AREVA (Transnuclear) Drawing No. NUH61BTH-4008 Revision 1. "NUHOMS 61BTH Type 1 & 2 Transportable Canister for BWR Fuel Field Welding."

5.6. ANSYS Version 14.0. ANSYS Inc. (Including the ANSYS Mechanical APDL Documentation).

5.7. ASME Boiler and Pressure Vessel Code, Section III Subsection NB. 1998 Edition with Addenda through 2000.

5.8. AREVA (Transnuclear) Document Number NUH-003 Revision 14. "Updated Final Safety Analysis Report for the Standardized NUHOMS Horizontal Modular Storage System for Irradiated Nuclear Fuel."

5.9. ASME Boiler and Pressure Vessel Code, Section III Appendices. 1998 Edition with Addenda through 2000.

5.10. ASME Boiler and Pressure Vessel Code, Section XI. Rules for Inservice Inspection of Nuclear Power Plant Components. 1998 Edition with Addenda through 2000.

5.11. AREVA (Transnuclear) Document No. NUH61BTH1-0101 Revision 2. "Design Criteria Specification for the NUHOMS-61BTH Transportable Storage Canister."

5.12. AREVA Calculation No. 11042-0204 Revision 3. "Allowable Flaw Size Evaluation in the Inner Top Cover Plate Closure Weld for DSC #16"

5.13. Chattopadhyay, Somnath. "Pressure Vessels Design and Practice." CRC Press. 2004.

5.14. TriVis Incorporated Welding Procedure Specification No. SS-8-M-TN Revision 10.

5.15. ASME Boiler and Pressure Vessel Code, Section II, Part C. "Specifications for Welding Rods, Electrodes, and Filler Metals." 1998 Edition with Addenda through 2000.

5.16. ASME Boiler and Pressure Vessel Code, Section II, Part D. "Properties." 1998 Edition with Addenda through 2000.

5.17. AREVA (Transnuclear) Calculation No. NUH61BTH-0253 Revision 0. "NUHOMS 61BTH Type 1 DSC Shell Assembly Outer Top Cover Plate Critical Flaw Size of Weld."

5.18. ASME Boiler and Pressure Vessel Code, Section VIII Division 2. 2010.

5.19. AREVA Document No. 54-PQ-114-001 Revision 0. "Phased Array Ultrasonic Examination of Dry Storage Canister Lid Welds."

5.20. NRC Spent Fuel Project Office Interim Staff Guidance -15. Materials Evaluation. (ISG-15). 1/10/2001.

6.0 ANALYSIS

Table 6 shows a summary of the results of all of the limit load analyses performed for this calculation and includes a comparison of the results with the acceptance criteria. Each limit load analysis case is discussed in more detail below.

6.1 Axisymmetric Analyses for Internal Pressure

6.1.1 Axisymmetric Case #1 – Initial Mesh Model

Two analyses are performed with the Axisymmetric Case #1 initial-mesh model described in Section 4.3.1: one case using the Service Level A/B material properties and one case using the Service Level D material properties. The collapse pressures were determined to be 95.9 psi for Service Level A/B and 136.6 psi for Service Level D. Figure 23 shows various plots of the plastic strain in the initial-mesh model for Service Level A/B at various locations and levels of loading. These strain plots are also representative of the behavior of the Service Level D analysis. Figure 24 shows the deflection history at the center of the lid, and indicates the expected plastic instability that occurs as the limit load is approached. Note that both the strains and displacements presented in these figures have no physical meaning and the displacement plots show only the loading (pressure) at which the solution fails to converge.

Since the initial mesh contains several element divisions at each critical cross-section, it is not expected that element shear locking (due to the default fully-integrated elements) will be significant. To confirm this, a test case was done using the Service Level A/B model but with the Simplified Enhanced Strain element formulation (KEYOP 1=3). The collapse pressure was found to be 96.1 psi, which is essentially identical to the initial results.

6.1.2 Axisymmetric Case #1 – Refined Mesh Models

Additional analyses are performed using the Service Level A/B material properties with the refined mesh models described in Section 4.3.1. Figure 25 and Figure 26 show the plastic strain results for the refined mesh at the weld region and the refined mesh at the weld and lid interior regions, respectively. The collapse pressures were found to be 94.8 psi and 93.8 psi, respectively, for these models. The OTCP deflection histories are shown in Figure 27. Note that both the strains and displacements presented in these figures have no physical meaning and the displacement plots show only the loading (pressure) at which the solution fails to converge.

Figure 28 shows a comparison of the maximum displacement history curves for the various Axisymmetric Case #1 models, done as part of the mesh sensitivity study. As seen in the figure, the results match very well. The results of the refined mesh models deviate at most (95.9-93.8)/93.8 = 2.2% from the initial mesh results. This is very close agreement particularly due to the non-linear nature of the analysis. Therefore, the initial mesh is considered sufficient. However since the analysis run times for the axisymmetric cases are reasonable even for the refined mesh model, the remaining axisymmetric cases use a refined mesh.

The Axisymmetric Case #1 with refined weld and lids for Service Level D criteria reported a collapse pressure of 132.6 psi.

Note that the nodal coupling in the axial direction between the ITCP and OTCP is a valid method to model the contact between the plates since the internal pressure loading ensures that the ITCP lid will bear against

the OTCP, and since the nodes that are coupled remain coincident throughout the analysis, with only very minor differences in radial position occurring at the later load steps. In order to confirm the behavior of the nodal coupling, the Axisymmetric Case #1 model with refined welds and lids was modified to include contact between the ITCP and OTCP. The model replaces the nodal coupling with CONTA171 and TARGE169 elements, using the default element parameters. Figure 29 shows a comparison between the model using DOF couples and the model using contact elements. As seen in the figure, the results are very similar, with the DOF-couple-model showing slightly more conservative results. Therefore, the nodal coupling is acceptable and is used in all other axisymmetric models.

Note that in all of the FEA models, the internal pressure loading was not applied to the faces of the ITCP weld root flaw that is exposed to the internal region of the cask. Pressure loading on this crack face is negligible since the flaw is only 0.09" high, and in reality the ITCP flaws are generally very short (i.e. not full-circumferential flaws). In order to support this conclusion, a sensitivity analysis is performed where the pressure loading is applied to the ITCP weld root crack faces. The results, shown in Figure 30, confirm that pressure loading on the faces of this flaw are negligible.

6.1.3 Axisymmetric Case #2

Two analyses are performed with the Axisymmetric Case #2 refined-mesh model described in Section 4.3.2: one case using the Service Level A/B material properties and one case using the Service Level D material properties. The collapse pressures were determined to be 93.7 psi for Service Level A/B and 132.9 psi for Service Level D. Figure 31 shows various plots of the plastic strain for Service Level A/B at various locations and levels of loading. These strain plots are also representative of the behavior of the Service Level D analysis. Note that both the strains and displacements presented in these figures have no physical meaning and the displacement plots show only the loading (pressure) at which the solution fails to converge.

6.1.4 Axisymmetric Case #0

One analysis is performed with the Axisymmetric Case #0 refined-mesh model described in Section 4.3.3 using the Service Level A/B material properties. The collapse pressures were determined to be 94.5 psi for Service Level A/B. Figure 32 shows various plots of the plastic strain at various locations and levels of loading. Note that both the strains and displacements presented in these figures have no physical meaning and the displacement plots show only the loading (pressure) at which the solution fails to converge.

Figure 33 shows a comparison of the maximum center-of-lid displacement history for all three axisymmetric cases. As seen in the figure, there is essential no difference between Axisymmetric Case #0, Case #1 and Case #2. The Case #1 and Case #2 analyses show slightly larger deflections early in the analysis due to the slightly reduced rotational fixity of the welds. However, the final collapse pressure are within (94.5-93.7)/93.7=0.9% of each other. This supports a supposition that the observed flaws have negligible impact on the governing failure mode of the top end closure plates and welds. Again, displacements from the limit load analyses have no physical meaning, other than to show the onset of non-convergence of the FE model.

6.2 Half Symmetry Analyses for Internal Pressure (Benchmark Cases)

The model described in Section 4.3.4 is used for an internal pressure collapse analysis in order to benchmark the model against the axisymmetric cases. The collapse pressure was calculated to be approximately 97 psi. (The run was terminated at 95 psi and the final collapse pressure was estimated to avoid excessive computer run time). Figure 34 shows various plots of the plastic strain at various locations and levels of loading. A comparison of the half-symmetry case to the refined-mesh axisymmetric case is shown in Figure 35. As seen in the figure, the half-symmetry case closely matches the behavior of the refined mesh axisymmetric model although the results indicate a slightly greater collapse pressure. Therefore, the half-symmetry model is considered sufficiently accurate for this analysis. As shown by the results, and as discussed in Section 7.0, there is significant safety margin available such that further mesh refinement of the half-symmetry model is not warranted. However, the effects of circumferential mesh density for the half-symmetry model can be seen in Section 6.3.1.

6.3 Half Symmetry Analyses for Side Drop Loading

6.3.1 Half-Symmetry Case #1

The model described in Section 4.3.4 is used to perform two side-drop limit load analysis. One case includes side-drop acceleration loading only, while the second case includes the DSC off-normal internal pressure of 20 psi. For this later case, the 20 psi internal pressure is applied simultaneously with a 75g acceleration, and then both the pressure and the acceleration are increased linearly until the collapse g-load is obtained. (For example, for collapse occurring at 181g, the internal pressure at collapse is 20*181/75 = 48.3 psi.)

Note that the side drop loading is combined with the design-basis off-normal internal pressure of 20 psi, as opposed to the internal pressure value of 32 psi used for the SL A/B cases which was the sum of the 10 psi normal pressure and an additional 22 psi to account for inertial handling/seismic loads. See Section 4.2

The collapse g-load for side-drop-only loading was found to be approximately 181g. The collapse g-load when internal pressure loading was included was found to be greater than 181g. This later run terminated at 181g, but based on the collapse behavior (see Figure 41) it is expected that smaller time steps would allow the solution to continue to larger loads.

Various images of the stress and strain in the side drop analyses are shown in Figure 36 to Figure 38. Note that both the strains and displacements presented in these figures have no physical meaning and the displacement plots show only the loading (pressure) at which the solution fails to converge.

The Half-Symmetry Case #1 model with refined mesh in the circumferential direction was used to evaluate the side drop load case (without internal pressure). This analysis was performed up until a load of 185 g's, at which time the analysis was terminated manually to avoid large file sizes and excessive run time. As seen in Figure 41, this model showed a greater resistance to the side-drop loading, and would eventually result in collapse g-loads in excess of 185 g if smaller timesteps and longer run times were provided. Images of the stress and strain from this analysis are shown in Figure 39. Note that both the strains and displacements presented in these figures have no physical meaning and the displacement plots show only the loading (pressure) at which the solution fails to converge.

This analysis confirms that the mesh used in the other half-symmetry cases is adequate, and conservative.

6.3.2 Half-Symmetry Case #0

One side drop analysis is performed with the Half-Symmetry Case #0 model (no flaws) described in Section 4.3.5. Based on the results discussed above, only the case without internal pressure loading was considered. This analysis resulted in a collapse load of 189g. Stress and strain plots from this analysis are shown in Figure 40. As noted previously, these strain plots have no physical meaning. As shown in Figure 41, the collapse behavior was nearly identical to the case with weld flaws, indicating that the flaws had negligible effect on the results.

6.4 Evaluation of the 25g Corner Drop

Reference 5.2 Section 10.2 evaluated the OTCP weld to resist a 25g inertial load on the entire DSC contents and neglecting the strength of the ITCP weld. Furthermore, a conservative stress was assumed in the weld due to internal pressure. The Reference 5.2 calculation is revised below to account for the strength of both welds and include a reduction in the weld thickness due to the observed flaws. The total weld thickness is taken as the combined weld throats from the ITCP and OTCP minus the height of the flaws present in the welds. (See Reference 5.2 Section 10.2 for the basis of the following values and calculations.)

Note that the allowable weld stress noted below includes a joint efficiency factor of 0.7 as described in Reference 5.2 Section 6.2. This reduction factor conservatively bounds the reduction factor of 0.8 discussed in Section 3.4. Therefore, no further reduction factor is applied, and the calculation below is conservative.

$W_{TOT} = 75{,}811 lbs$ $\quad$ $(total\ weight\ of\ fuel + basket + lids\ and\ shield\ plug)$

$W_P = 68{,}943\ lbs$ $\quad$ $(load\ due\ to\ axial\ component\ of\ pressure)$

$W_{TOT25g} = 25 \times 75{,}811 + 68{,}943 = 1{,}964{,}218\ lbs$

$w_{25g} = \frac{W_{TOT25g}}{L_{weld}} = \frac{1{,}964{,}218}{208.131} = 9{,}437 \frac{lb}{in}$ $\quad$ $(length\ of\ weld\ is\ 208.131")$

$t_{weld} = \frac{3}{16} + \frac{1}{2} - (0.23 + 0.11) = 0.3475\ in$ $(*\ See\ Note)$

$\tau_{25g} = \frac{w_{25g}}{t_{weld}} = \frac{9{,}437}{0.3475} = 27{,}157\ psi$ $\quad$ $(weld\ shear\ stress\ due\ to\ 25g\ corner\ drop)$

$\tau_{20psi} = 4{,}120\ psi$ $\quad$ $(weld\ stress\ radial\ component\ due\ to\ 20\ psi\ internal\ pressure)$

$\tau_{TOT} = \tau_{25g} + \tau_{20psi} = 27{,}157 + 4{,}120 = 31{,}277\ psi$

$\tau_{Allow} = 32{,}400\ psi$

$$\frac{\tau_{TOT}}{\tau_{Allow}} = \frac{31{,}277}{32{,}400} = 0.97 \leq 1\ (OK)$$

*Note: the reduction of the weld to account for the flaws is based on the maximum flaw heights in any one plane through each of the welds. This is taken as 0.23" for the OTCP weld and 0.11" for the ITCP weld.)

Therefore, the top end closure welds, with the observed flaws, are OK for the Service Level D corner drop event.

7.0 DISCUSSION AND CONCLUSIONS

This calculation qualifies the as-welded DSC-16 canister using a combination of limit load analyses and elastic-plastic analyses. The limit load analyses are used to show that the DSC satisfies the primary stress limits of ASME Section III Subsection NB. The elastic-plastic analyses are used to show that the actual predicted strain values are below the material ductility limits and that adequate design margin above and beyond the specified loading exists. Both the limit load and elastic-plastic analyses account for any remaining uncertainty in the weld (e.g. non-inspected weld regions and PAUT technique limitations) by including an uncertainty factor of 0.8 which is described in detail in Section 3.4.

Limit Load Analyses:

The lower bound collapse pressure for Service Level A/B criteria was found to be 93.7 psi which is greater than the required pressure of 1.5x32/0.8=60 psi (where 1.5 is the code-required [Ref. 5.7] factor on the 32 psi design pressure loading and 0.8 is the weld strength reduction factor- see Section 4.2). Therefore the Service Level A/B criteria is satisfied.

The lower bound collapse pressure for Service Level D criteria was found to be 132.6 psi which is greater than the required pressure of 1.11x65/0.8=90.2 psi (where 1.11 is the code-required [Ref. 5.7] factor on the 65 psi design pressure loading and 0.8 is the weld strength reduction factor - see Section 4.2). Therefore the Service Level D criteria for internal pressure is satisfied.

As noted in Section 6.1.4 and as shown in Figure 33, there is essentially no difference in the collapse pressure and extremely little difference in the overall collapse behavior of the DSC subjected to internal pressure loading with and without flaws in the weld.

The lower bound collapse acceleration for side drop (Service Level D) loading was found to be 181g which is greater than the required load of 1.11x75/0.8=104g. Therefore the Service Level D criteria for side drop loading is satisfied.

As noted in Section 6.3.2 and as shown in Figure 41, there is essentially no difference in the collapse load and behavior between the as-designed DSC and the DSC with closure weld flaws.

Elastic-Plastic Analyses:

Table 7 lists the peak strains predicted by the elastic-plastic analyses for the bounding Service Level D load cases performed in Appendix A. As shown in the table, the peak strain values remain below the material ductility limits at the specified loading conditions, and also at 1.5x the specified loads. The ductility limit conservatively includes a reduction factor of 0.8 to account for weld uncertainties as discussed in Section 3.4.

The Reference 5.12 and 5.17 calculations document the ITCP and OTCP closure weld critical flaw sizes, respectively, based on the maximum radial stresses in the welds. The guidance and safety factors of Reference 5.10 are used in the critical flaw size analysis. The critical flaw sizes are determined to be 0.19 and 0.29 inches for surface and subsurface flaws, respectively, in the OTCP weld and 0.15 inches for surface and subsurface flaws in the ITCP weld. The largest single OTCP flaw size documented in Reference 5.1 is 0.14 inches. As discussed in Section 3.2 a very conservative maximum combined flaw height of 0.195 inches is assumed in this analysis. The largest single ITCP flaw size documented in Reference 5.1 is 0.11 inches. Therefore, the observed flaws actually are smaller than the critical flaw size limits and therefore it is not surprising that the flaws are shown to have little effect on the capacity of the structure. This analysis

shows that the quantity and close proximity of some of the flaws also has no significant adverse effects on the structural capacity of the DSC.

Even though all observed flaws in the ITCP and OTCP welds are included in the analysis models using conservative representations, an additional weld strength reduction factor of 0.8 is considered by increasing the limit load acceptance criteria by a factor of 1/0.8=1.25 times and by reducing the elastic-plastic strain limit by a factor of 0.8. The 0.8 factor, which is the same magnitude reduction factor as in ISG-15 [Ref. 5.20], conservatively accounts for any additional limitations in the efficacy of the PAUT examinations and also accounts for the inaccessible area around the vent and siphon block as well as the geometric reflectors at the root and near the toe of the weld.

Therefore it is concluded that Monticello DSC-16, remains in compliance with the ASME Section III Subsection NB [Ref. 5.7] stress limits and has adequate design margin above and beyond the specified loadings with the presence of the ITCP and OTCP closure weld flaws as documented in Reference 5.1.

8.0 LISTING OF COMPUTER FILES

Analyses performed on Computer HEA-0213A using ANSYS Version 14.0 [Ref. 5.6].

File Date & Time listing is as displayed by the Windows 7 Operating System – Differences may occur due local time zone and daylight savings settings.

Analysis Case	File Name	Date & Time
Axisymmetric 1 Initial Mesh Internal Pressure SL A/B	61BTH_WeldFlaw_1F_AX_2_DETACH.db	4/7/2015 10:45 AM
	61BTH_WeldFlaw_1F_AX_2_DETACH.rst	4/7/2015 10:45 AM
	61BTH_WeldFlaw_1F_AX_2_DETACH.mntr	4/7/2015 10:45 AM
	SOLUTION_AXISYMM_IP_LimitLoad.INP	4/7/2015 10:20 AM
Axisymmetric 1 Refined Weld Mesh Internal Pressure SL A/B	61BTH_WeldFlaw_1F_AX_2_DETACH.db	4/7/215 11:59 AM
	61BTH_WeldFlaw_1F_AX_2_DETACH.rst	4/7/215 11:58 AM
	61BTH_WeldFlaw_1F_AX_2_DETACH.mntr	4/7/215 11:59 AM
	SOLUTION_AXISYMM_IP_LimitLoad.INP	4/7/2015 11:55 AM
Axisymmetric 1 Refined Weld and Lid Mesh Internal Pressure SL A/B	61BTH_WeldFlaw_1F_AX_2_DETACH.db	4/21/2015 9:04 AM
	61BTH_WeldFlaw_1F_AX_2_DETACH.rst	4/21/2015 9:03 AM
	61BTH_WeldFlaw_1F_AX_2_DETACH.mntr	4/21/2015 9:04 AM
	SOLUTION_AXISYMM_IP_LimitLoad.INP	4/7/2015 11:55 AM
Axisymmetric 1 Initial Mesh Internal Pressure SL D	61BTH_WeldFlaw_1F_AX_2_DETACH.db	4/20/2015 10:43 AM
	61BTH_WeldFlaw_1F_AX_2_DETACH.rst	4/20/2015 11:09 AM
	61BTH_WeldFlaw_1F_AX_2_DETACH.mntr	4/20/2015 11:09 AM
	SOLUTION_AXISYMM_IP_LimitLoad_SLD.INP	4/7/2015 11:20 AM
Axisymmetric 1 Refined Weld and Lid Mesh Internal Pressure SL D	61BTH_WeldFlaw_1F_AX_2_DETACH.db	4/30/2015 8:12 AM
	61BTH_WeldFlaw_1F_AX_2_DETACH.rst	4/30/2015 8:12 AM
	61BTH_WeldFlaw_1F_AX_2_DETACH.mntr	4/30/2015 8:12 AM
	SOLUTION_AXISYMM_IP_LimitLoad_SLD.INP	4/7/2015 12:02 PM
Axisymmetric 2 Refined Weld and Lid Mesh Internal Pressure SL A/B	61BTH_WeldFlaw_2G_AX_2.db	4/21/2015 3:06 PM
	61BTH_WeldFlaw_2G_AX_2.rst	4/21/2015 2:58 PM
	61BTH_WeldFlaw_2G_AX_2.mntr	4/21/2015 3:06 PM
	SOLUTION_AXISYMM_IP_LimitLoad.INP	4/7/2015 11:55 AM
Axisymmetric 2 Refined Weld and Lid Mesh Internal Pressure SL D	61BTH_WeldFlaw_2G_AX_2.db	4/21/2015 3:10 PM
	61BTH_WeldFlaw_2G_AX_2.rst	4/21/2015 3:10 PM
	61BTH_WeldFlaw_2G_AX_2.mntr	4/21/2015 3:10 PM
	SOLUTION_AXISYMM_IP_LimitLoad_SLD.INP P	4/7/2015 12:02 PM
Axisymmetric 0 Refined Weld and Lid Mesh Internal Pressure SL A/B	61BTH_WeldFlaw_1F_AX_2_DETACH.db	4/21/2015 10:39 AM
	61BTH_WeldFlaw_1F_AX_2_DETACH.rst	4/21/2015 10:31 AM
	61BTH_WeldFlaw_1F_AX_2_DETACH.mntr	4/21/2015 10:39 AM
	SOLUTION_AXISYMM_IP_LimitLoad.INP	4/15/2015 11:07 AM
Axisymmetric 1 Initial Mesh with Keyoption 1=3 Internal Pressure SL A/B	61BTH_WeldFlaw_1F_AX_2_DETACH.db	4/17/2015 5:40 PM
	61BTH_WeldFlaw_1F_AX_2_DETACH.rst	4/17/2015 5:40 PM
	61BTH_WeldFlaw_1F_AX_2_DETACH.mntr	4/17/2015 5:40 PM
	SOLUTION_AXISYMM_IP_LimitLoad.INP	4/16/2015 12:27 PM

Analysis Case	File Name	Date & Time
Axisymmetric 1 Refined Weld and Lid Mesh Internal Pressure, SL A/B ITCP/OTCP couples replaced with Contact	61BTH_WeldFlaw_1F_AX_2_DETACH.db	5/19/2015 8:45 AM
	61BTH_WeldFlaw_1F_AX_2_DETACH.rst	5/19/2015 8:02 AM
	61BTH_WeldFlaw_1F_AX_2_DETACH.mntr	5/19/2015 8:45 AM
	SOLUTION_AXISYMM_IP_LimitLoad.INP	5/18/2015 5:03 PM
Axisymmetric 1 Refined Weld and Lid Mesh Internal Pressure, SL A/B With Pressure on ITCP Weld Root Flaw Surfaces	61BTH_WeldFlaw_1F_AX_2_DETACH.db	5/18/2015 2:42 PM
	61BTH_WeldFlaw_1F_AX_2_DETACH.rst	5/18/2015 1:37 PM
	61BTH_WeldFlaw_1F_AX_2_DETACH.mntr	5/18/2015 2:42 PM
	SOLUTION_AXISYMM_IP_LimitLoad.INP	5/18/2015 1:25 PM
Half Symmetry 1 Initial Mesh Internal Pressure SL A/B	61BTH_WeldFlaw_1GC.db	4/29/2015 2:10 PM
	61BTH_WeldFlaw_1GC.rst	4/29/2015 4:52 PM
	61BTH_WeldFlaw_1GC.mntr	4/29/2015 4:52 PM
	SOLUTION_HALFSYM_LimitLoad.INP	4/29/2015 2:10 PM
Half Symmetry 1 Initial Mesh Side Drop SL D	61BTH_WeldFlaw_1GC.db	4/30/2015 8:20 AM
	61BTH_WeldFlaw_1GC.rst	4/30/2015 3:35 PM
	61BTH_WeldFlaw_1GC.mntr	4/30/2015 3:35 PM
	SOLUTION_HALFSYM_SD.INP	4/30/2015 8:21 AM
Half Symmetry 1 Initial Mesh Side Drop + Internal Pressure SL D	61BTH_WeldFlaw_1GC.db	5/1/2015 6:58 PM
	61BTH_WeldFlaw_1GC.rst	5/1/2015 4:29 PM
	61BTH_WeldFlaw_1GC.mntr	5/1/2015 4:13 PM
	SOLUTION_HALFSYM_SD.INP	4/30/2015 10:26 PM
Half Symmetry 1 Refined Circumferential Mesh Side Drop SL D	61BTH_WeldFlaw_1GD_Refined.db	5/6/2015 1:54 PM
	61BTH_WeldFlaw_1GD_Refined.rst	5/6/2015 11:48 AM
	61BTH_WeldFlaw_1GD_Refined.mntr	5/6/2015 11:47 AM
	SOLUTION_HALFSYM_SD.INP	5/5/2015 9:01 PM
Half Symmetry 0 Initial Mesh Side Drop SL D	61BTH_WeldFlaw_1GC.db	5/2/2015 6:53 AM
	61BTH_WeldFlaw_1GC.rst	5/2/2015 6:53 AM
	61BTH_WeldFlaw_1GC.mntr	5/2/2015 3:37 AM
	SOLUTION_HALFSYM_SD.INP	4/30/2015 8:21 AM

9.0 TABLES AND FIGURES

Table 1 – Summary of Design Basis Load Combinations for the 61BTH DSC [Ref. 5.8]

Load Case	Horizontal DW		Vertical DW		Internal Pressure[9]	External Pressure	Thermal Condition	Lifting Loads	Other Loads	Service Level
	DSC	Fuel	DSC	Fuel						
Non-Operational Load Cases										
NO-1 Fab. Leak Testing	—	—	—	—	—	14.7 psig	70°F	—	155 kip axial	Test
NO-2 Fab. Leak Testing	—	—	—	—	15/23 psig[13]	—	70°F	—	155 kip axial	Test
NO-3 DSC Uprighting	x	—	—	—	—	—	70°F	x	—	A
NO-4 DSC Vertical Lift	—	—	x	—	—	—	70°F	x	—	A
Fuel Loading Load Cases										
FL-1 DSC/Cask Filling	—	—	Cask	—	—	Hydrostatic	120°F Cask	x	x	A
FL-2 DSC/Cask Filling	—	—	Cask	—	Hydrostatic	Hydrostatic	120°F Cask	x	x	A
FL-3 DSC/Cask Xfer	—	—	Cask	—	Hydrostatic	Hydrostatic	120°F Cask	—	—	A
FL-4 Fuel Loading	—	—	Cask	x	Hydrostatic	Hydrostatic	120°F Cask	—	—	A
FL-5 Xfer to Decon	—	—	Cask	x	Hydrostatic	Hydrostatic	120°F Cask	—	—	A
FL-6 Inner Cover plate Welding	—	—	Cask	x	Hydrostatic	Hydrostatic	120°F Cask	—	—	A
FL-7 Fuel Deck Seismic Loading	—	—	Cask	x	Hydrostatic	Hydrostatic	120°F Cask	—	Note 10	C
Draining/Drying Load Cases										
DD-1 DSC Blowdown	—	—	Cask	x	Hydrostatic + 10/15 psig	Hydrostatic	120°F Cask	—	—	A
DD-2 Vacuum Drying	—	—	Cask	x	0 psia	Hydrostatic + 14 psig	120°F Cask	—	—	A
DD-3 Helium Backfill	—	—	Cask	x	12 psig	Hydrostatic	120°F Cask	—	—	A
DD-4 Final Helium Backfill	—	—	Cask	x	3.5 psig	Hydrostatic	120°F Cask	—	—	A
DD-5 Outer Cover Plate Weld	—	—	Cask	x	3.5 psig	Hydrostatic	120°F Cask	—	—	A
Transfer Trailer Loading										
TL-1 Vertical Xfer to Trailer	—	—	Cask	x	10/15 psig	—	0°F Cask	—	—	A
TL-2 Vertical Xfer to Trailer	—	—	Cask	x	10/15 psig	—	120°F Cask	—	—	A
TL-3 Laydown	Cask	X	—	—	10/15 psig	—	0°F Cask	—	—	A
TL-4 Laydown	Cask	X	—	—	10/15 psig	—	120°F Cask	—	—	A

Load Case	Horizontal DW		Vertical DW		Internal Pressure[9]	External Pressure	Thermal Condition	Lifting Loads	Other Loads	Service Level
	DSC	Fuel	DSC	Fuel						
Transfer To/From ISFSI										
TR-1 Axial Load - Cold	Cask	X	—	—	10/15 psig	—	0°F	1g Axial	—	A
TR-2 Transverse Load - Cold	Cask	X	—	—	10/15 psig	—	0°F	1g Transverse	—	A
TR-3 Vertical Load - Cold	Cask	X	—	—	10/15 psig	—	0°F	1g Vertical	—	A
TR-4 Oblique Load - Cold	Cask	X	—	—	10/15 psig	—	0°F	½ g Axial + ½ g Trans + ½ g Vert.	—	A
TR-5 Axial Load – Hot	Cask	X	—	—	10/15 psig	—	100°F	1g Axial	—	A
TR-6 Transverse Load - Hot	Cask	X	—	—	10/15 psig	—	100°F	1g Trans.	—	A
TR-7 Vertical Load - Hot	Cask	X	—	—	10/15 psig	—	100°F	1g Vertical	—	A
TR-8 Oblique Load - Hot	Cask	X	—	—	10/15 psig	—	100°F	½ g Axial + ½ g Trans + ½ g Vert.	—	A
TR-9 25g Corner Drop[12]	Note 1, 14		Note 1, 14		20 psig	—	100°F[4]		25g Corner Drop	D
TR-10 75g Side Drop[12]	Note 1		—	—	20 psig	—	100°F[4]		75g Side Drop	D
TR-11 Top or Bottom End Drops[12]			Note 1, 12		20 psig	—	100°F[4]		60g End Drop	D

Table 1 (Continued) - Summary of Design Basis Load Combinations for the 61BTH DSC [Ref. 5.8]

HSM LOADING	Horizontal DW		Vertical DW		Internal Pressure[9]	External Pressure[9]	Thermal Condition	Handling Loads	Other Loads	Service Level
	DSC	Fuel	DSC	Fuel						
LD-1 Normal Loading - Cold	Cask	X	--	--	10/15 psig	--	0°F Cask	+80 Kip	--	A
LD-2 Normal Loading –Hot	Cask	X	--	--	10/15 psig	--	100° F Cask	+80 Kip	--	A
LD-3	Cask	X	--	--	10/15 psig	--	117° F w/shade[5]	+80 Kip	--	A
LD-4 Off-Normal Loading –Cold	Cask	X	--	--	20 psig	--	0° F Cask	+80 Kip	FF	B
LD-5 Off-Normal Loading - Hot	Cask	X	--	--	20 psig	--	100° F Cask[5]	+80 Kip	FF	B
LD-6	Cask	X	--	--	20 psig	--	117° F w/shade[5]	+80 Kip	FF	B
LD-7 Accident Loading	Cask	X	--	--	20 psig	--	117° F w/shade[5]	+80 Kip	FF	C/D

HSM STORAGE	Horizontal DW		Vertical DW		Internal Pressure[9]	External Pressure[9]	Thermal Condition	Handling Loads	Other Loads	Service Level
	DSC	Fuel	DSC	Fuel						
HSM-1 Off-Normal	HSM	X	--	--	15 psig	--	-40° F HSM	--	--	B
HSM-2 Normal Storage	HSM	X	--	--	15 psig	--	0° F HSM	--	--	A
HSM-3 Off-Normal	HSM	X	--	--	15 psig	--	117° F HSM	--	--	B
HSM-4 Off-Normal Temp. + Failed Fuel	HSM	X	--	--	20 psig	--	117° F HSM	--	FF	C
HSM-5 Blocked Vent Storage	HSM	X	--	--	65/120 psig	--	117° F HSM/BV[2][4]	--	--	D
HSM-6 B.V. + Failed Fuel Storage	HSM	X	--	--	65/120 psig	--	117° F HSM/BV[2][4]	--	FF	D
HSM-7 Earthquake Loading –Cold	HSM	X	--	--	10/15 psig	--	0° F HSM	--	EQ	C/D[12]
HSM-8 Earthquake Loading –Hot	HSM	X	--	--	10/15 psig	--	100°F HSM	--	EQ	C/D[12]
HSM-9 Flood Load (50' H_2O) –Cold	HSM	X	--	--	10/15 psig	22 psig	0° F HSM	--	Flood[3]	C
HSM-10 Flood Load (50' H_2O) - Hot	HSM	X	--	--	10/15 psig	22 psig	100°F HSM	--	Flood[3]	C

HSM UNLOADING	Horizontal DW		Vertical DW		Internal Pressure[9]	External Pressure[9]	Thermal Condition	Handling Loads	Other Loads	Service Level
	DSC	Fuel	DSC	Fuel						
UL-1 Normal Unloading – Cold	HSM	X	--	--	10/15 psig	--	0°F HSM	+60 Kip	--	A
UL-2 Normal Unloading –Hot	HSM	X	--	--	10/15 psig	--	100° F HSM	+60 Kip	--	A
UL-3	HSM	X	--	--	10/15 psig	--	117° F w/shade	+60 Kip	--	A
UL-4 Off-Normal Unloading –Cold	HSM	X	--	--	20 psig	--	0° F HSM	+60 Kip	FF	B
UL-5 Off-Normal Unloading – Hot	HSM	X	--	--	20 psig	--	100° F HSM	+60 Kip	FF	B
UL-6	HSM	X	--	--	20 psig	--	117° F w/shade	+60 Kip	FF	B
UL-7 Off. Norm. Unloading-FF/Hot[6,11]	HSM	X	--	--	20 psig	--	100° F HSM	+80 Kip	FF	C
UL-8 Accident Unloading –FF/Hot[7,11]	HSM	X	--	--	65/120[7] psig	--	100° F HSM	+80 Kip	FF	D
RF-1 DSC Reflood	--	--	Cask	X	20 psig (max)	Hydrostatic	120° F Cask	--	--	D

Table 1 (Concluded) – Summary of Design Basis Load Combinations for the 61BTH DSC [Ref. 5.8]

(Notes for the preceding portions of Table 1)

1. 25g and 75g drop acceleration includes gravity effects. Therefore, it is not necessary to add an additional 1.0g load.
2. For Level D events, only maximum temperature case is considered. (Thermal stresses are not limited for level D events and maximum temperatures give minimum allowables).
3. Flood load is an external pressure equivalent to 50 feet of water.
4. BV = HSM vents are blocked.
5. At temperature over 100°F a sunshade is required over the Transfer Cask. Temperatures for these cases are enveloped by the 100°F (without sunshade) case.
6. As described in Section T.4, this pressure assumes release of the fuel cover gas and 30% of the fission gas. Since unloading requires the HSM door to be removed, the pressure and temperatures are based on the normal (unblocked vent) condition. Pressure is applied to the confinement boundary.
7. As described in Section T.4, this pressure assumes release of the fuel cover gas and 30% of the fission gas. Although unloading requires the HSM door to be removed, the pressure and temperatures are based on the blocked vent condition. Pressure is applied to the shell, inner bottom and inner and outer top cover plates.
8. Not used.
9. Unless noted otherwise, pressure is applied to the confinement boundary. 10 psig and 65 psig are applicable to Type 1 DSC, while 15 psig and 120 psig are applicable to Type 2 DSC.
10. Fuel deck seismic loads are assumed enveloped by handling loads.
11. Load Cases UL-7 and UL-8 envelop loading cases where the stresses due to insertion loading of 80 kips are added to stresses due to internal pressure (in reality, the insertion force is opposed by internal pressure).
12. The 60g top end drop and bottom end drop are not credible events, therefore these drop analyses are not required. However, consideration of 60g end drop and 75g side drop conservatively envelops the effect of 25g corner drop.
13. Conservatively based on normal operating pressure times 1.5 to cover future 10CFR Part 71 requirements.
14. A 25g corner drop analysis (30° from horizontal) of 61BTH DSC without support from the TC is to be documented.
15. *Service Level C is for the standard seismic event and Service Level D is for the high seismic event.*

Table 2 – Internal Pressure in the 61BTH Type 1 DSC

Design Condition	Maximum Calculated Pressure [psi]	Design Pressure used in Ref. 5.2 and This Calculation [psi]	Reference
Normal	7.3	10	Ref. 5.8 Table T.4-16
Off-Normal	10.9	20	Ref. 5.8 Table T.4-20
Accident	56.1	65	Ref. 5.8 Table T.4-24

Table 3 – Maximum Temperatures in the 61BTH Type 1 DSC Shell

Design Condition		Maximum Calculated Temperature [°F]	Design Temperature used in This Calculation [°F]	Reference
Normal	Storage	374	500	Ref. 5.8 Table T.4-13
	Transfer	439	500	
Off-Normal	Storage	399	500	Ref. 5.8 Table T.4-18
	Transfer	416	500	
Accident	Storage	611	625	Ref. 5.8 Table T.4-22
	Transfer	467	500	

Table 4 – Properties of SA-240 Type 304. [Ref. 5.11]

Temp [°F]	E Modulus of Elasticity [ksi]	S_m Allowable Stress Intensity [ksi]	S_y Yield Stress [ksi]	S_u Ultimate Tensile Strength [ksi]	Yield Stress for SL A/B Limit Load Analysis (Note 1) [ksi]	Yield Stress for SL D Limit Load Analysis (Note 2) [ksi]
70	28,300	20.0	30.0	75.0	30.0	46.0
100	28,138	20.0	30.0	75.0	30.0	46.0
200	27,600	20.0	25.0	71.0	30.0	46.0
300	27,000	20.0	22.4	66.2	30.0	46.0
400	26,500	18.7	20.7	64.0	28.1	43.0
500	25,800	17.5	19.4	63.4	26.3	40.3
600	25,300	16.4	18.4	63.4	24.6	37.7
625	25,175	16.3	18.2	63.4	24.5	37.5
700	24,800	16.0	17.6	63.4	24.0	36.8

(1) The yield strength to be used in a Limit Analysis for Service Level A and B Loading is 1.5*Sm, per Paragraph NB-3228.1 of Reference 5.7.

(2) The yield strength to be used in a Limit Analysis for Service Level D Loading is the lesser of 2.3*Sm and 0.7*Su, per Paragraph F-1341.3 of Reference 5.9.

Table 5 –Properties of SA-36. [Ref. 5.11]

Temp [°F]	E Modulus of Elasticity [ksi]	S_m Allowable Stress Intensity [ksi]	S_y Yield Stress [ksi]	S_u Ultimate Tensile Strength [ksi]	Yield Stress for SL A/B Limit Load Analysis (Note 1) [ksi]	Yield Stress for SL D Limit Load Analysis (Note 2) [ksi]
70	29,500	19.3	36.0	58.0	29.0	40.6
100	29,338	19.3	36.0	58.0	29.0	40.6
200	28,800	19.3	33.0	58.0	29.0	40.6
300	28,300	19.3	31.8	58.0	29.0	40.6
400	27,700	19.3	30.8	58.0	29.0	40.6
500	27,300	19.3	29.3	58.0	29.0	40.6
600	26,700	17.7	27.6	58.0	26.6	40.6
625(3)	26,400	17.6	27.2	58.0	26.4	40.4
700	25,500	17.3	25.8	58.0	26.0	39.8

(1) The yield strength to be used in a Limit Analysis for Service Level A and B Loading is 1.5*Sm, per Paragraph NB-3228.1 of Reference 5.7.

(2) The yield strength to be used in a Limit Analysis for Service Level D Loading is the lesser of 2.3*Sm and 0.7*Su, per Paragraph F-1341.3 of Reference 5.9.

(3) All values are interpolated from the 600 °F and 700 °F values.

Table 6 –Summary of Load Cases, Mesh Refinement Results, and NB-3228.1 Limit Load Analysis Results

Name	Mesh Level	Loading	Temp. [ºF]	Analysis Criteria	Required/ Design Pressure (Note 4) [psi]	Required Pressure to Satisfy Limit Load Criteria (Note 5) [psi]	Limit Load Collapse Pressure [psi]	Code Limit Load Criteria Satisfied?
Axisymmetric 1	Initial	Internal Pressure	500	SL A/B	32	60.0	95.9	Yes
Axisymmetric 1	Refined Welds	Internal Pressure	500	SL A/B	32	60.0	94.8	Yes
Axisymmetric 1	Refined Welds and Lid	Internal Pressure	500	SL A/B	32	60.0	93.8	Yes
Axisymmetric 1	Initial	Internal Pressure	625	SL D	65	90.2	136.6	Yes
Axisymmetric 1	Refined Welds and Lid	Internal Pressure	625	SL D	65	90.2	132.6	Yes
Axisym. 2	Refined Welds and Lid	Internal Pressure	500	SL A/B	32	60.0	93.7	Yes
Axisym. 2	Refined Welds and Lid	Internal Pressure	625	SL D	65	90.2	132.9	Yes
Axy-0 (No Flaws)	Refined Welds and Lid	Internal Pressure	500	SL A/B	32	60.0	94.5	Yes
Half-Symm 1 Benchark	Initial (Note 2)	Internal Pressure	500	SL A/B	32	60.0	97	Yes

Name	Mesh Level	Loading	Temp. [ºF]	Analysis Criteria	Required/ Design G-Load [g]	Required G-Load to Satisfy Limit Load Criteria (Note 5) [g]	Collapse G-Load [g]	Code Limit Load Criteria Satisfied?
Half Symmetry 1	Initial	Side Drop	500	SL D	75	104.0	181	Yes
Half Symmetry 1	Refined Circumferential Mesh (Note 3)	Side Drop	500	SL D	75	104.0	185	Yes
Half Symmetry 1	Initial (Note 3)	Side Drop with Off-Normal IP	500	SL D	75	104.0	181	Yes
Half-Symm-0 (No Flaws)	Initial	Side Drop	500	SL D	75	104.0	189	Yes

Notes:

1) [Not Used]

2) The 97 psi collpase load is estimated / extrapolated from the final obtained solution at 95 psi. Excessive run times make more precise results impractical.

3) The reported collapse load is conservative - based on the collapse behavior it is expected that smaller analysis time steps would yield larger collapse loads. This was deemed impractical due to the long run time and the large margin available.

4) The Service Level A/B required pressure of 32 psi is based on the design internal pressure of 10 psi plus an equivalent internal pressure of 22 psi which accounts for other Service Level A loads. See Section 4.2

5) Includes both the ASME code required factor and the 0.8 weld strength reduction factor to account for examination limitations.

Table 7 –Evaluation of Peak Strain Values at Specified Loads and at 1.5x Specified Loads from Elastic-Plastic Analyses.

Load Case	Specified Loading Internal Pressure [psi]	Peak Equivalent Plastic Strain [in/in]		Material Strain Limit (Note 1)	Margin of Safety at Specified Loading (Note 2)
		at 65 psi internal pressure	at 100 psi internal pressure		
Internal Pressure Service Level D	65	0.0597 (5.97%)	0.126 (12.6%)	0.28 (28%)	3.69
Load Case	Specified Loading Side Drop G-Load [g]	Peak Equivalent Plastic Strain [in/in]		Material Strain Limit (Note 1)	Margin of Safety at Specified Loading (Note 2)
		at 75g loading	at 112.5g loading		
Side Drop Service Level D	75	0.0609 (6.09%)	0.126 (12.6%)	0.28 (28%)	3.60

Notes:

1) The weld uncertainty factor of 0.8 (See Section 3.4) is applied to the minimum of the ASME specified minimum elongations of SA-240 Type 304 (40%) and E308-XX electrode (35%). Therefore the strain limit is taken as 0.8*0.35=0.28.

2) Margin of Safety is calculated as [(Strain Limit)/(Actual Strain)]-1

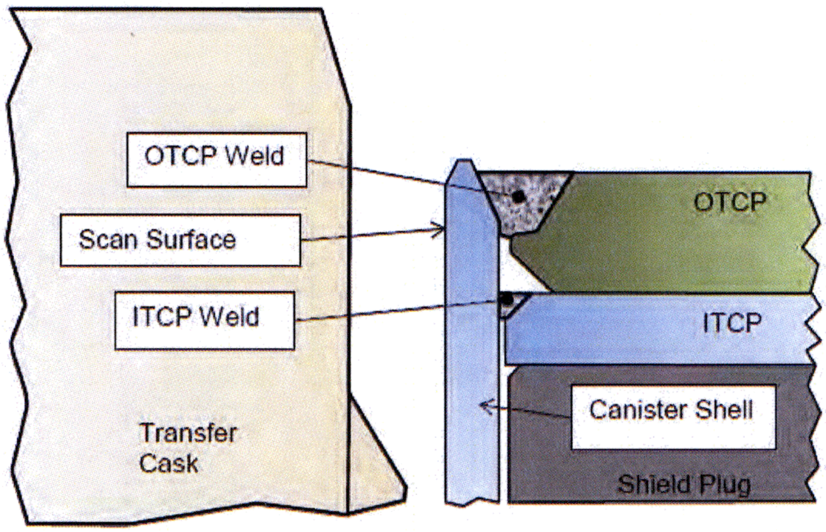

Figure 1 – Sketch of the 61BTH DSC Top End and Transfer Cask from Reference 5.1

Security-Related Information Figure Withheld Under 10 CFR 2.390.

Figure 2 – Details of the 61BTH Top End Component Interfaces

Security-Related Information Figure Withheld Under 10 CFR 2.390.

Figure 3 – ITCP and OTCP Closure Weld Details from Reference 5.5
(Note: Section B-B above is rotated 90 degrees clockwise from Figure 2.)

Security-Related Information Figure Withheld Under 10 CFR 2.390.

Figure 4 – DSC Top End Detailed Dimensions

(Note: See Section 2.0 Assumption No. 6 and Section 4.3 for discussions and justifications regarding the modeled dimensions and lid-to-shell gaps.)

Security-Related Information Figure Withheld Under 10 CFR 2.390.

Figure 6 – OTCP Flaws – Main Flaw Group Reduced and Bounded

Security-Related Information Figure Withheld Under 10 CFR 2.390.

Figure 8 – OTCP Flaws –Bounding Set #2 for ANSYS Collapse Analysis

Security-Related Information Figure Withheld Under 10 CFR 2.390.

Figure 10 – ITCP Flaws – Bounding Flaw Set for ANSYS Collapse Analysis

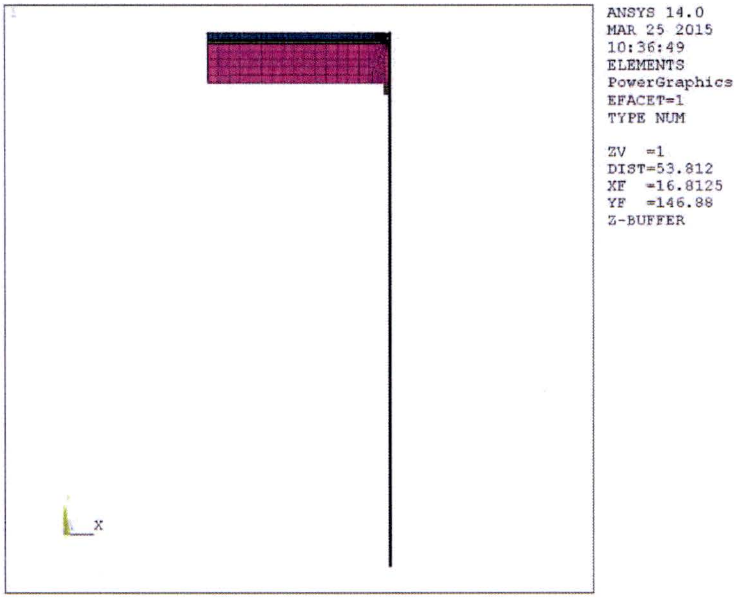

Figure 11 – Overview of the Axisymmetric Model

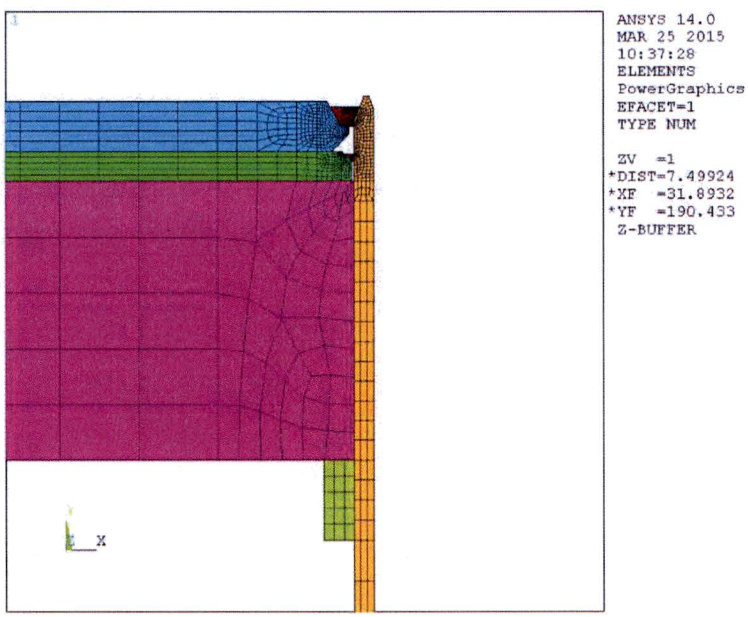

Figure 12 – Mesh Details Near the Lid Regions of the Axisymmetric Model
(Small differences in the mesh exist amongst the sub-models)

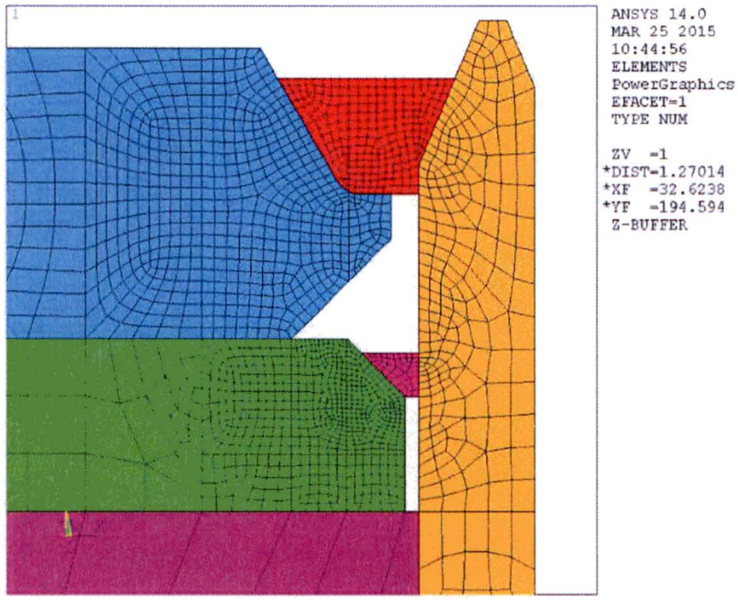

Figure 13 – Mesh Details at the Welds for Axisymmetric Case #1

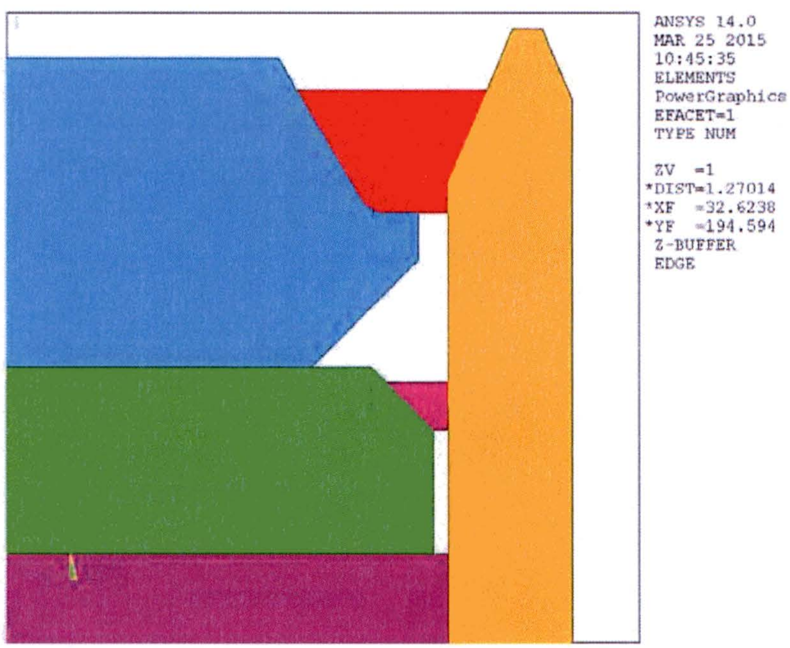

Figure 14 – Flaw Locations for Axisymmetric Case #1

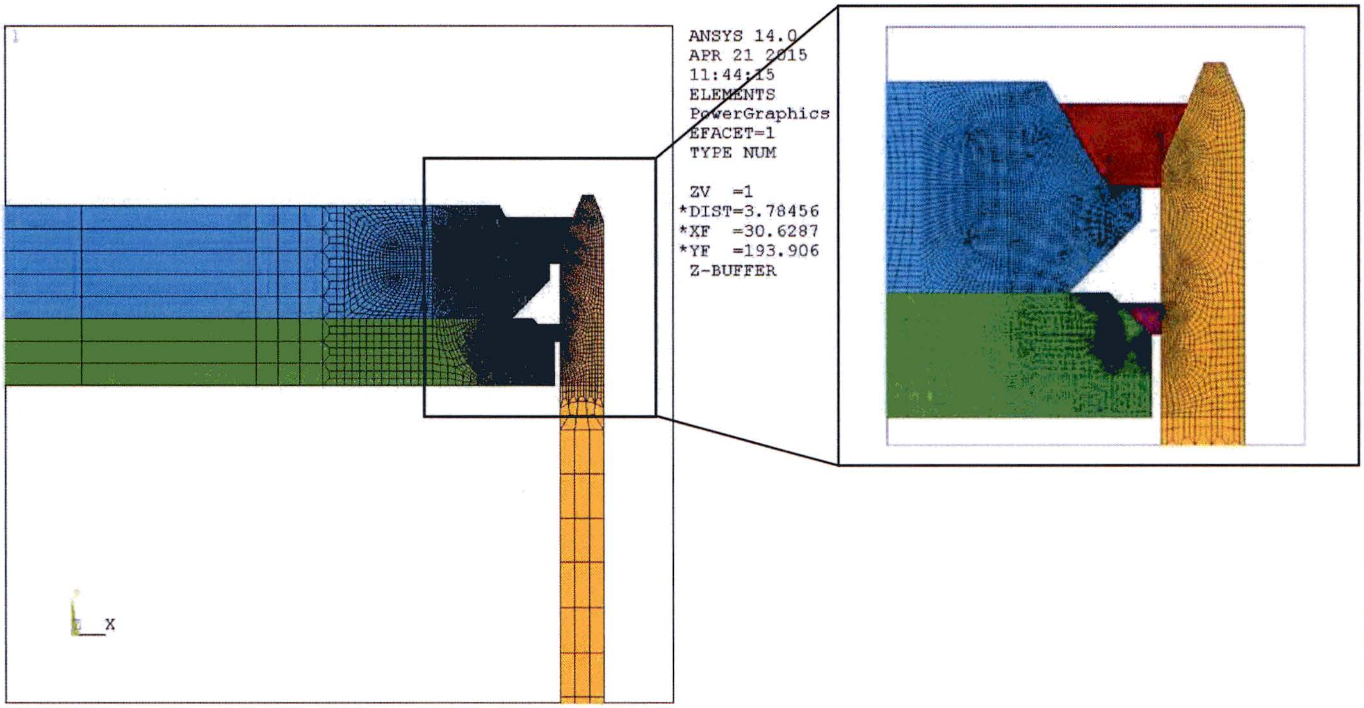

Figure 15 – Refined Mesh (Weld Region) for Axisymmetric Case #1

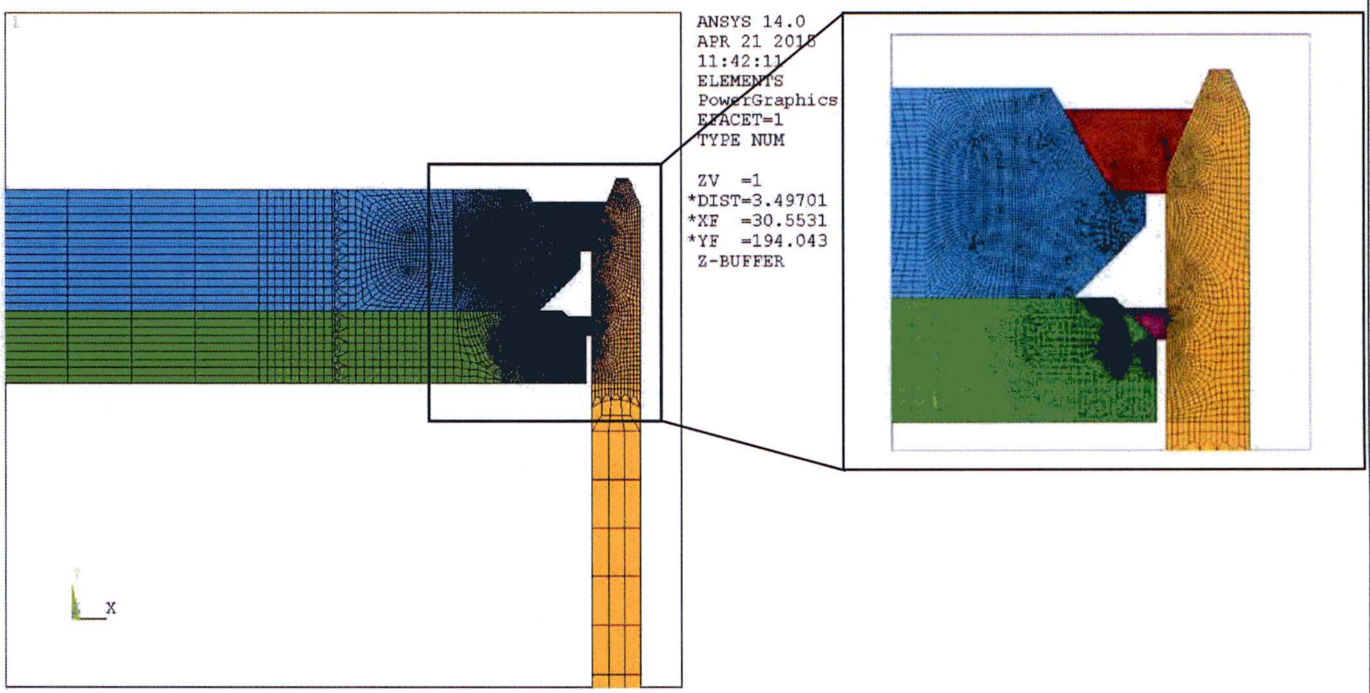

Figure 16 – Refined Mesh (Weld and Lid Interior Region) for Axisymmetric Case #1

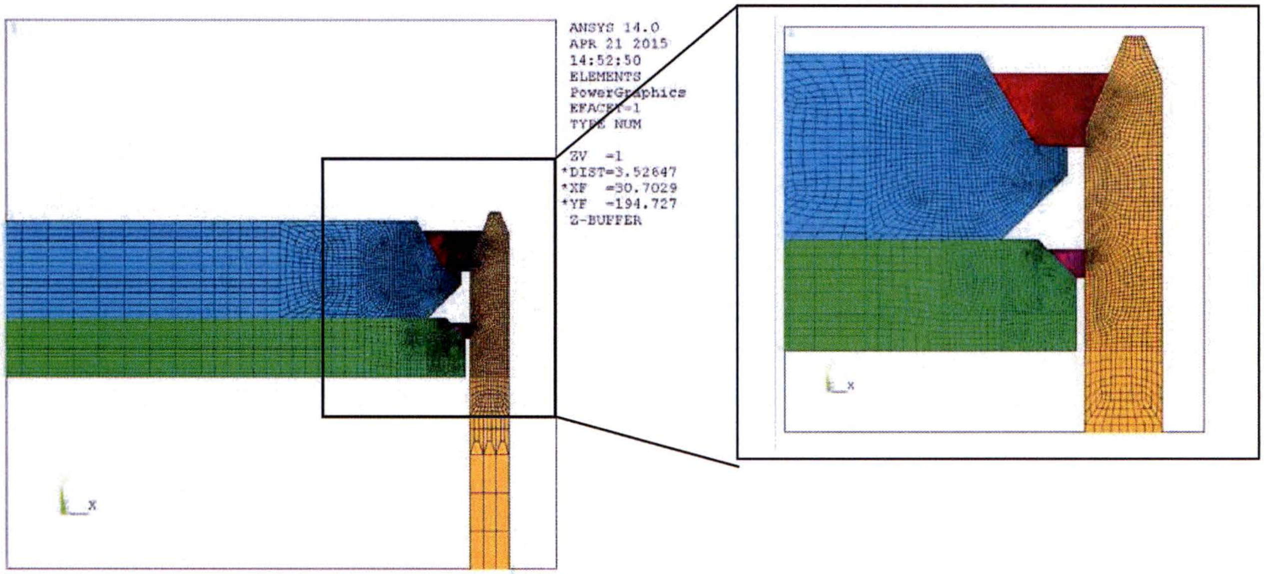

Figure 17 – Mesh Details at the Welds for Axisymmetric Case #2

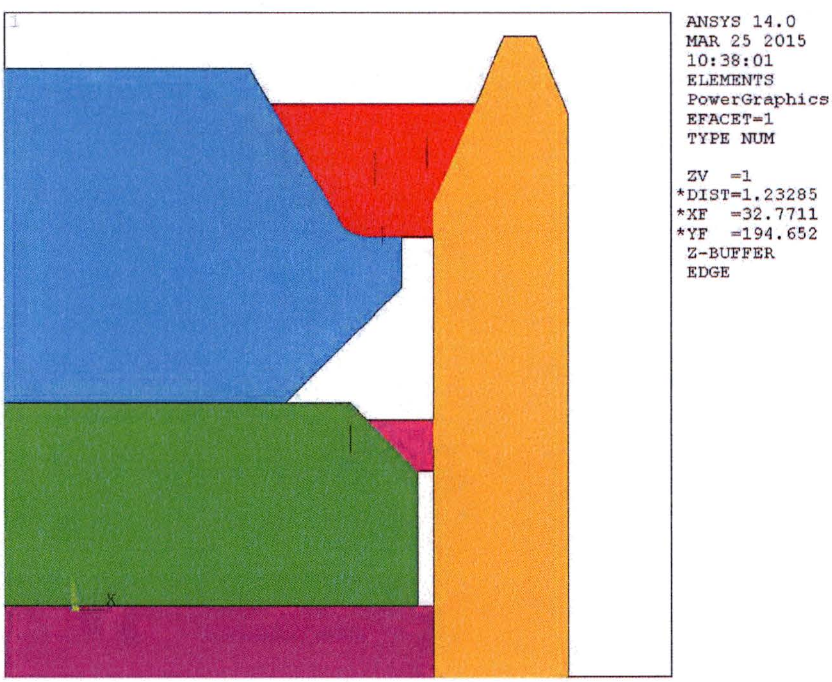

Figure 18 – Flaw Locations for Axisymmetric Case #2

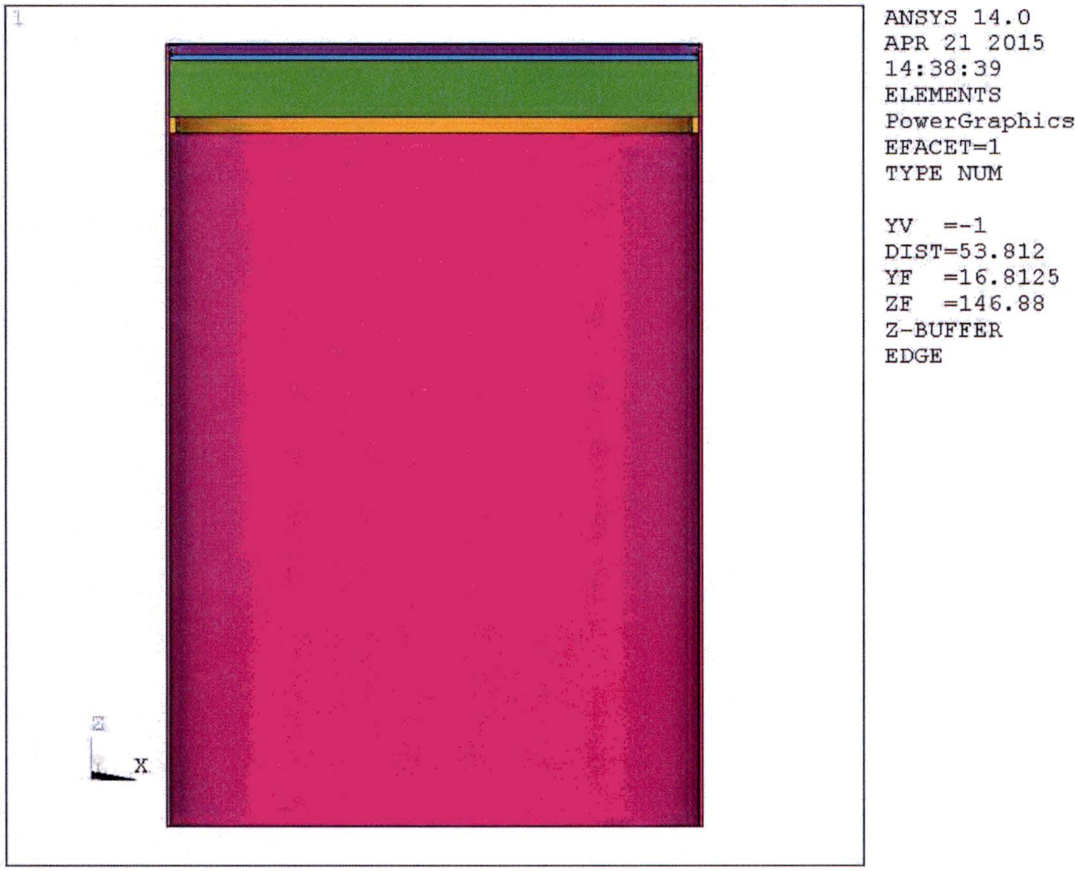

Figure 19 – Overview of the Half-Symmetry Model

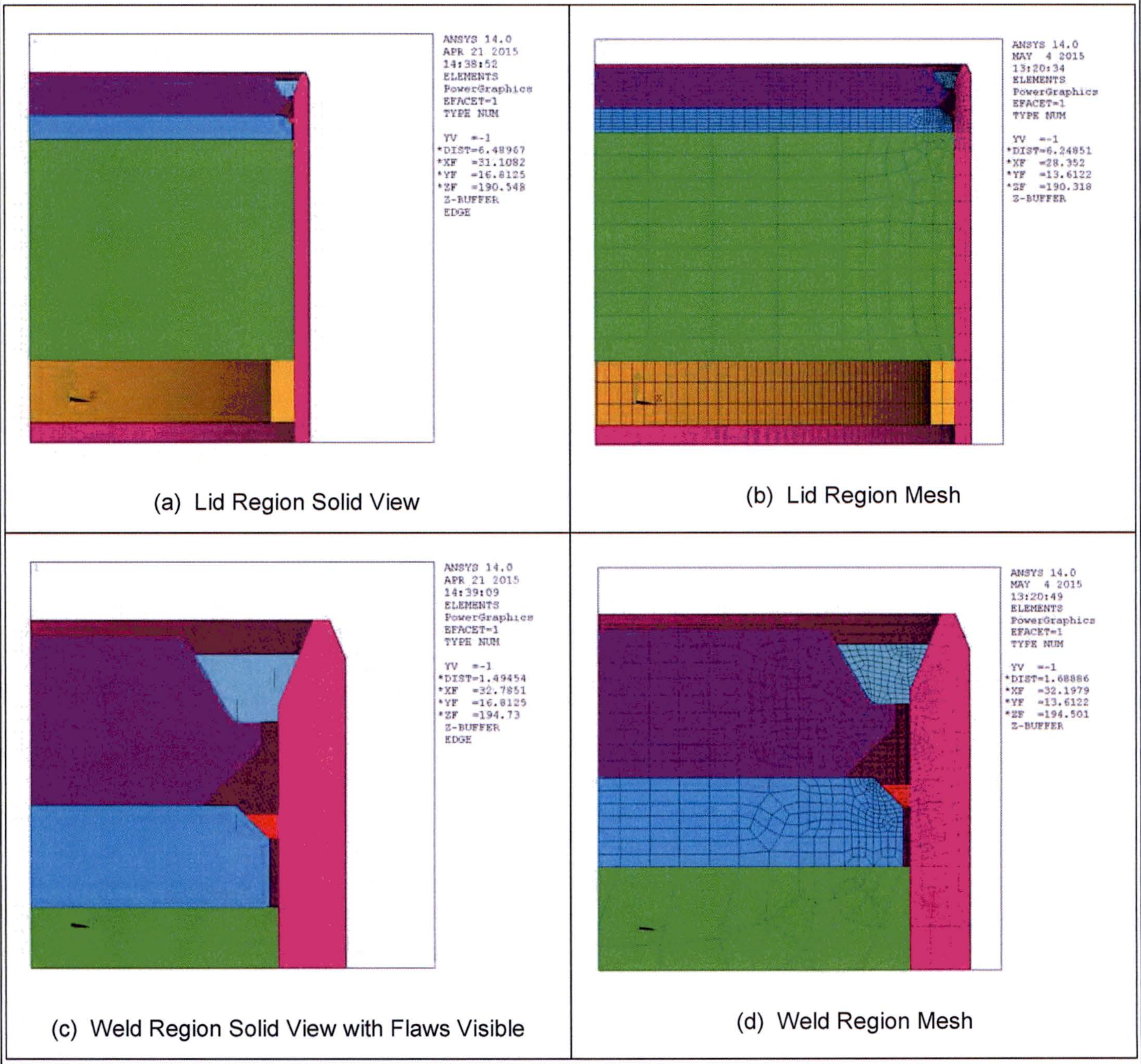

(a) Lid Region Solid View

(b) Lid Region Mesh

(c) Weld Region Solid View with Flaws Visible

(d) Weld Region Mesh

Figure 20 – Detail Views and Mesh Plots of the Half Symmetry Model

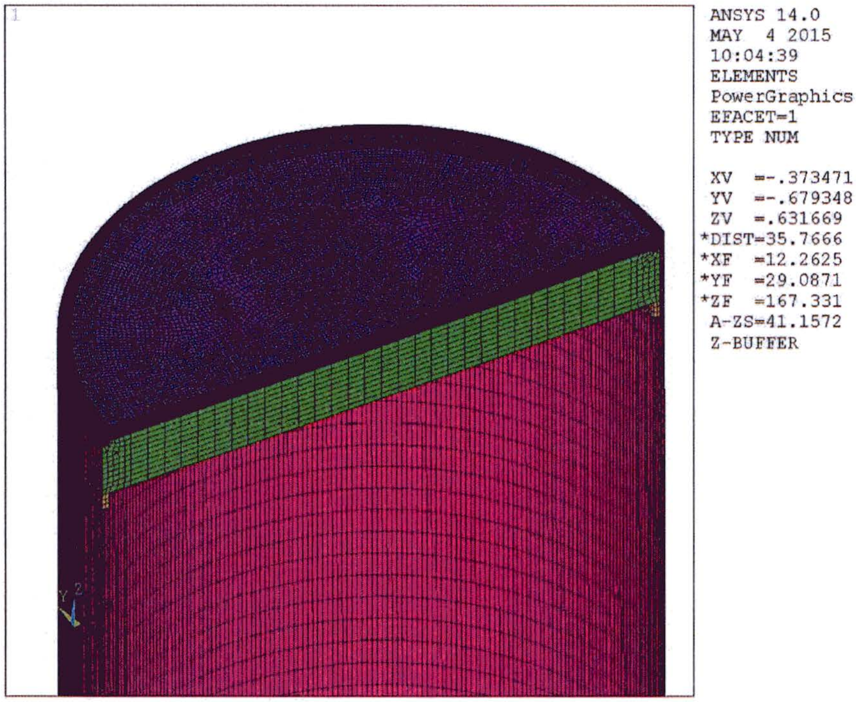

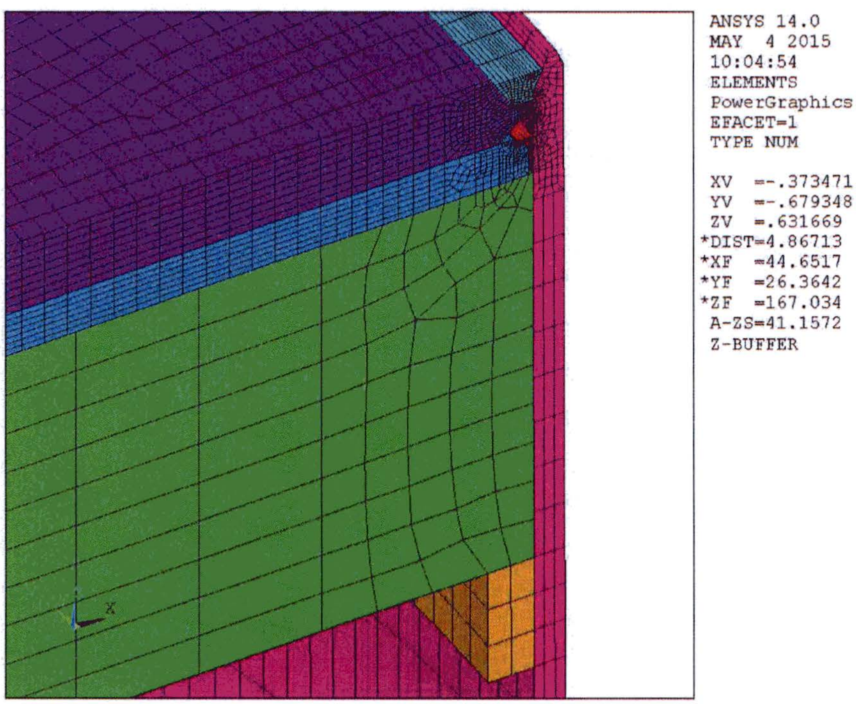

Figure 21 – Isometric Views of Half-Symmetry Model

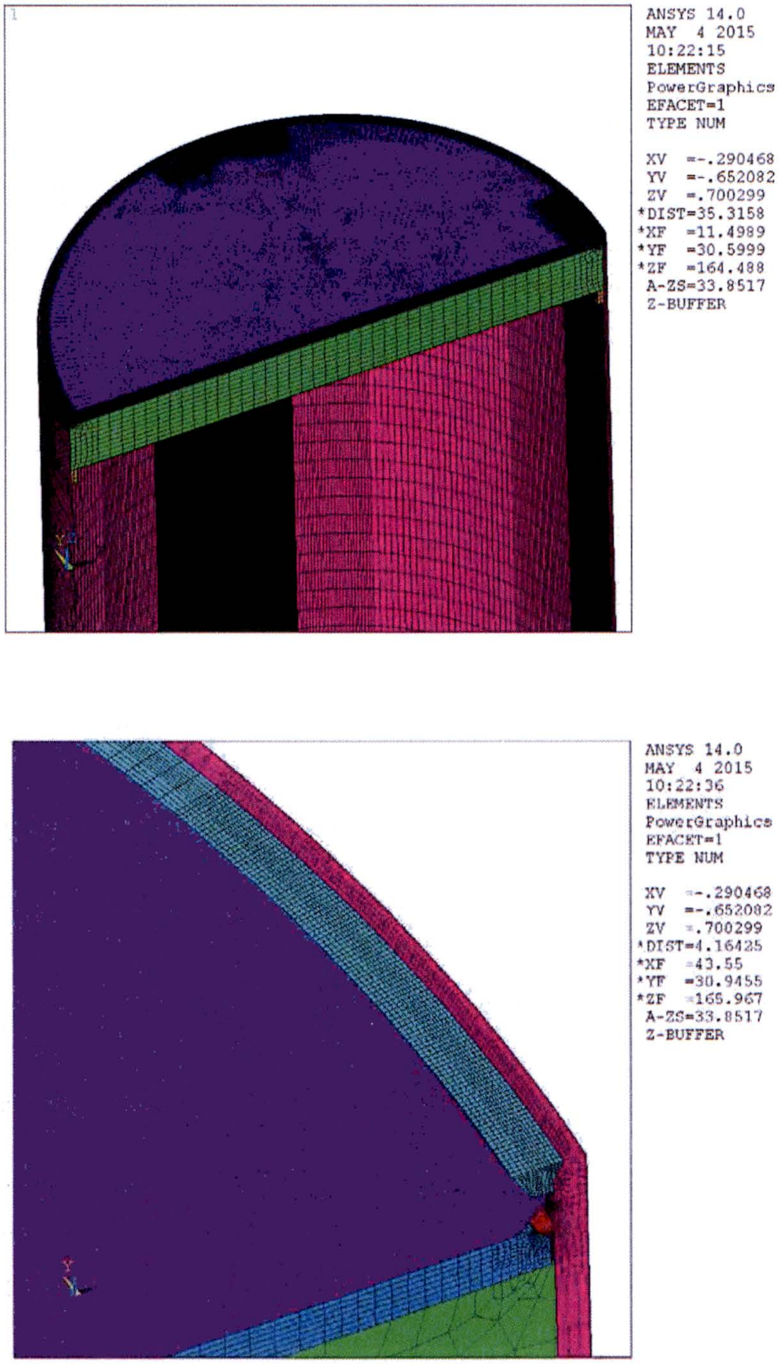

Figure 22 – Isometric Views of Half-Symmetry Model (Refined Circumferential Mesh)

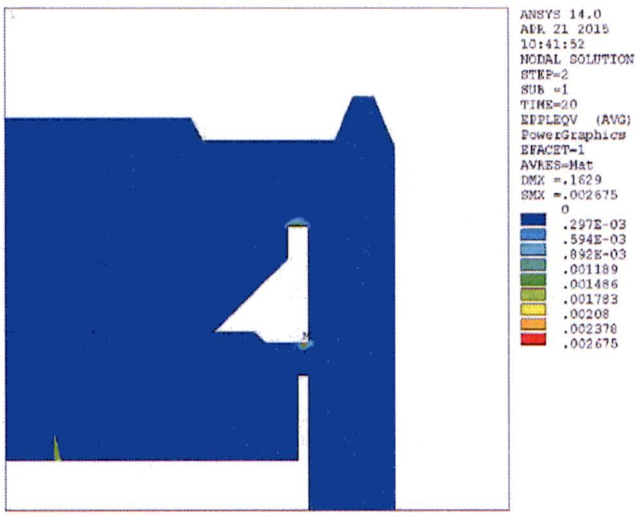

(a) Equivalent Plastic Strain in Weld Region [in/in] at 20 psi Internal Pressure

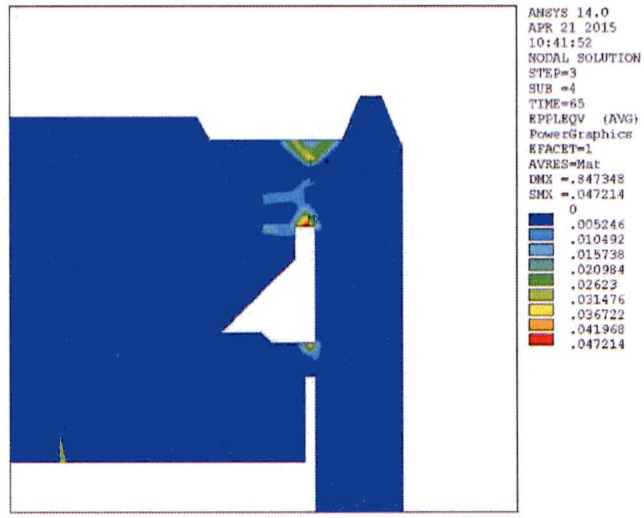

(b) Equivalent Plastic Strain in Weld Region [in/in] at 65 psi Internal Pressure

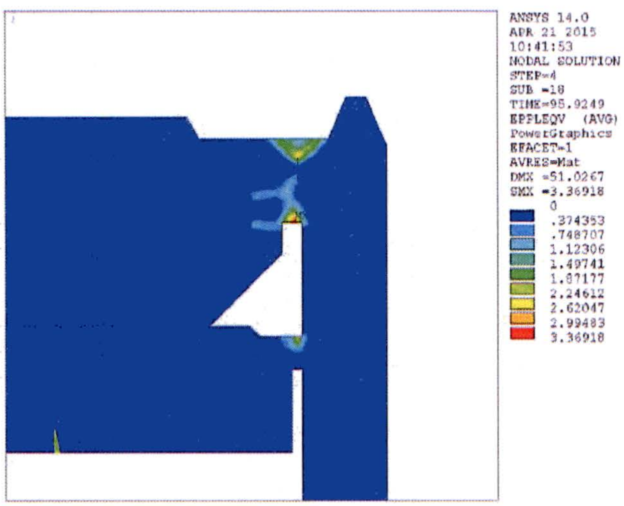

(c) Equivalent Plastic Strain in Weld Region [in/in] at 95.9 psi Internal Pressure

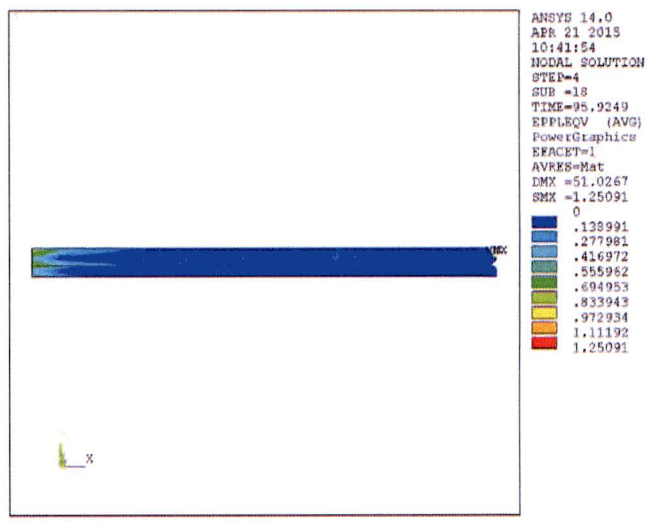

(d) EQV Plastic Strain in the Cover Plates at 95.9 psi

Figure 23 – Results for Axisymmetric Case #1 – Initial Mesh – Service Level A/B

(Note that the magnitude of the strains and deflections has no true physical meaning due to the nature of limit load analysis)

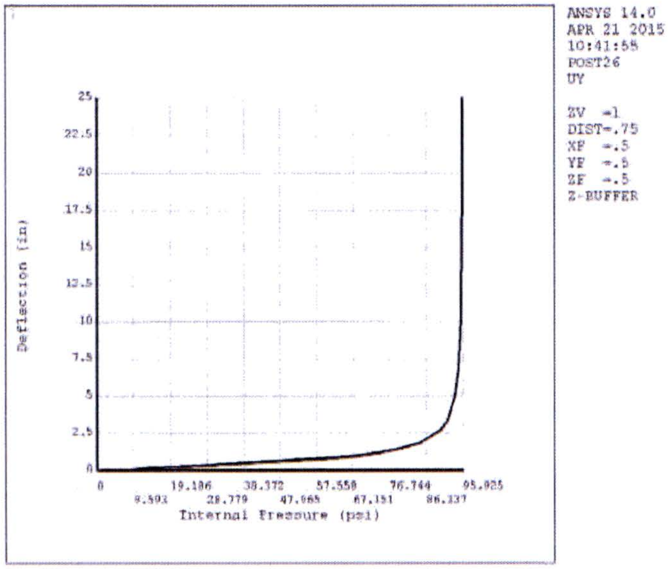

(a) Service Level A/B Material Properties

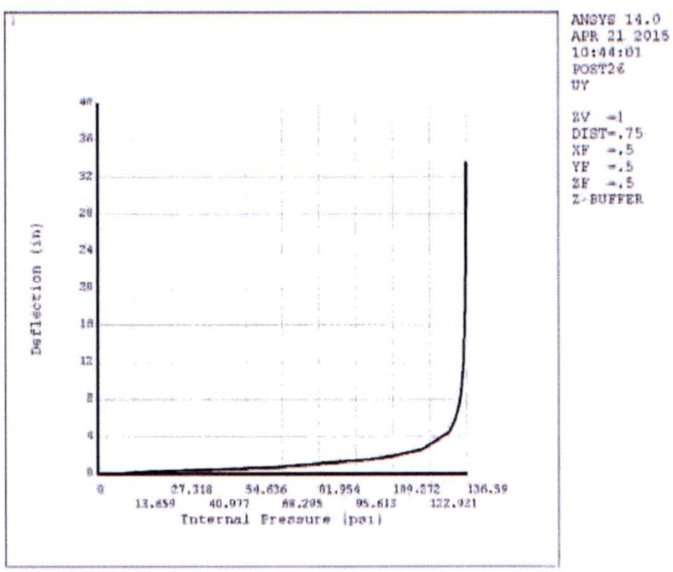

(b) Service Level D Material Properties

Figure 24 – Deflection History of the Center of the OTCP for the Axisymmetric Case #1 Initial Mesh

(Maximum deflection occurs at the center point of the lids, in the outward axial direction)

(Note that the magnitude of the deflections has no true physical meaning due to the nature of limit load analysis)

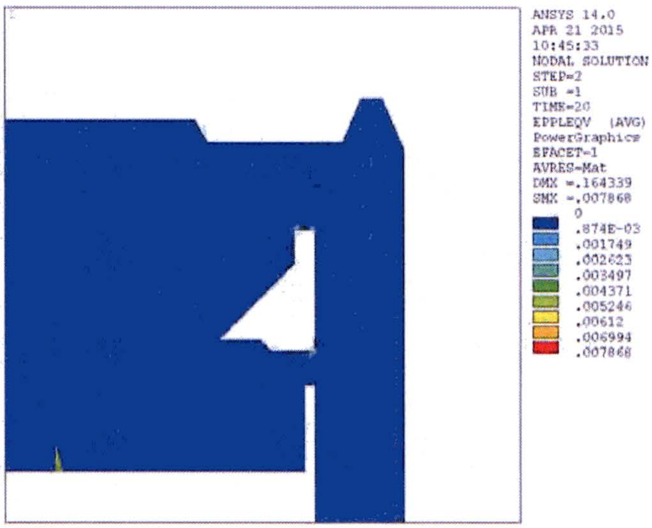

(a) Equivalent Plastic Strain in Weld Region [in/in] at 20 psi Internal Pressure

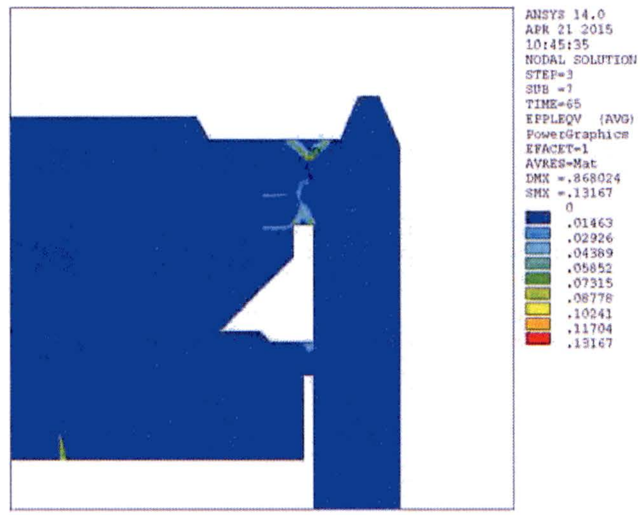

(b) Equivalent Plastic Strain in Weld Region [in/in] at 65 psi Internal Pressure

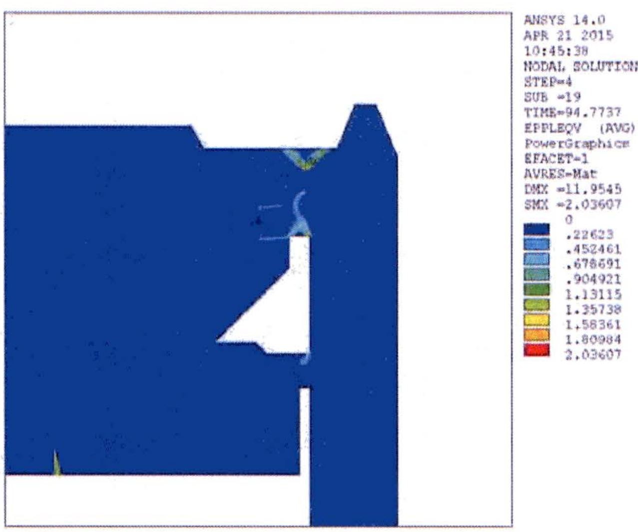

(c) Equivalent Plastic Strain in Weld Region [in/in] at 94.8 psi Internal Pressure

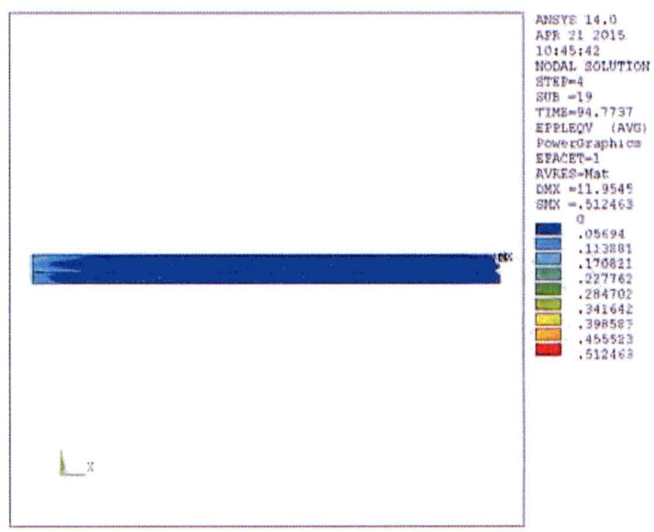

(d) EQV Plastic Strain in the Cover Plates at 94.8 psi

Figure 25 – Results for Axisymmetric Case #1 – Refined Mesh in Weld Region – Service Level A/B

(Note that the magnitude of the strains and deflections has no true physical meaning due to the nature of limit load analysis)

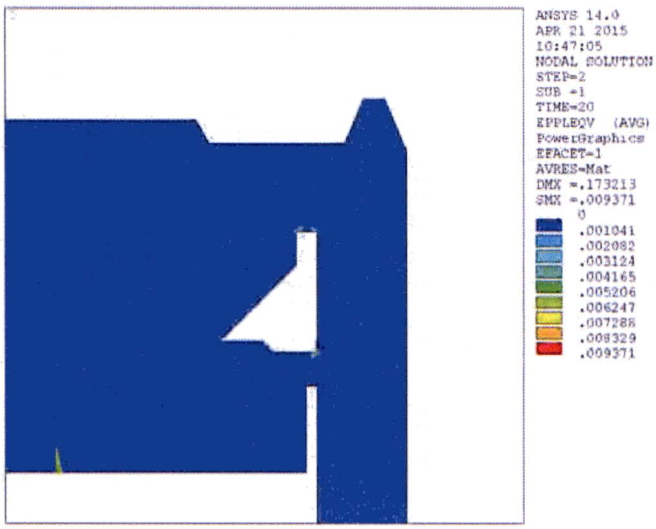

(a) Equivalent Plastic Strain in Weld Region [in/in] at 20 psi Internal Pressure

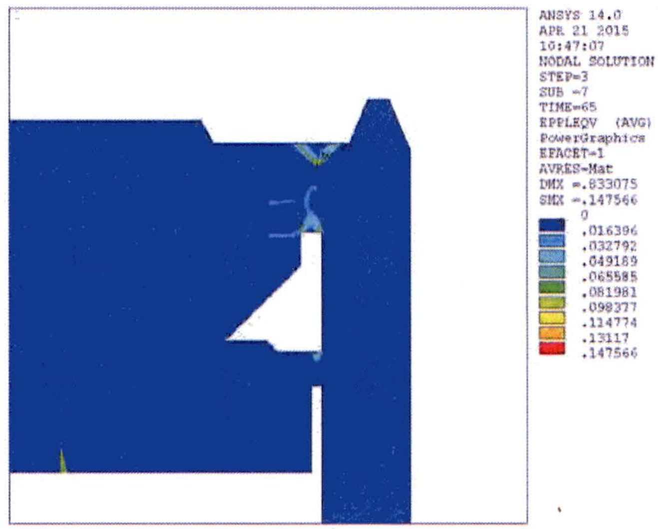

(b) Equivalent Plastic Strain in Weld Region [in/in] at 65 psi Internal Pressure

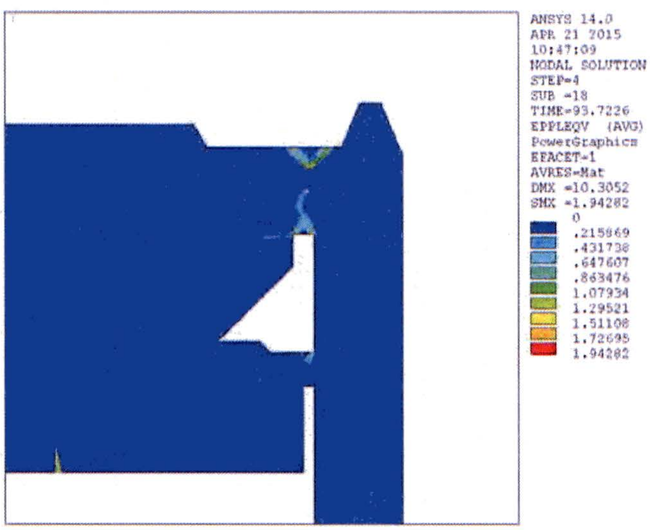

(c) Equivalent Plastic Strain in Weld Region [in/in] at 93.7 psi Internal Pressure

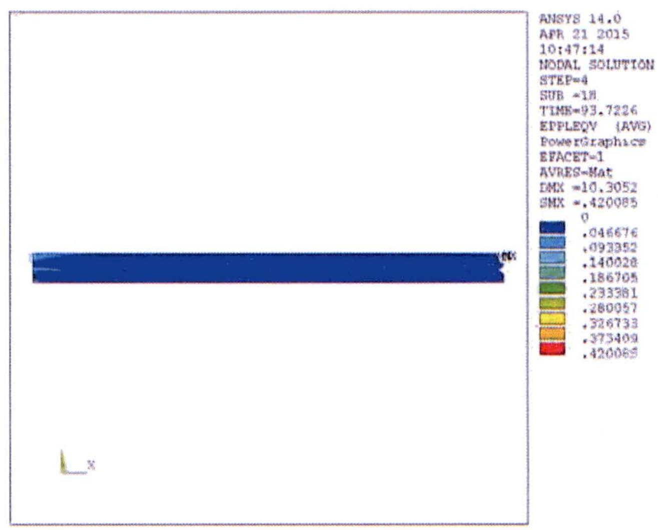

(d) EQV Plastic Strain in the Cover Plates at 93.7 psi

Figure 26 – Results for Axisymmetric Case #1 – Refined Mesh in Weld and Lid Interior Region – Service Level A/B

(Note (c) and (d) are plotted one timestep before the collapse pressure)

(Note that the magnitude of the strains and deflections has no true physical meaning due to the nature of limit load analysis)

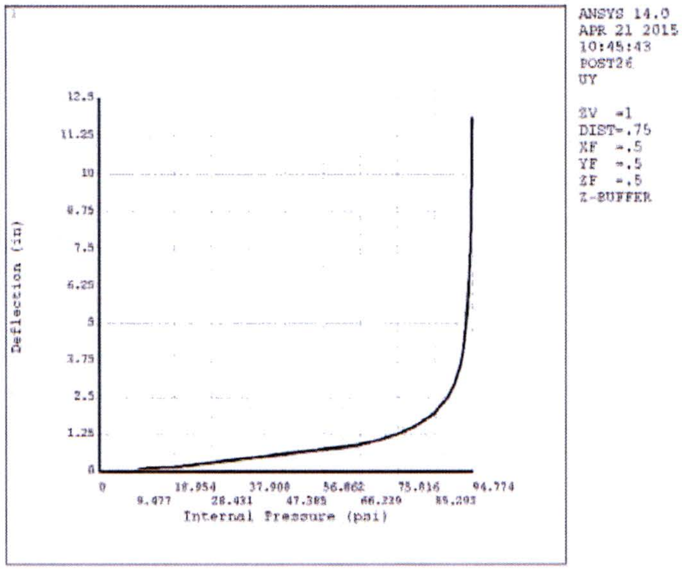

(a) Service Level A/B Material Properties

Refined Mesh at Weld Region Only

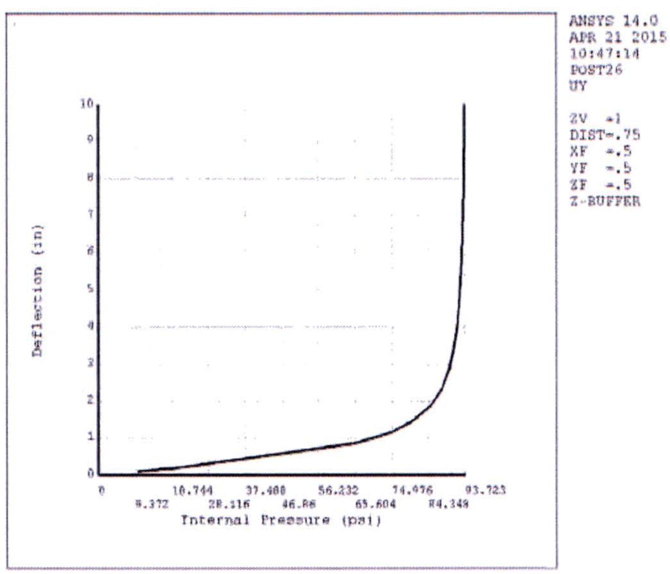

(b) Service Level A/B Material Properties

Refined Mesh at the Weld and Lid Interior Regions

Figure 27 – Deflection History of the Center of the OTCP for the Axisymmetric Case #1 Refined Mesh

(Maximum deflection occurs at the center point of the lids, in the outward axial direction)

(Note that the magnitude of the deflections has no true physical meaning due to the nature of limit load analysis)

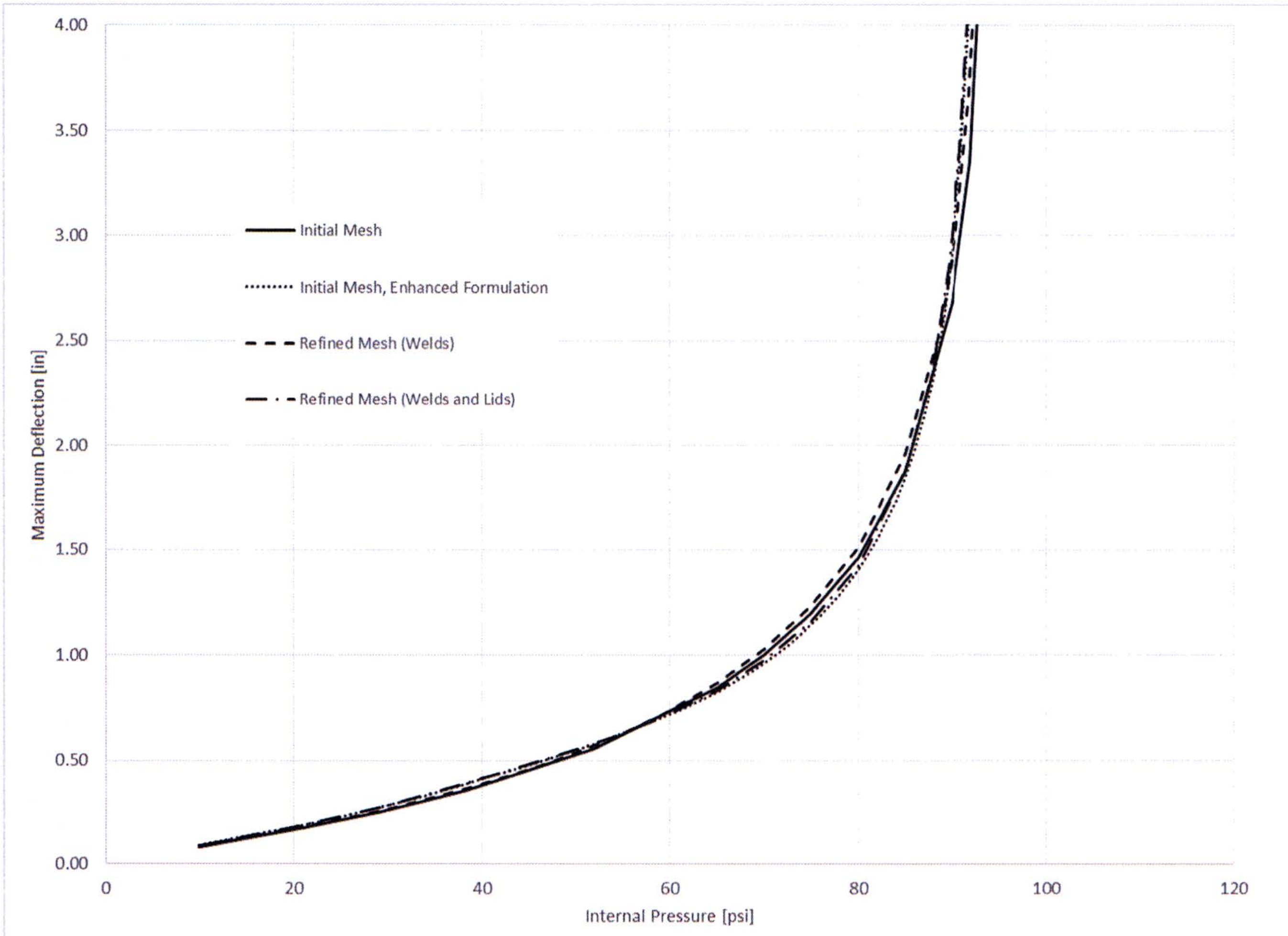

Figure 28 – Comparison of Maximum Displacement Histories for Axisymmetric Model Sensitivity Studies

(Maximum deflection occurs at the center point of the lids, in the outward axial direction)

(Note that the magnitude of the deflections has no true physical meaning due to the nature of limit load analysis)

(Service Level A/B material Properties)

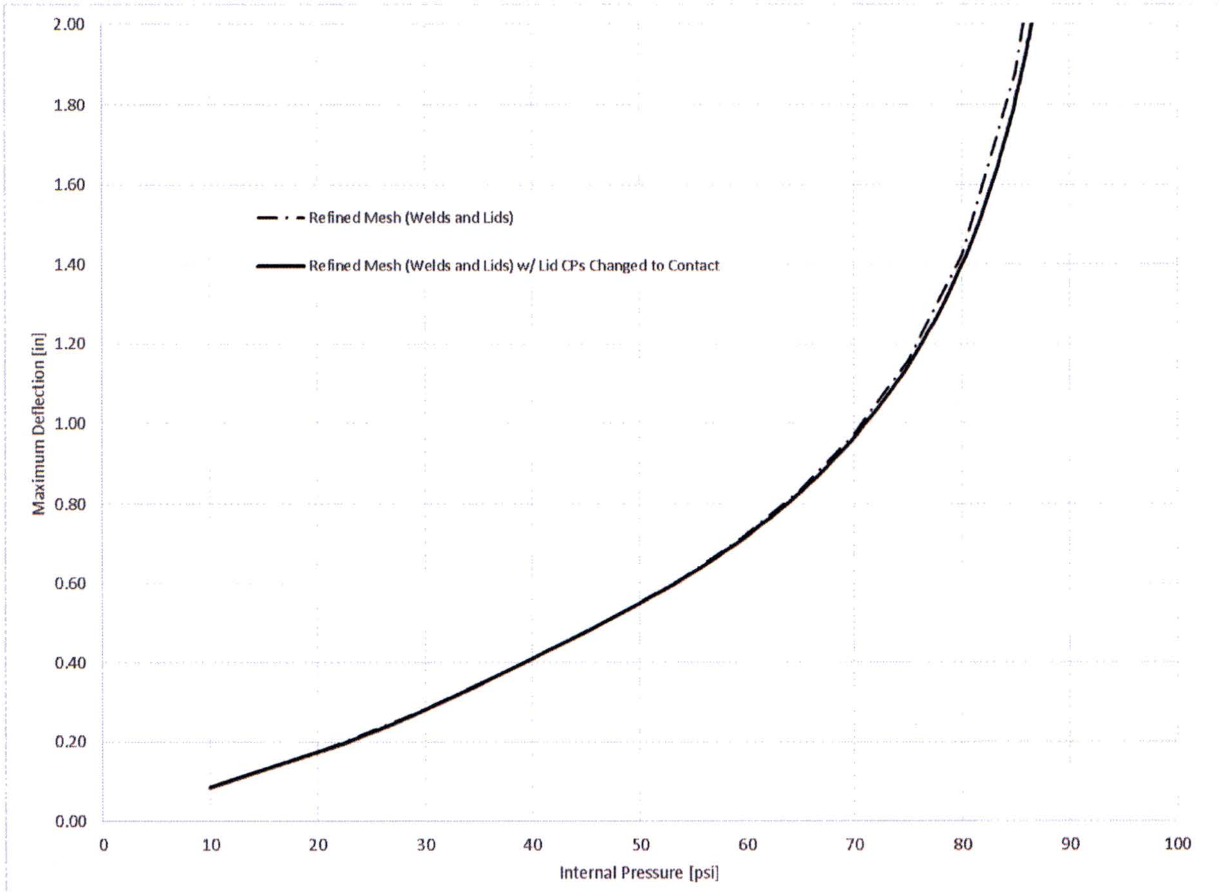

Figure 29 – Comparison of Maximum Displacement Histories for Axisymmetric Model with Lid Contact Defined using Nodal DOF Couples vs. Contact Elements

(Maximum deflection occurs at the center point of the lids, in the outward axial direction)

(Note that the magnitude of the deflections has no true physical meaning due to the nature of limit load analysis)

(Service Level A/B material properties)

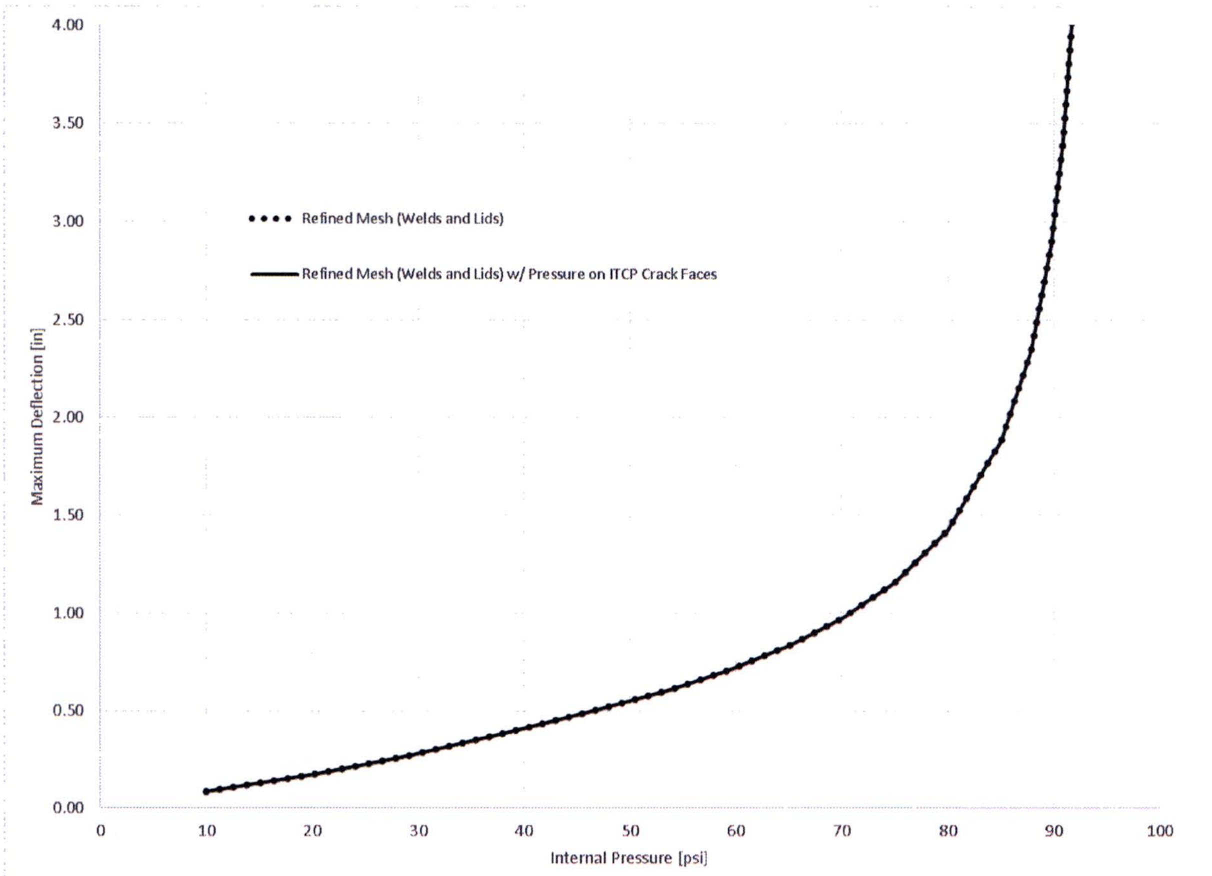

Figure 30 – Comparison of Maximum Displacement Histories for Axisymmetric Model With and Without Pressure Loading Applied to the ITCP Weld Root Flaw Faces

(Maximum deflection occurs at the center point of the lids, in the outward axial direction)

(Note that the magnitude of the deflections has no true physical meaning due to the nature of limit load analysis)

(Service Level A/B material properties)

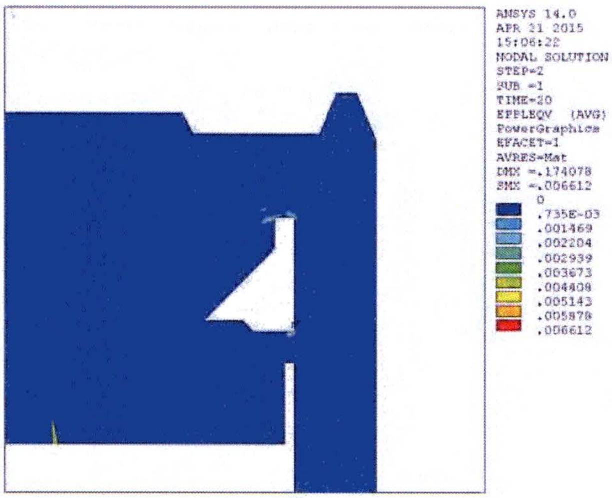

(a) Equivalent Plastic Strain in Weld Region [in/in] at 20 psi Internal Pressure

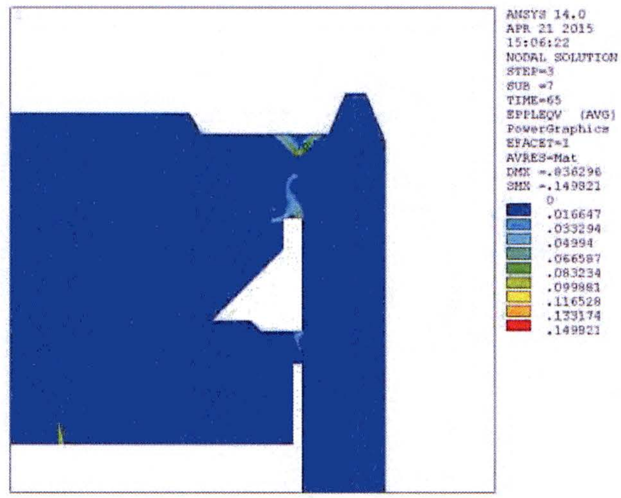

(b) Equivalent Plastic Strain in Weld Region [in/in] at 65 psi Internal Pressure

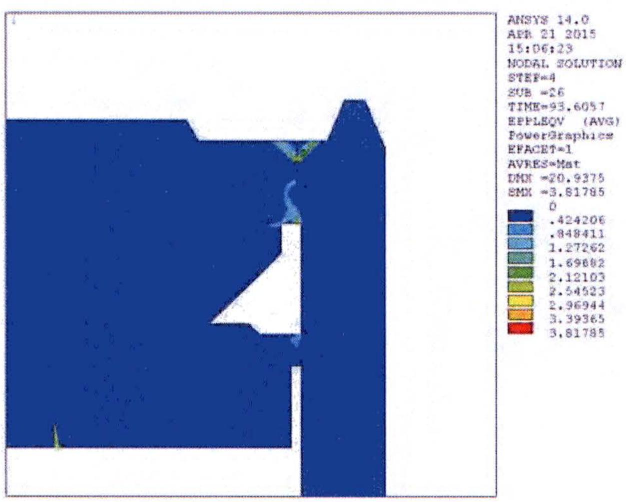

(c) Equivalent Plastic Strain in Weld Region [in/in] at 93.6 psi Internal Pressure

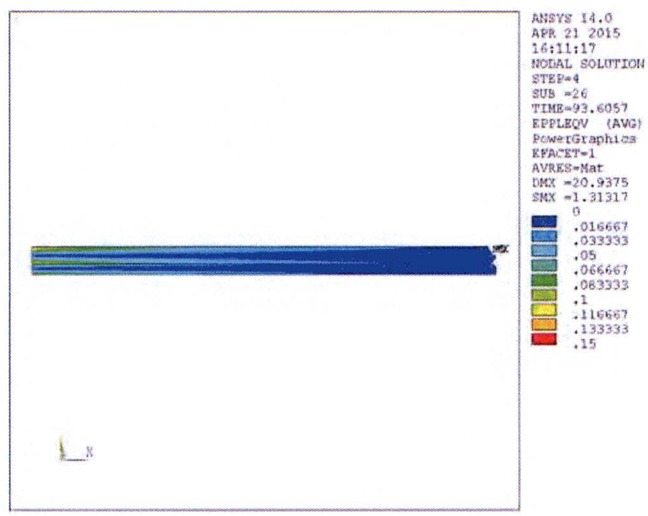

(d) EQV Plastic Strain in the Cover Plates at 93.6 psi

Figure 31 – Results for Axisymmetric Case #2 – Refined Mesh in Weld and Lid Interior Region – Service Level A/B

(Note (c) and (d) are plotted one timestep before the collapse pressure)

(Note that the magnitude of the strains and deflections has no true physical meaning due to the nature of limit load analysis)

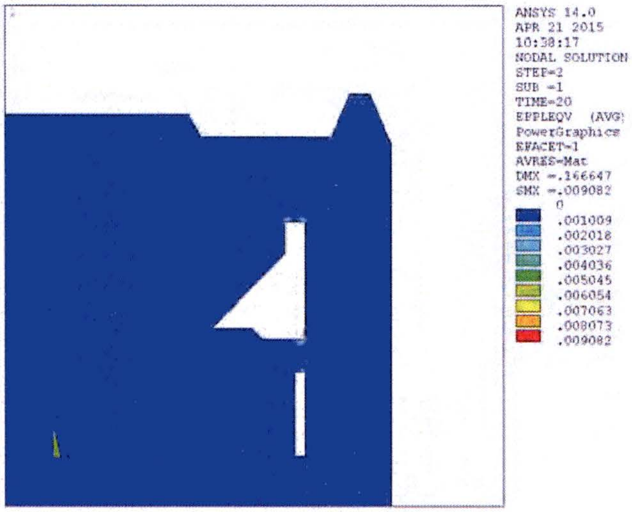

(a) Equivalent Plastic Strain in Weld Region [in/in] at 20 psi Internal Pressure

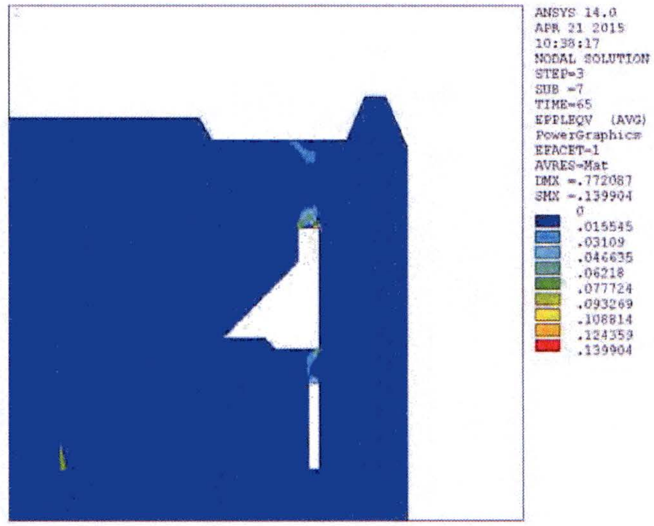

(b) Equivalent Plastic Strain in Weld Region [in/in] at 65 psi Internal Pressure

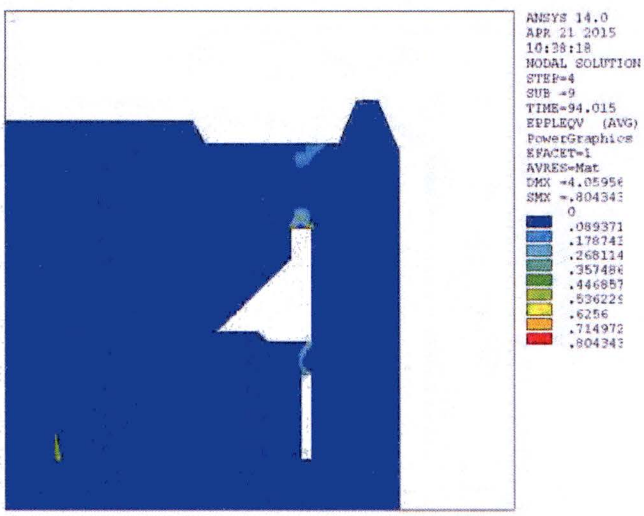

(c) Equivalent Plastic Strain in Weld Region [in/in] at 94.0 psi Internal Pressure

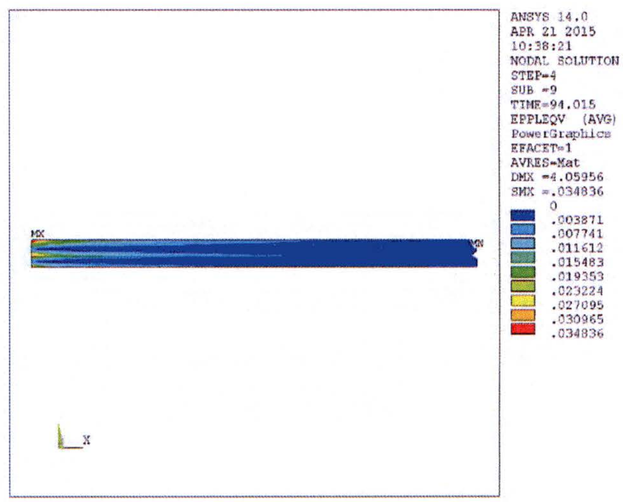

(d) EQV Plastic Strain in the Cover Plates at 94.0 psi

Figure 32 – Results for Axisymmetric Case #0 – Refined Mesh in Weld and Lid Interior Region – Service Level A/B

(Note (c) and (d) are plotted one timestep before the collapse pressure)

(Note that the magnitude of the strains and deflections has no true physical meaning due to the nature of limit load analysis)

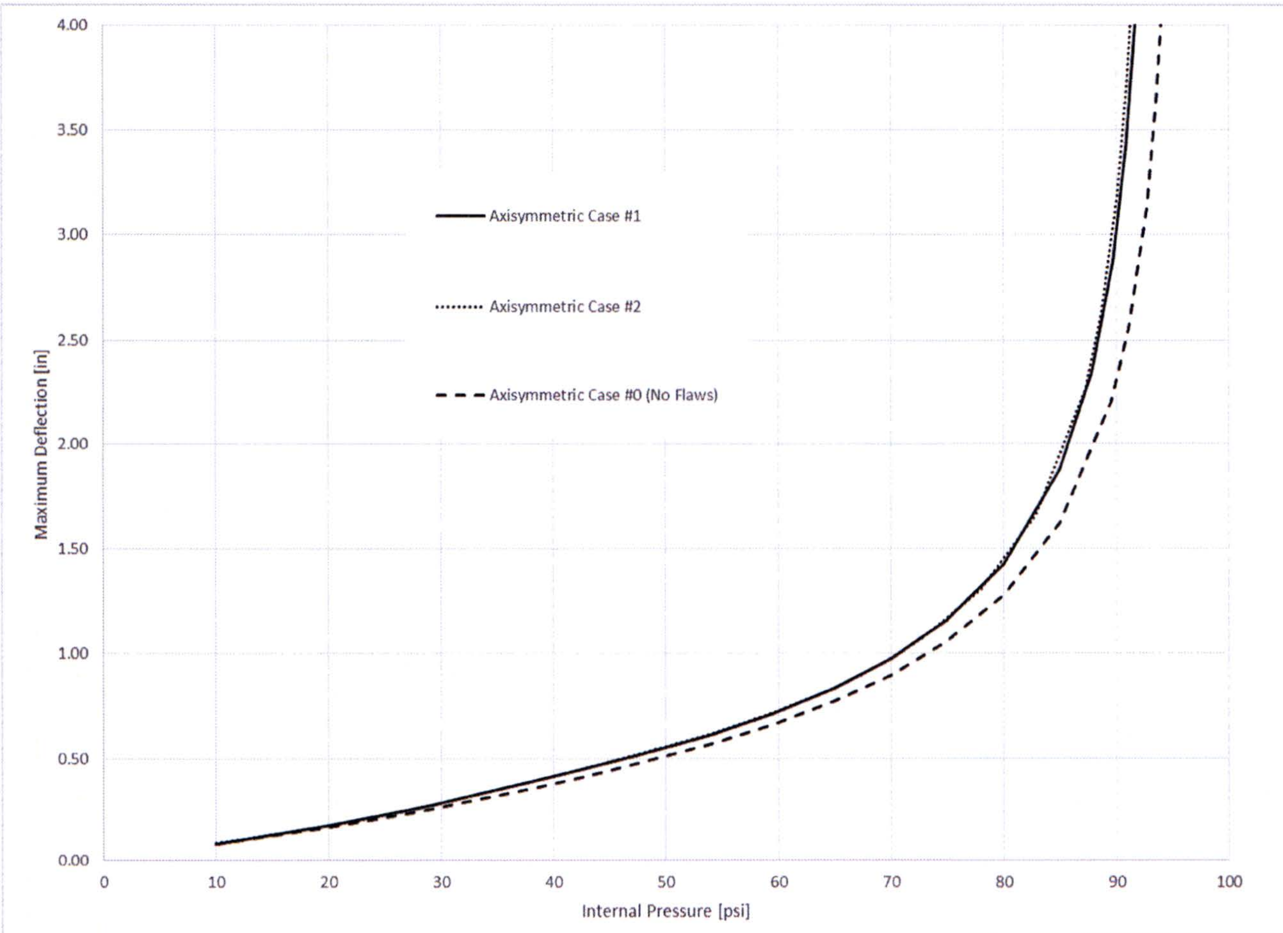

Figure 33 – Comparison of Maximum Center-of-Lid Displacement Histories for the Various Flaw Models

(Service Level A/B material properties)

(Note that the magnitude of the deflections has no true physical meaning due to the nature of limit load analysis)

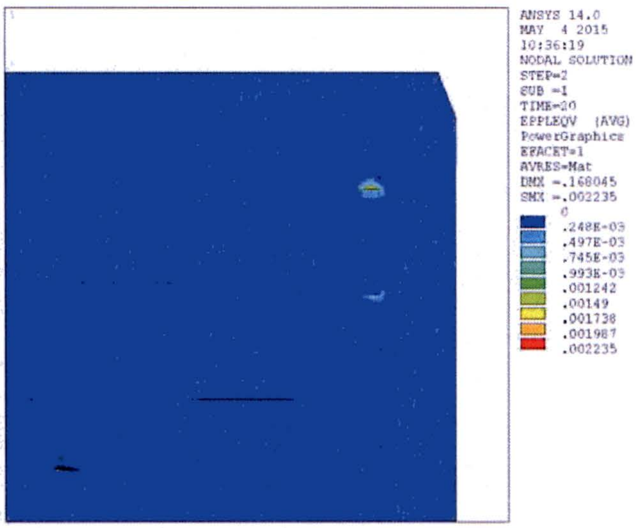

(a) Equivalent Plastic Strain in Weld Region [in/in] at 20 psi Internal Pressure

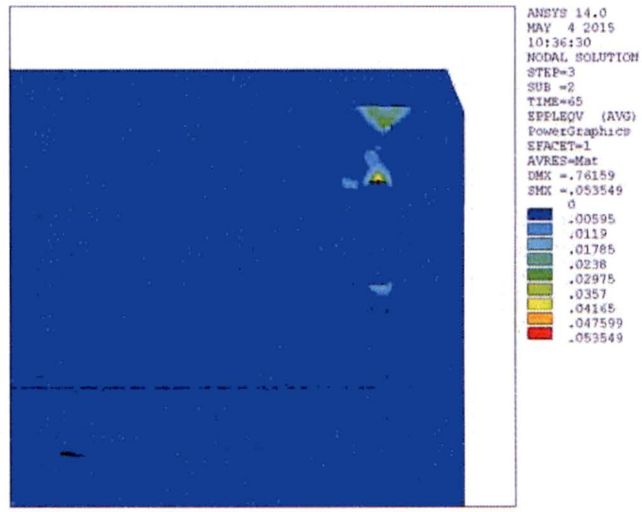

(b) Equivalent Plastic Strain in Weld Region [in/in] at 65 psi Internal Pressure

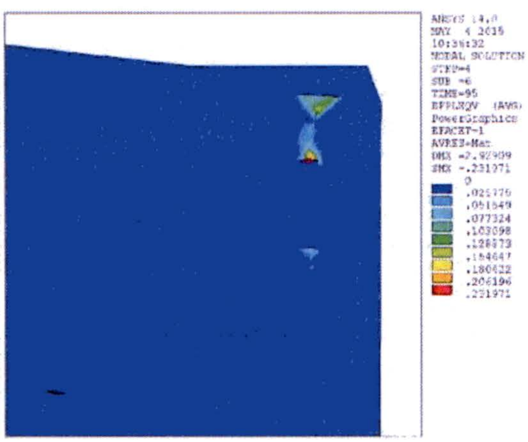

(c) Equivalent Plastic Strain in Weld Region [in/in] at 95 psi Internal Pressure

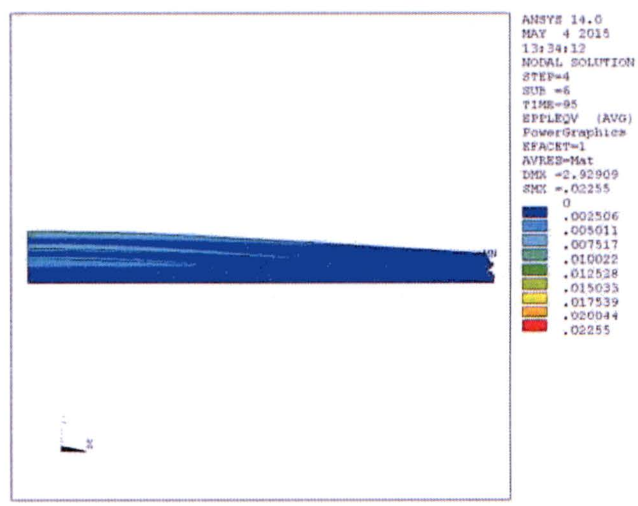

(d) EQV Plastic Strain in the Cover Plates at 95 psi

Figure 34 – Results for Half-Symmetry Case #1 Internal Pressure Loading Benchmark Analysis – Service Level A/B

(Note that the magnitude of the strains and deflections has no true physical meaning due to the nature of limit load analysis)

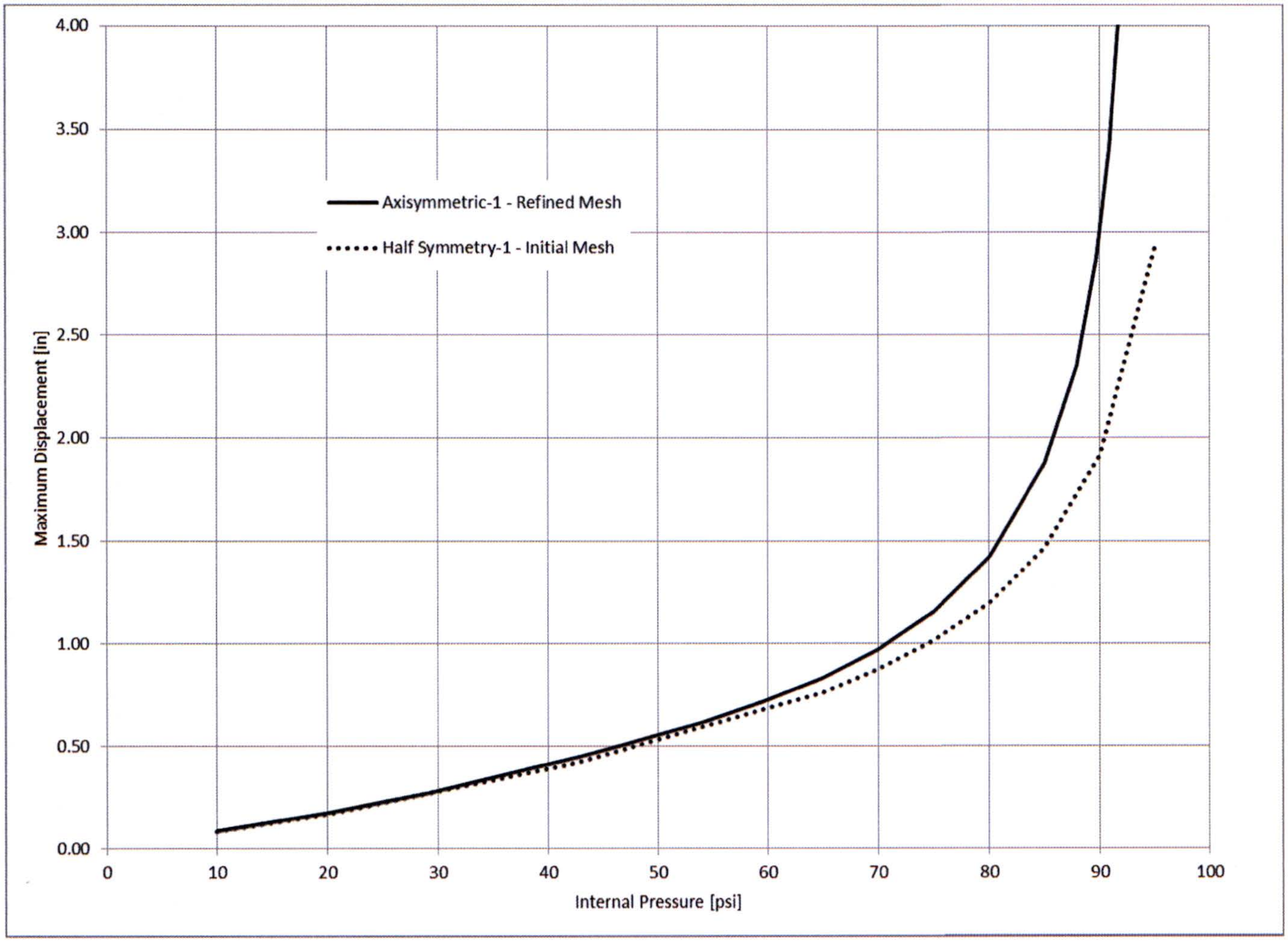

Figure 35 – Benchmark of the Half Symmetry model with the Axisymmetric Analysis

(Service Level A/B material properties)

(Note that the magnitude of the deflections has no true physical meaning due to the nature of limit load analysis)

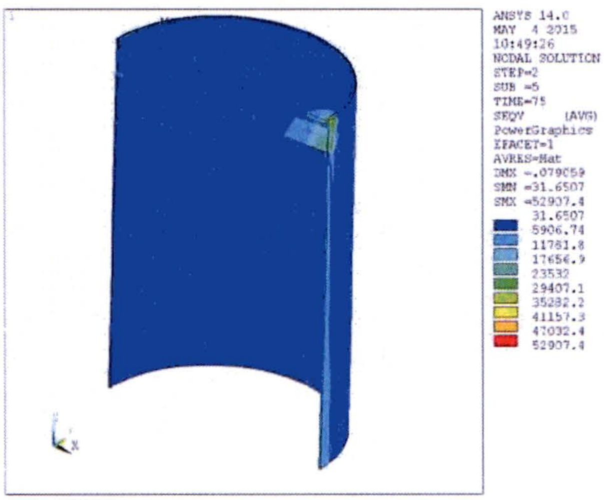

(a) Equivalent (von Mises) Stress [psi] at 75g

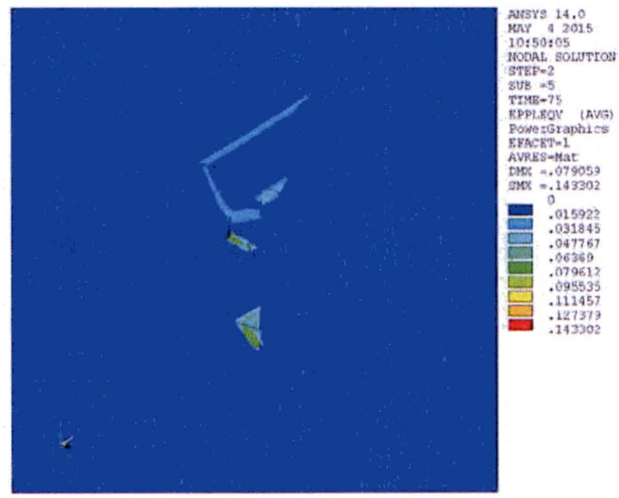

(b) Equivalent Plastic Strain in Weld Region [in/in] at 75g.

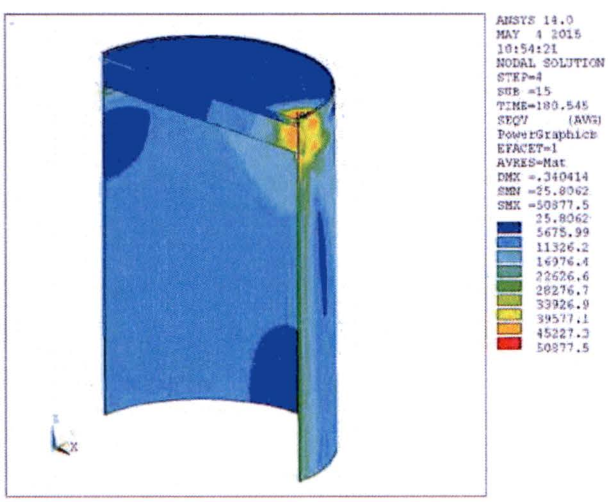

(c) Equivalent (von Mises) Stress [psi] at 181g

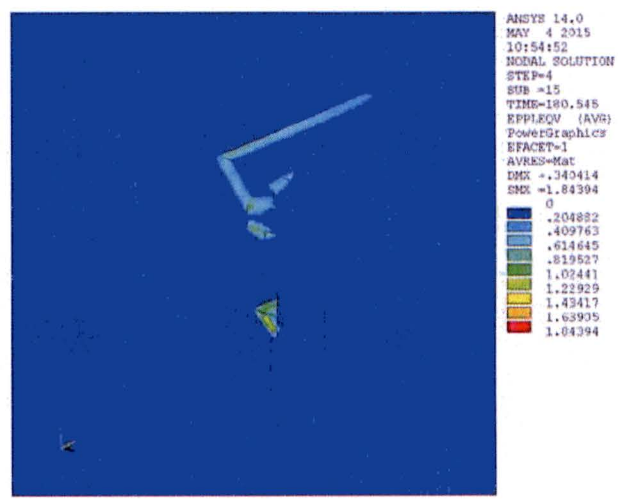

(d) Equivalent Plastic Strain in Weld Region [in/in] at 181g.

Figure 36 – Equivalent Stress and Plastic Strain Plots from the Half-Symmetry #1 Side Drop Analysis

(Note that the magnitude of the strains and deflections has no true physical meaning due to the nature of limit load analysis)

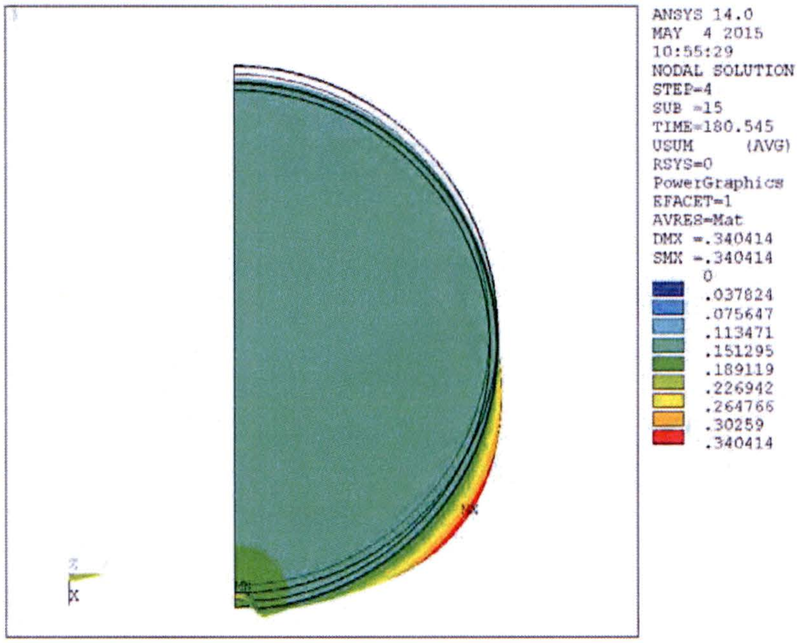

(a) Deformed Shape Plot – Axial View – Exaggerated Scale

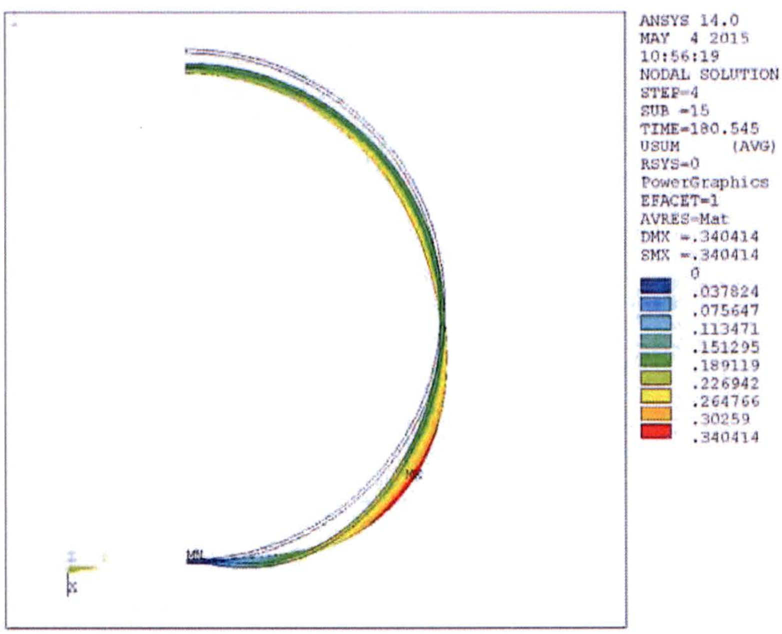

(b) Deformed Shape Plot of DSC Shell – Axial View – Exaggerated Scale

Figure 37 – Additional Results Plots from the Half-Symmetry #1 Side Drop Analysis

(Note that the magnitude of the deflections has no true physical meaning due to the nature of limit load analysis)

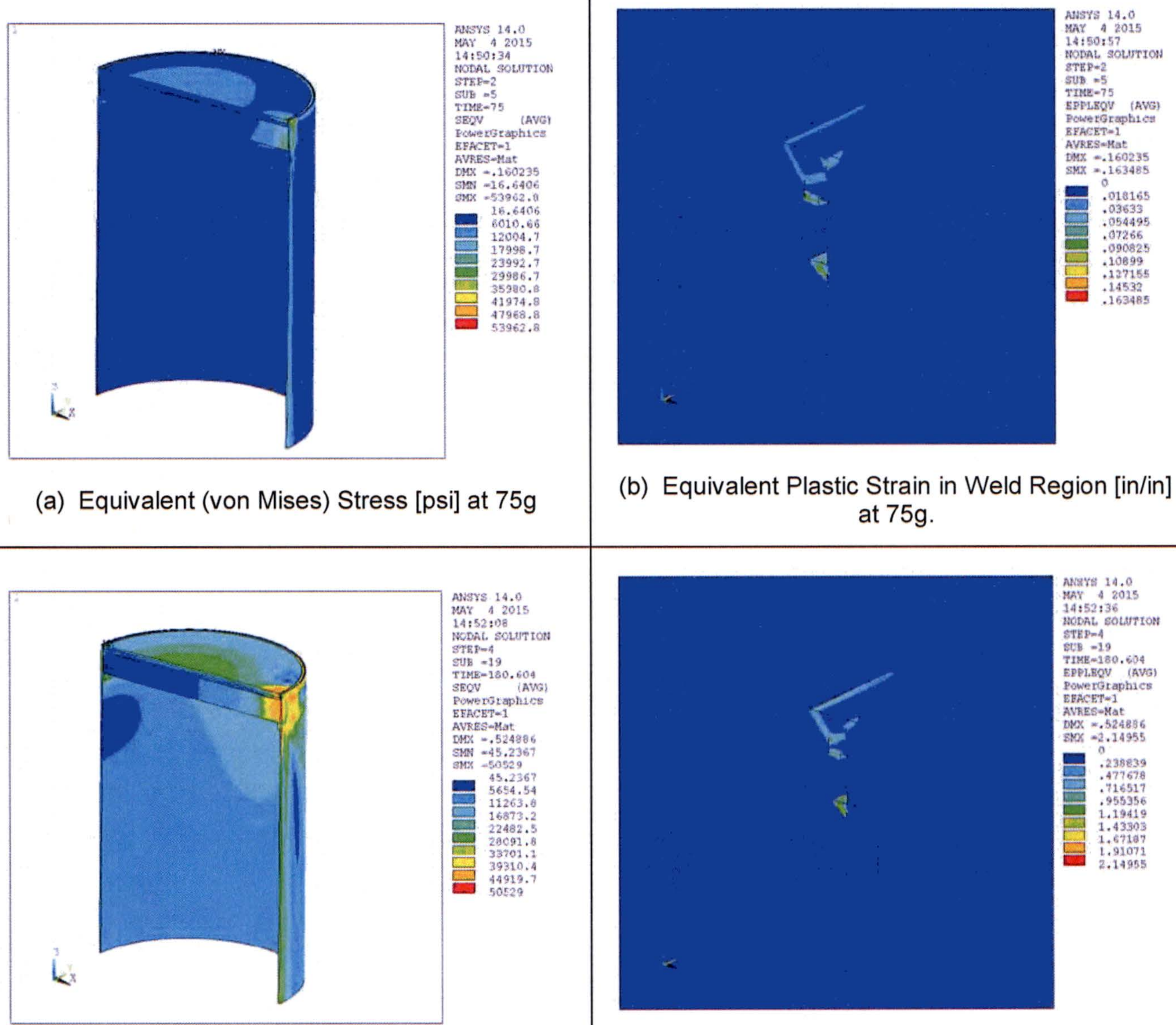

(a) Equivalent (von Mises) Stress [psi] at 75g

(b) Equivalent Plastic Strain in Weld Region [in/in] at 75g.

(c) Equivalent (von Mises) Stress [psi] at 181g

(d) Equivalent Plastic Strain in Weld Region [in/in] at 181g.

Figure 38 – Equivalent Stress and Plastic Strain Plots from the Half-Symmetry #1 Side Drop Analysis with Off-Normal Internal Pressure

(Note that the magnitude of the strains and deflections has no true physical meaning due to the nature of limit load analysis)

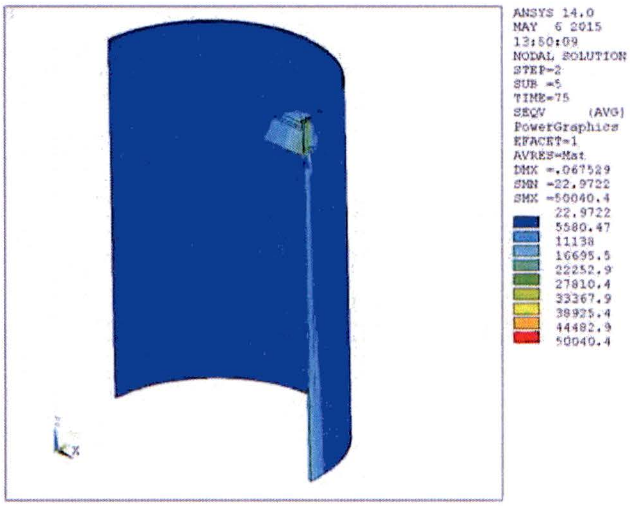

(a) Equivalent (von Mises) Stress [psi] at 75g

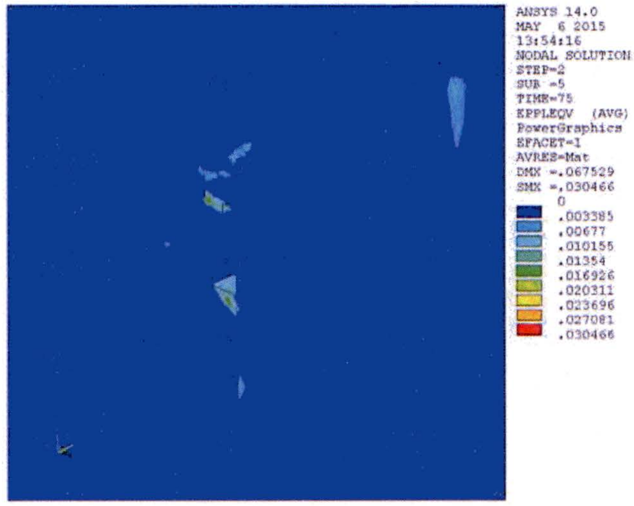

(b) Equivalent Plastic Strain in Weld Region [in/in] at 75g.

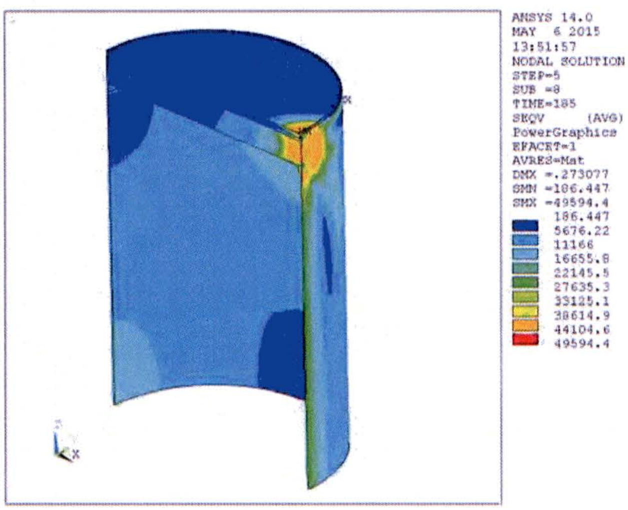

(c) Equivalent (von Mises) Stress [psi] at 185g

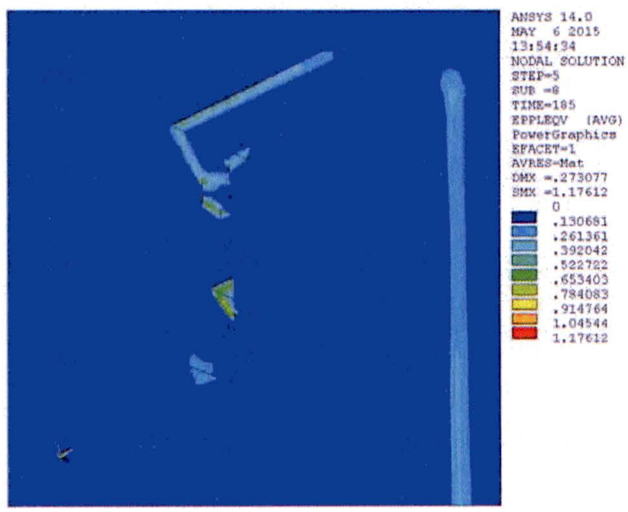

(d) Equivalent Plastic Strain in Weld Region [in/in] at 185g.

Figure 39 – Equivalent Stress and Plastic Strain Plots from the Half-Symmetry #1 Side Drop Analysis with Refined Circumferential Mesh

(Note that the magnitude of the strains and deflections has no true physical meaning due to the nature of limit load analysis)

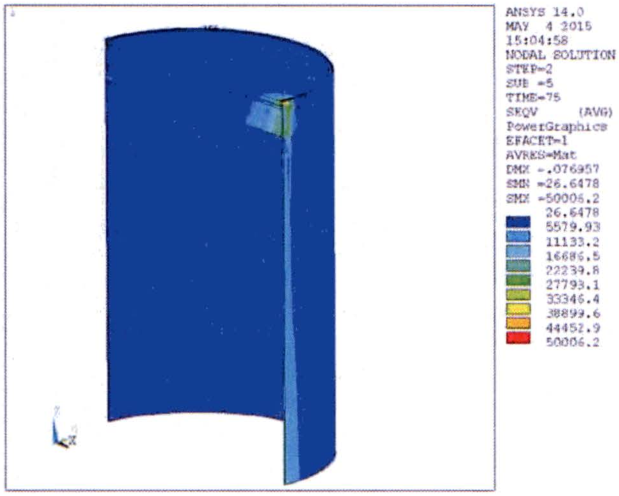

(a) Equivalent (von Mises) Stress [psi] at 75g

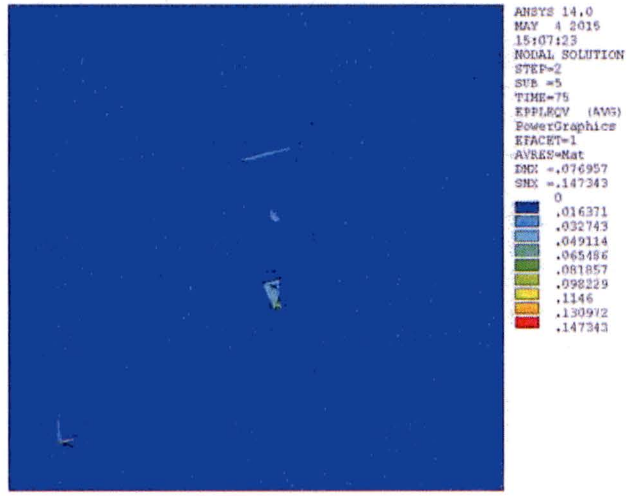

(b) Equivalent Plastic Strain in Weld Region [in/in] at 75g.

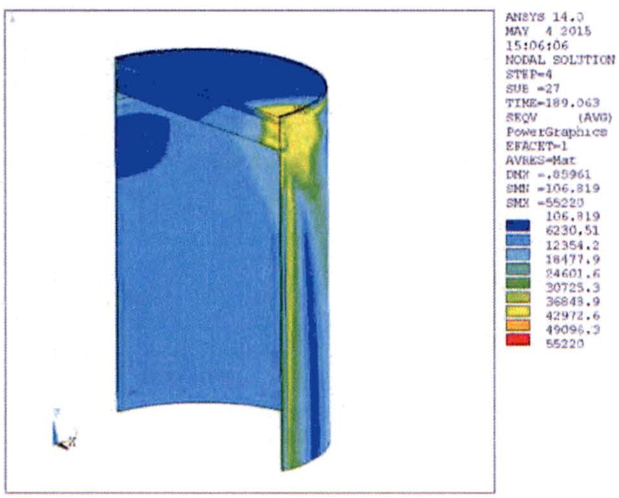

(c) Equivalent (von Mises) Stress [psi] at 189g

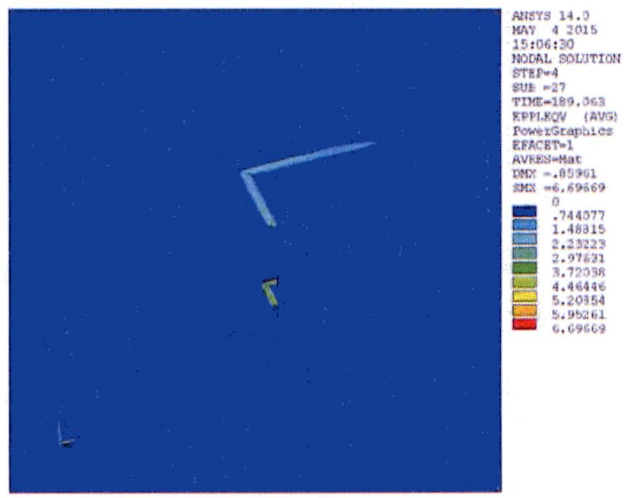

(d) Equivalent Plastic Strain in Weld Region [in/in] at 189g.

Figure 40 – Equivalent Stress and Plastic Strain Plots from the Half-Symmetry #0 (No Flaws) Side Drop Analysis

(Note that the magnitude of the strains and deflections has no true physical meaning due to the nature of limit load analysis)

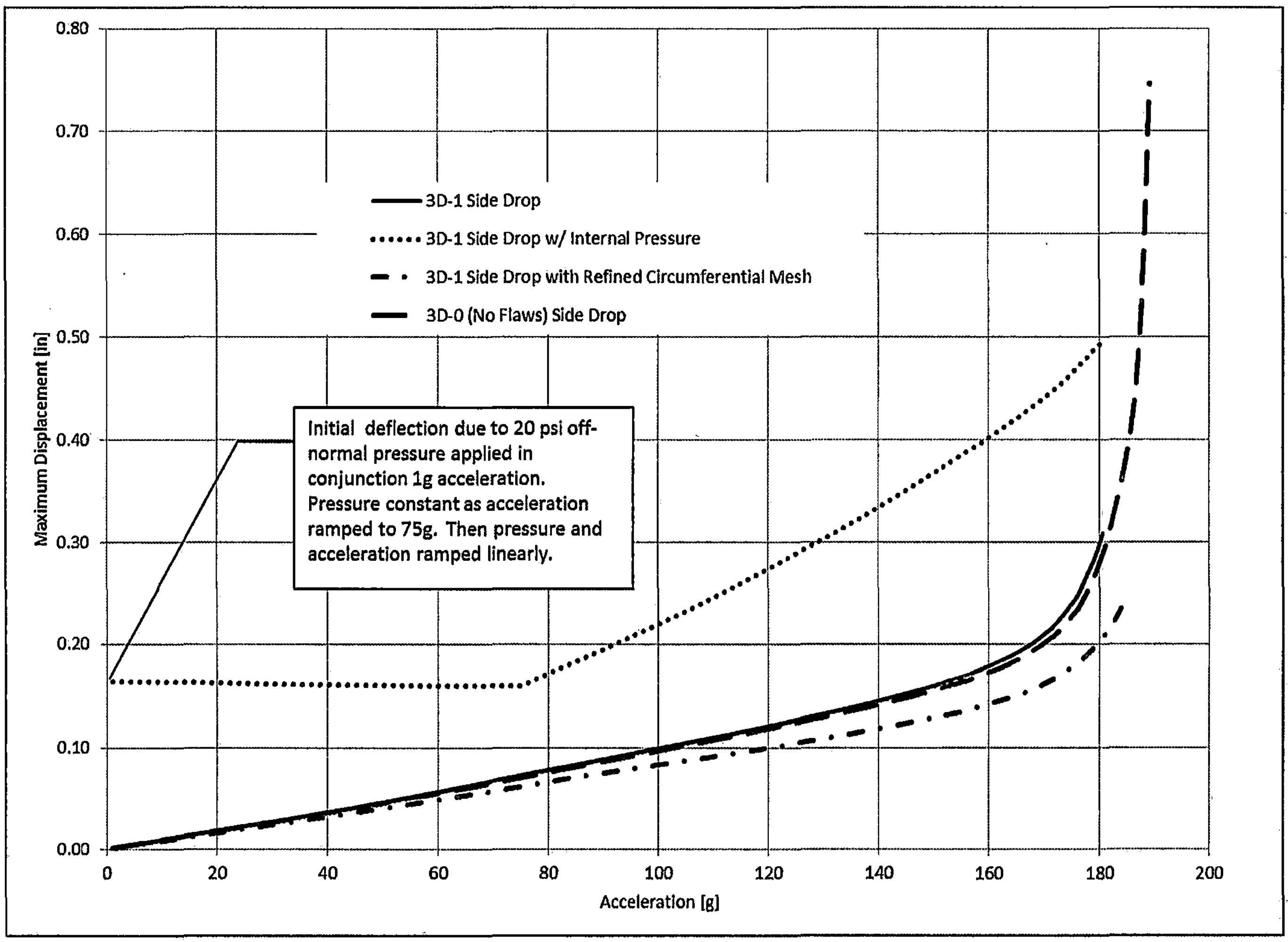

Figure 41 – Comparison of Maximum Displacement Histories for the Various Half-Symmetry Analyses

(Service Level D material properties)

(Note that the magnitude of the strains and deflections has no true physical meaning due to the nature of limit load analysis)

10.0 APPENDIX A –ELASTIC-PLASTIC ANALYSES

Purpose

The purpose of this appendix is to document elastic-plastic analyses of DSC-16. The models listed below are used as a basis for the analyses.

Axisymmetric 1 with Refined Welds and Lid Mesh

Half Symmetry 1 with Initial Mesh

These models produced the bounding results using the limit load methodology. The models are updated to include the elastic-plastic material properties described below. In addition, these new runs consider the effects of large-deformations (NLGEOM,ON). The intent of these analyses is to provide a more realistic prediction of the actual material strains that would occur under the design basis loading, as opposed to the over-estimated strains and deformations which result from the limit-load analysis methodology.

Material Properties

The elastic-plastic behavior of SA-240 Type 304 stainless steel is idealized using Ramberg-Osgood stress-strain curve constants calculated using the equations in Appendix B of Reference A1[2]. The constants are calculated using the ASME code [Ref.5.16] specified minimum yield and ultimate strength values at the applicable temperatures. In order to incorporate the curves into the ANSYS analysis, the initial slope of the curves must match the defined elastic modulus. Therefore the first data point in the curves is defined at the (strain,stress) data point (S_y/E,S_y). The material behavior is based on true stress and true strain, since the ANSYS analysis accounts for changes in geometry (e.g. necking). The following equations from Reference A1 were used to develop the curves:

$$\frac{\epsilon}{\epsilon_o} = \frac{\sigma}{\sigma_o} + \alpha\left(\frac{\sigma}{\sigma_o}\right)^n$$

$\epsilon = true\ strain$

$\epsilon_o = true\ strain\ at\ yield$

$\sigma = true\ stress$

$\sigma_o = true\ stress\ at\ yield$

$$n = \frac{1}{ln(1 + e_u)}$$

$$\alpha = \left[\frac{ln(1 + e_u)}{ln\left(1 + \frac{\sigma_y}{E}\right)} - \frac{\sigma_u(1 + e_u)}{\sigma_y\left(1 + \frac{\sigma_y}{E}\right)}\right]\left[\frac{\sigma_u(1 + e_u)}{\sigma_y\left(1 + \frac{\sigma_y}{E}\right)}\right]^{-n}$$

$e_u = engineering\ strain\ at\ the\ ultimate\ tensile\ strength$

$\sigma_y = engineering\ yield\ stress$

[2] The equations in Reference A1 to develop the full-range true stress-strain curve are based on curve fits of tensile test data. The resulting curve is not indicative of a specific failure type or analysis approach. Rather, it is a method to develop a full-range stress-strain curve of a material using a limited set of data (i.e. minimum specified yield and ultimate strengths.)

$$\sigma_u = engineering\ ultimate\ strength$$

The value of e_u is taken as 0.35, which is assumed to be e_{tot}-0.05, where e_{tot} is taken as the minimum specified elongation of the material (40%), per Reference A2.

The relationship between true and engineering stress and strain is per the following equations:

$$\sigma_{true} = \sigma_{eng}(e_{eng} + 1)$$
$$\epsilon_{true} = ln(e_{eng} + 1)$$

Figure A-1 shows both the true and engineering stress strain curves based on the Ramberg-Osgood equations. The curves at various temperatures as coded into the ANSYS analysis are shown in Figure A-2.

The SA-36 shield plugs use a bi-linear stress strain curve with a tangent modulus of 1% of the initial elastic modulus. This results in a less stiff representation of the shield plug, which will result in conservatively greater strains in the DSC.

Load Cases

Analyses are performed for the following load cases:

1. Internal pressure loading (32 psi) for Service Level A/B.
2. Internal pressure loading (65 psi) for Service Level D.
3. Side drop Loading (75g) for Service Level D.

As discussed in Section 4.2, these three load cases bound all of the design loading conditions for the DSC OTCP and ITCP welds.

Results and Conclusion

Plots of the equivalent plastic strain for the three analyses are shown in Figure A-3 through A-5. The results are summarized in Table A-1. As shown by the results, the strain levels remain well below the minimum specified elongation limits of Type 304 steel and Type 308 weld electrodes [Ref. A2 and A3]. Therefore, material rupture will not occur at the design conditions.

The maximum strains at loads up to 1.5x the specified loading are also extracted. These results are shown in Table 7, which also includes a comparison of the peak strain values to the ductility limit of the material reduced by the weld uncertainty factor of 0.8 discussed in Section 3.4. See Section 7.0 for further discussion and conclusions.

References

A1. EPRI NP-5531. Evaluation of High-Energy Pipe Rupture Experiments. January 1988.

A2. ASME Section II Part A. Ferrous Material Specifications. 1998 Edition with Addenda through 2000.

A3. ASME Section II Part C. Specifications for Welding Rods, Electrodes, and Filler Metals. 1998 Edition with Addenda through 2000.

Computer Files

Analyses performed on Computer HEA-0213A using ANSYS Version 14.0 [Ref. 5.6]

File date & time listing is as displayed by the Windows 7 Operating System – Differences may occur due to local time zone and daylight savings settings.

Analysis Case	File Name	Date & Time
Elastic-Plastic Axisymmetric 1 Refined Lids and Welds Internal Pressure SL A/B	61BTH_WeldFlaw_1F_AX_2_DETACH.db	11/29/2015 8:41 AM
	61BTH_WeldFlaw_1F_AX_2_DETACH.rst	11/29/2015 8:18 AM
	SOLUTION_AXISYMM_IP_500F.INP	11/27/2015 4:03 PM
Elastic-Plastic Axisymmetric 1 Refined Lids and Welds Internal Pressure SL D	61BTH_WeldFlaw_1F_AX_2_DETACH.db	11/27/2015 3:36 PM
	61BTH_WeldFlaw_1F_AX_2_DETACH.rst	11/27/2015 3:33 PM
	SOLUTION_AXISYMM_IP_625F.INP	11/19/2015 11:46 AM
Elastic-Plastic Half-Symmetry 1 Initial Mesh Side Drop SL D	61BTH_WeldFlaw_1GC.db	11/29/2015 8:16 AM
	61BTH_WeldFlaw_1GC.rst	11/27/2015 6:26 PM
	SOLUTION_HALFSYM_SD.INP	11/20/2015 10:08 AM
Stress-Strain Curve Development	Stress-Strain.xls	11/30/2015 10:59 AM

Table A-1 – Summary of Elastic-Plastic Analysis Results.

Analysis Case	Result	Value [in/in]
Internal Pressure Service Level A Axisymmetric (Note 1)	Equivalent Plastic Strain at 32 psi Internal Pressure (Note 1)	0.0183 (1.83%)
Internal Pressure Service Level D Axisymmetric	Equivalent Plastic Strain at 65 psi Internal Pressure	0.0597 (5.97%)
Side Drop Service Level D Half-Symmetry	Equivalent Plastic Strain at 75g Acceleration	0.0609 (6.09%)

Note 1: The 32 psi internal pressure is bounding for Service Levels A and B and includes design internal pressure of 10 psi plus an additional 22 psi to account for inertial loading of the DSC contents onto the lid. See Section 4.2 for details.

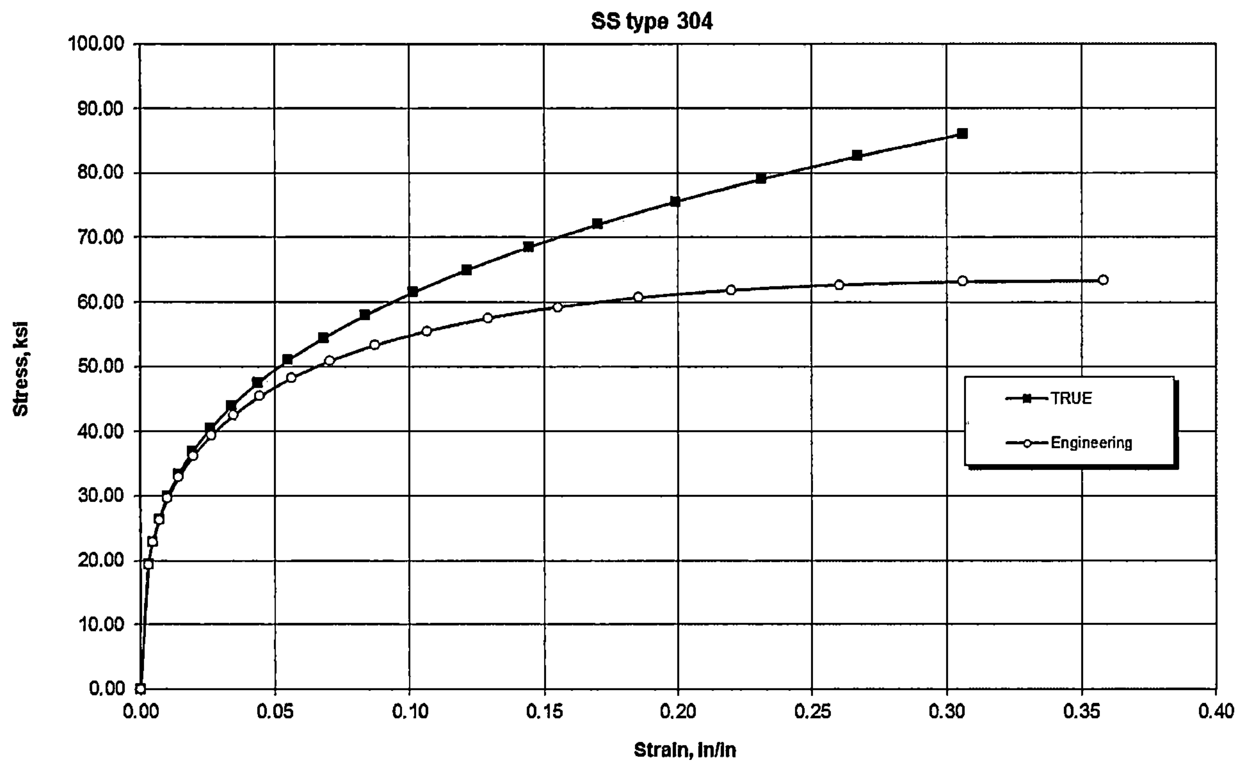

Figure A-1 – Ramberg-Osgood Derived Stress Strain Curve for SA-240 Type 304 at 500 °F.

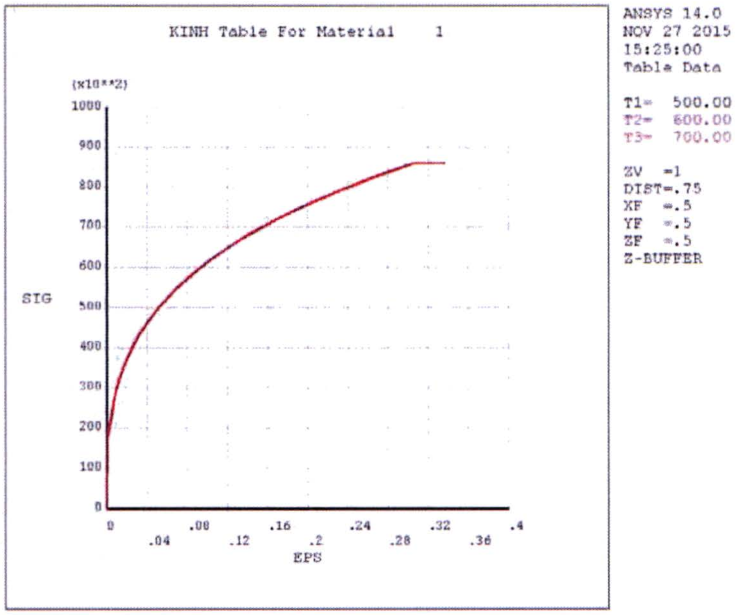

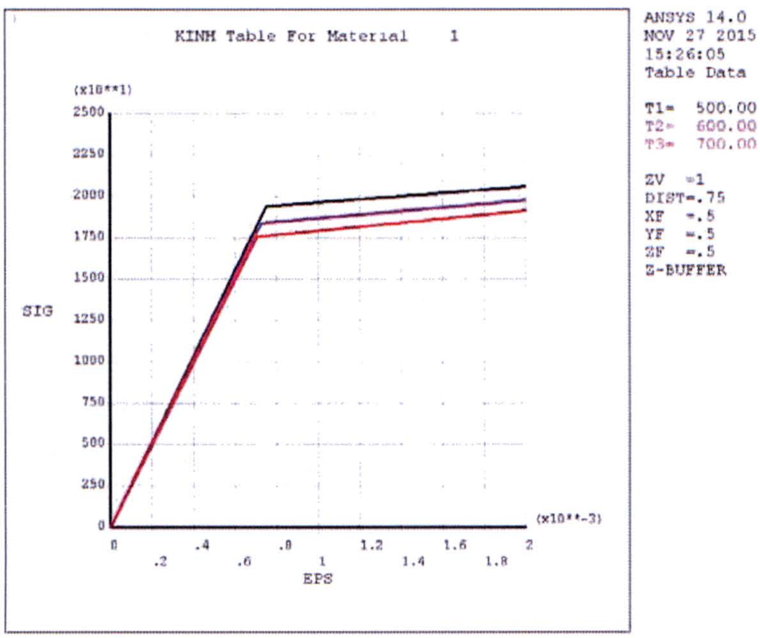

Figure A-2 – Ramberg-Osgood Stress Strain Curves for SA-240 Type 304 from ANSYS Model at Various Temperatures.
Upper image shows full range of curves (strain axis from 0 to 40%), lower image shows detail of the initial yield point (strain axis from 0 to 0.2%)

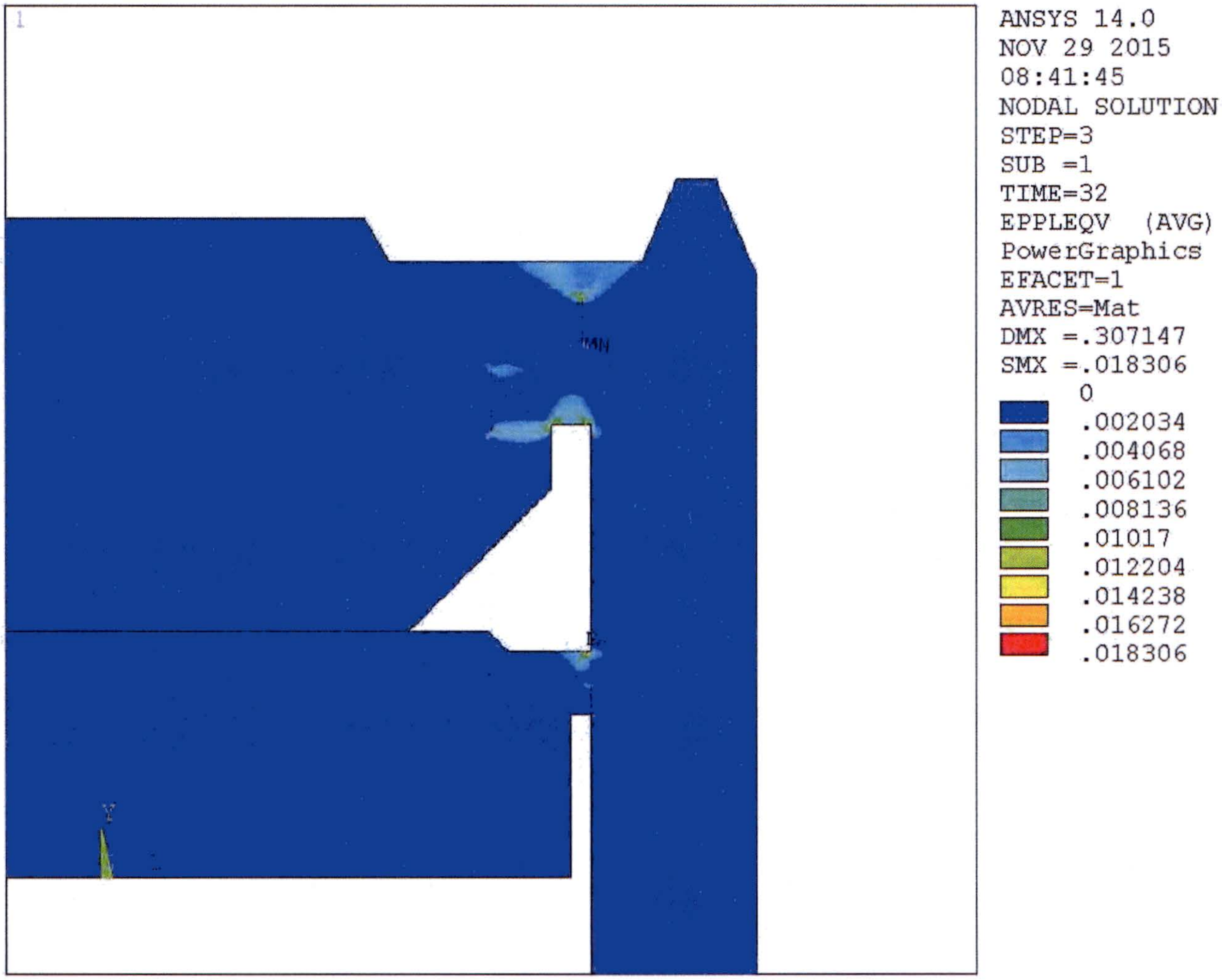

Figure A-3 – Service Level A Internal Pressure - Equivalent Plastic Strain at 32 psi *Note

*Note: The 32 psi internal pressure is bounding for Service Levels A and B and includes design internal pressure of 10 psi plus an additional 22 psi to account for inertial loading of the DSC contents onto the lid. See Section 4.2 for details.

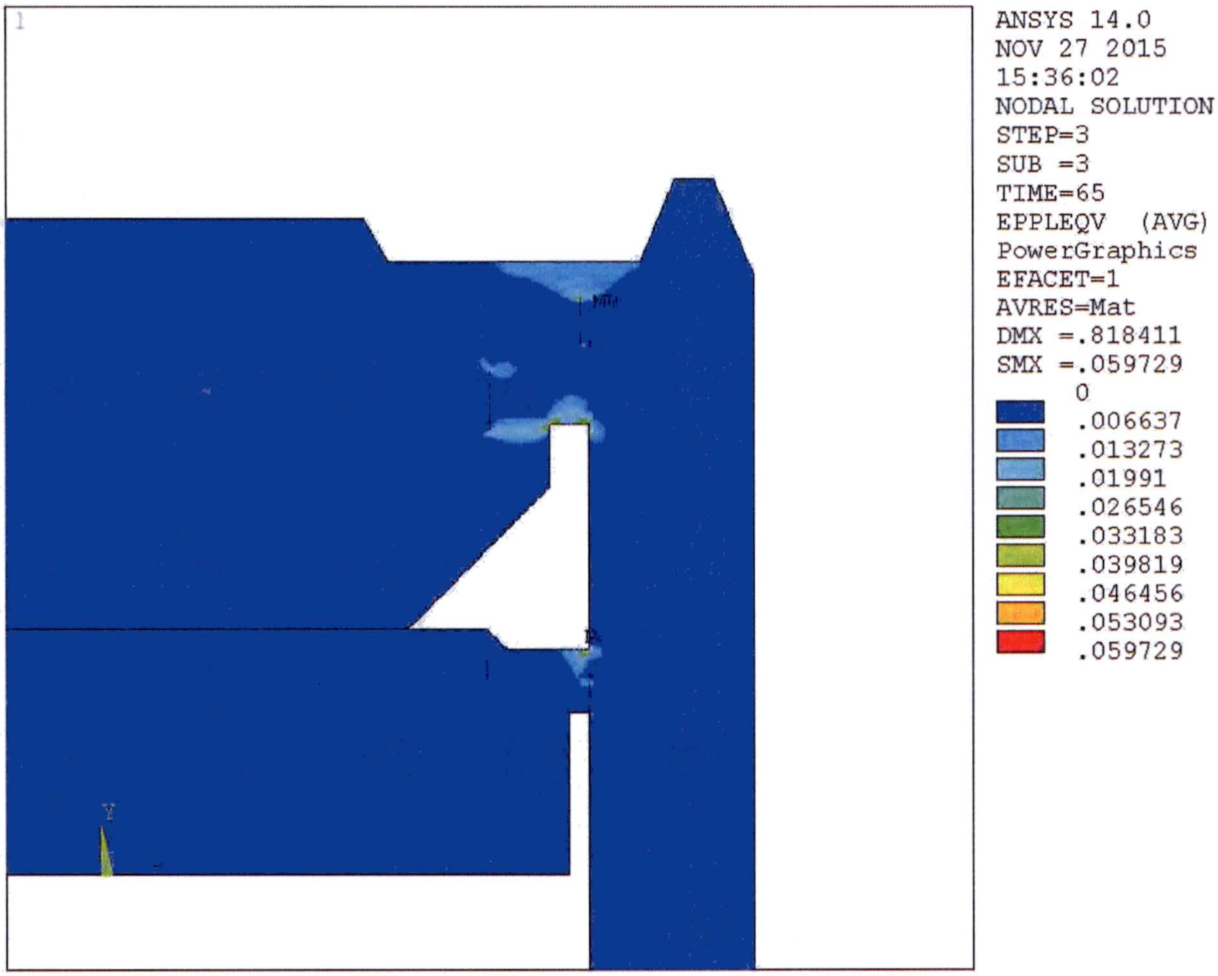

Figure A-4 – Service Level D Internal Pressure - Equivalent Plastic Strain at 65 psi

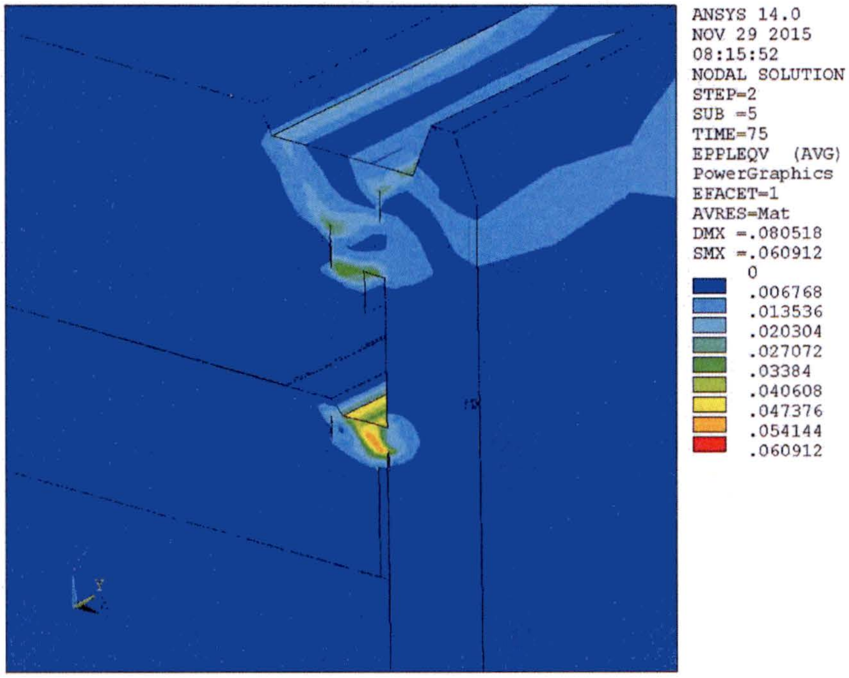

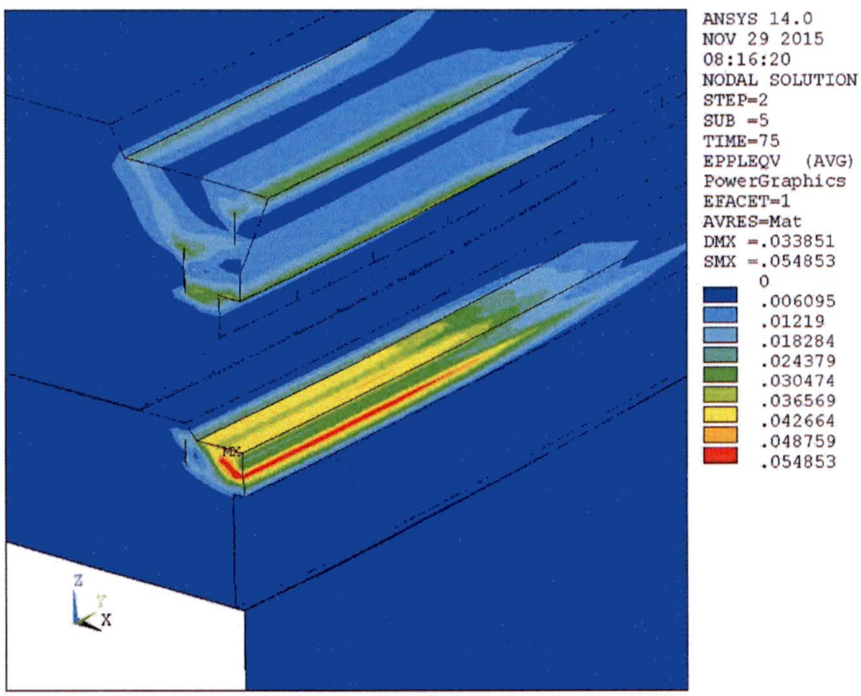

Figure A-5 – Service Level D Side Drop - Equivalent Plastic Strain at 75g. Upper image shows all DSC components, lower image is without shell to allow view of the weld surface. The peak strain of 6.09% occurred on the surface of the shell. Therefore, when the shell was removed for the lower image, the peak strain reported reduced to 5.49%.

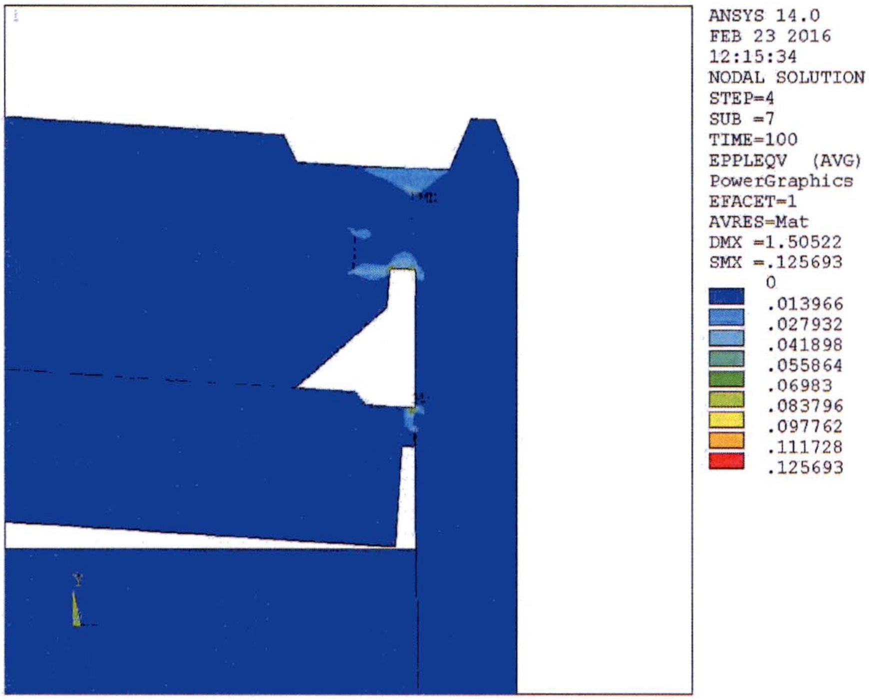

Figure A-6 – Service Level D Internal Pressure - Equivalent Plastic Strain at 100 psi.

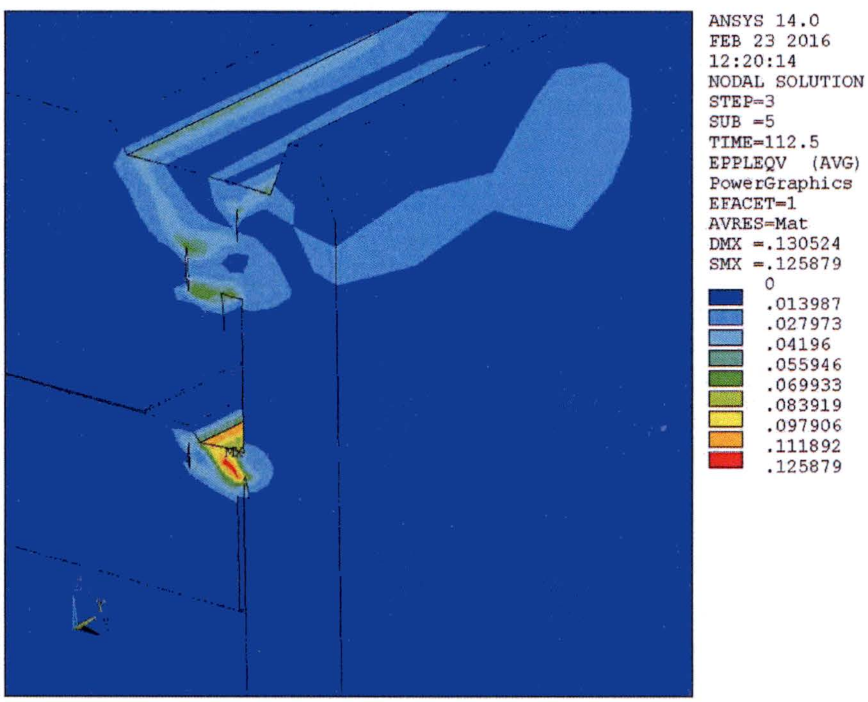

Figure A-7 – Service Level D Side Drop - Equivalent Plastic Strain at 112.5g.